APPENDICES

Appendix A

Units Systems and Conversions

A.1 Introduction

In any book of this nature, it is worthwhile to include a comprehensive list of units conversion factors, since data are often reported in units different from those used in the equations. Such factors are presented in this appendix. Because of the possibility of eventual conversion of engineering calculations to a metric standard, we also include information about the "SI" system of weights and measures.[1] Finally, we compare some important units and equations in five different unit systems.

A.2 The International (SI) Metric System

"SI" is the official abbreviation, *in all languages*, for the International System of Units (les Systéme International d'Unités). That system is neither the centimetre-gram-second (cgs) system nor the metre-kilogram-second (mks) system. Rather, it is a modernized version of mks. A complete description of SI is presented by Hopkins.[1] The American Petroleum Institute has proposed a set of metric standards for use in the petroleum industry.[2]

TABLE A.1—SI SYSTEM UNITS.

Base SI Units Used in Well Test Analysis

Quantity	Name	Symbol
length	metre	m
time	second	s
mass	kilogram	kg
temperature	kelvin	K
amount of substance	mole	mol

Units That Are Multiples or Submultiples of SI Base Units Given Special Names

Quantity	Name of Unit	Symbol	Definition	SI Term
mass	tonne	t	$1t=10^3kg$	Mg
volume	litre*	l	$1l=1\ dm^3$	dm^3

SI-Derived Units With Special Names Used in Well Test Analysis

Quantity	Name	Symbol	Expression in Terms of Other Units	Expression in Terms of SI Base Units
force	newton	N	—	$m\cdot kg\cdot s^{-2}$
pressure	pascal	Pa	N/m^2	$m^{-1}\cdot kg\cdot s^{-2}$
energy, work, quantity of heat	joule	J	$N\cdot m$	$m^2\cdot kg\cdot s^{-2}$

*In 1964, the 12th Conférence Générale des Poids et Mesures (CGPM) redefined the litre to be $1\ dm^3 = 0.001\ m^3$. At the same time, it abrogated the 1901 definition of the litre given by the third CGPM.

Table A.1 lists the five *base* SI units encountered in well test analysis. The approved spelling is the French spelling. Names of units are never capitalized, although some of the abbreviations are. Most units are abbreviated with a single symbol. Table A.1 also lists two SI units that have been given special names and three derived units with special SI names. No units are normally used in well test analysis other than those presented in Table A.1.

SI allows prefixes to indicate multiples of the base units. The prefixes are summarized in Table A.2. Compound prefixes, such as micro-micro, are not allowed; the correct prefix, in this case pico, should always be used.

A.3 Constants and Conversion Factors

Table A.3 presents values for several physical constants useful in petroleum engineering, in several sets of units. Table A.4 summarizes useful conversion factors. SI units are indicated by boldface type. To use Table A.4, multiply the quantity given in the left-hand column by the number given in the "multiply by" column to obtain units in the second column. For simplicity, the "inverse" column may be used to reverse this procedure. Thus, to convert from square feet to acres, one would multiply the number of square feet by 2.296×10^{-5}.

Some permeability units are given under the heading "area" in Table A.4, since permeability has the units of area. Table A.5 is also supplied to simplify other conver-

TABLE A.2—SI PREFIXES.

Factor	Prefix	Symbol*
10^{12}	tera	T
10^{9}	giga	G
10^{6}	mega	M
10^{3}	kilo	k
10^{2}	hecto	h
10	deka	da
10^{-1}	deci	d
10^{-2}	centi	c
10^{-3}	milli	m
10^{-6}	micro	μ
10^{-9}	nano	n
10^{-12}	pico	p
10^{-15}	femto	f
10^{-18}	atto	a

*Only the symbols T (tera), G (giga), and M (mega) are capital letters. Compound prefixes are not allowed — for example, use nm (nano metre) rather than mμm (milli micro metre).

TABLE A. 3—PHYSICAL CONSTANTS AND VALUES.*

Quantity	Magnitude	Unit
Triple point of water	273.16 exactly	**K**
	0.01 exactly	°C
	491.688 exactly	°R
	32.018 exactly	°F
Absolute zero	0.00 exactly	**K**
	−273.15 exactly	°C
	0.00 exactly	°R
	−459.67 exactly	°F
Gas constant (R)	8.3143	**J·mol^{-1}·K^{-1}**
	8.3143 E + 07	erg·(gm mole)$^{-1}$·°K^{-1}
	10.732	psi·ft^3·(lb mole)$^{-1}$·°R^{-1}
Maximum density of water	999.973	**kg·m^{-3}**
	0.999 973	g·cm^{-3}
	62.426 1	lb_m·ft^{-3}
Density of water at 60 °F (15.56 °C, 288.71 K)	999.014	**kg·m^{-3}**
	0.999 014	g·cm^{-3}
	62.366 4	lb_m·ft^{-3}
Water gradient at 60 °F (15.56 °C, 288.71 K)	9,796.98	**Pa·m^{-1}**
	979.698	dyne·cm^{-3}
	0.433 100	psi·ft^{-1}
Standard atmosphere	1.013 25 E + 05	**Pa**
	1.013 25 E + 06	dyne·cm^{-2}
	14.695 9	psi
Density of air at 1 atm, 60 °F (15.56 °C, 288.71 K)	1.223 2	**kg·m^{-3}**
	1.223 2 E − 03	g·cm^{-3}
	0.076 362	lb_m·ft^{-3}
Earth's gravitational acceleration,		
g	9.806 650	**m·s^{-2}**
	980.665 0	cm·s^{-2}
	32.174 05	ft·s^{-2}
g_c	1.000 000	**kg·m·N^{-1}·sec^{-2}**
	1.000 000	g·cm·dyne^{-1}·sec^{-2}
	32.174 05	lb_m·ft·lb_f^{-1}·s^{-2}
π	3.141 593	
e	2.718 282	
ln (10)	2.302 585	
γ (Euler's constant)	0.577 215 66	
°API	$\frac{141.5}{\gamma(60\ °F)} - 131.5$	

*SI values are in boldface type. All quantities are consistent with conversion factors for the current SI system.

sions using permeability. That table is similar to data given by Amyx, Bass, and Whiting[3] but there is some variation in numbers. Differences occur because numerical values are shown only to the significance possible (in this case, limited by the SI agreed-on accuracy of atmospheric pressure and the density of water and mercury), and are based on conversion factors derived from the SI Standards. Some of those factors are slightly different from those used previously because of more precise definitions for certain quantities.

Table A.6 provides conversions for various temperature scales. The SI standard temperature unit is the kelvin; that unit is neither capitalized nor associated with the word "degree." One kelvin is equivalent to 1 degree Celsius (the SI system drops the use of the term Centigrade). The triple point of water is *defined* as 273.16 kelvin exactly. All other temperatures are derived from that. The normal Celsius and Fahrenheit scales are the same, as are their conversions to the other scales.

Table A.7 compares units and equations from five systems of units. The oilfield units are used exclusively throughout this monograph. The column for SI units is a coherent system (that is, one in which basic equations contain no units conversion factors). The preferred API standard SI unit system[2] is not a coherent system, but has the advantages of providing reasonable size values for most physical quantities. The cgs units column is the standard cgs system used for many years in petroleum engineering. Finally, the column for groundwater units is provided for those who practice in that field. The symbols used in groundwater hydrology vary from reference to reference, so the reader should check carefully when using groundwater literature. Table A.8 shows the correspondence between some groundwater quantities and oilfield quantities for any consistent unit system.

Many of the conversion factors provided in Tables A.3 through A.7 have been calculated from SI-stated factors for other unit conversions. Depending on the approach used in performing such a calculation, the seventh significant digit may vary by a few units. The reader should be aware of that when attempting to verify the values given, or to use them in precision computations.

References

1. Hopkins, Robert A.: *The International (SI) Metric System and How It Works*, Polymetric Services, Inc., Tarzana, Calif. (1974).
2. "Conversion of Operational and Process Measurement Units to the Metric (SI) System," *Manual of Petroleum Measurement Standards*, Pub. API 2564, American Petroleum Institute (March 1974) Chap. 15, Sec. 2.
3. Amyx, James W., Bass, Daniel, M., Jr., and Whiting, Robert L.: *Petroleum Reservoir Engineering: Physical Properties*, McGraw-Hill Book Co., Inc., New York (1960) 79.

TABLE A.4—CONVERSION FACTORS USEFUL IN WELL TEST ANALYSIS.

SI conversions are in boldface type. All quantities are current to SI standards as of 1974. An asterisk (*) after the sixth decimal indicates the conversion factor is exact and all following digits are zero. All other conversion factors have been rounded. The notation E+03 is used in place of 10^3, and so on.

To Convert From	To	Multiply by	Inverse
AREA			
acre	**metre² (m^2)**	4.046 856 E+03	2.471 054 E−04
	foot²	4.356 000* E+04	2.295 684 E−05
darcy	**metre² (m^2)**	9.869 23 E−13	1.013 25 E+12
	centimetre² (cm^2)	9.869 23 E−09	1.013 25 E+08
	micrometre² (μm^2)	9.869 23 E−01	1.013 25 E+00
	millidarcy	1.000 000* E+03	1.000 000*E−03
	$cm^2 \cdot cp \cdot sec^{-1} \cdot atm^{-1}$	1.000 000* E+00	1.000 000*E+00
foot²	**metre² (m^2)**	9.290 304* E−02	1.076 391 E+01
	centimetre²	9.290 304* E+02	1.076 391 E−03
	inch²	1.440 000* E+02	6.944 444 E−03
hectare	**metre² (m^2)**	1.000 000* E+04	1.000 000*E−04
	acre	2.471 054 E+00	4.046 856 E−01
mile²	**metre² (m^2)**	2.589 988 E+06	3.861 022 E−07
	acre	6.400 000* E+02	1.562 500*E−03
DENSITY			
gram/centimetre³	**kilogram/metre³ ($kg \cdot m^{-3}$)**	1.000 000* E+03	1.000 000*E−03
	pound-mass/foot³	6.242 797 E+01	1.601 846 E−02
	pound-mass/gallon	8.345 405 E+00	1.198 264 E−01
	pound-mass/barrel	3.505 070 E+02	2.853 010 E−03
pound-mass/foot³	**kilogram/metre³ ($kg \cdot m^{-3}$)**	1.601 846 E+01	6.242 797 E−02
	pound-mass/gallon	1.336 805 E−01	7.480 520 E+00
	pound-mass/barrel	5.614 583 E+00	1.781 076 E−01
pound-mass/gallon	**kilogram/metre³ ($kg \cdot m^{-3}$)**	1.198 264 E+02	8.345 406 E−03
	pound-mass/barrel	4.200 000 E+01	2.380 952 E−02
FORCE			
dyne	**newton (N)**	1.000 000* E−05	1.000 000*E+05
	pound-force	2.248 089 E−06	4.448 222 E+05
kilogram-force	**newton (N)**	9.806 650* E+00	1.019 716 E−01
	pound-force	2.204 622 E+00	4.535 924 E−01
pound-force	**newton (N)**	4.448 222 E+00	2.248 089 E−01
LENGTH			
angstrom	**metre (m)**	1.000 000* E−10	1.000 000*E+10
centimetre	**metre (m)**	1.000 000* E−02	1.000 000*E+02
foot	**metre (m)**	3.048 000* E−01	3.280 840 E+00
	centimetre	3.048 000* E+01	3.280 840 E−02
inch	**metre (m)**	2.540 000* E−02	3.937 008 E+01
	centimetre	2.540 000* E+00	3.937 008 E−01
micron	**metre (m)**	1.000 000* E−06	1.000 000*E+06
mile (U.S. statute)	**metre (m)**	1.609 344* E+03	6.213 712 E−04
	foot	5.280 000* E+03	1.893 939 E−04
MASS			
gram-mass	**kilogram (kg)**	1.000 000* E−03	1.000 000*E+03
ounce-mass (av)	**kilogram (kg)**	2.834 952 E−02	3.527 397 E+01
	gram	2.834 952 E+01	3.527 397 E−02
pound-mass	**kilogram (kg)**	4.535 923 7*E−01	2.204 623 E+00
	ounce-mass	1.600 000* E+01	6.250 000*E−02
slug	**kilogram (kg)**	1.459 390 E+01	6.852 178 E−02
	pound-mass	3.217 405 E+01	3.108 095 E−02
ton (U.S. short)	**kilogram (kg)**	9.071 847 E+02	1.102 311 E−03
	pound-mass	2.000 000* E+03	5.000 000*E−04
ton (U.S. long)	**kilogram (kg)**	1.016 047 E+03	9.842 064 E−04
	pound-mass	2.240 000* E+03	4.464 286 E−04
ton (metric)	**kilogram (kg)**	1.000 000* E+03	1.000 000*E−03
tonne	**kilogram (kg)**	1.000 000* E+03	1.000 000*E−03

TABLE A.4—CONT'D.

To Convert From	To	Multiply by	Inverse
PRESSURE			
atmosphere (normal—760 mm Hg)	**pascal (Pa)**	1.013 25 E+05	9.869 23 E−06
	mm Hg (0 °C)	7.600 000*E+02	1.315 789 E−03
	feet water (4 °C)	3.389 95 E+01	2.949 90 E−02
	psi	1.469 60 E+01	6.804 60 E−02
	bar	1.013 25 E+00	9.869 23 E−01
bar	**pascal (Pa)**	1.000 000*E+05	1.000 000*E−05
	psi	1.450 377 E+01	6.894 757 E−02
centimetre of Hg (0 °C)	**pascal (Pa)**	1.333 22 E+03	7.500 64 E−04
	psi	1.933 67 E−01	5.171 51 E+00
dyne/centimetre^2	**pascal (Pa)**	1.000 000*E−01	1.000 000*E+01
	psi	1.450 377 E−05	6.894 757 E+04
feet of water (4 °C)	**pascal (Pa)**	2.988 98 E+03	3.345 62 E−04
	psi	4.335 15 E−01	2.306 73 E+00
kilogram-force/centimetre^2	**pascal (Pa)**	9.806 650*E+04	1.019 716 E−05
	bar	9.806 650*E−01	1.019 716 E+00
	psi	1.422 334 E+01	7.030 695 E−02
psi	**pascal (Pa)**	6.894 757 E+03	1.450 377 E−04
TIME			
day	**second (s)**	8.640 000*E+04	1.157 407 E−05
	minute	1.440 000*E+03	6.944 444 E−04
	hour	2.400 000*E+01	4.166 667 E−02
hour	**second (s)**	3.600 000*E+03	2.777 778 E−04
	minute	6.000 000*E+01	1.666 667 E−02
minute	**second (s)**	6.000 000*E+01	1.666 667 E−02
VISCOSITY			
centipoise	**pascal-second (Pa·s)**	1.000 000*E−03	1.000 000*E+03
	dyne-second/centimetre^2	1.000 000*E−02	1.000 000*E+02
	pound-mass/(foot-second)	6.719 689 E−04	1.488 164 E+03
	pound-force-second/foot^2	2.088 543 E−05	4.788 026 E+04
	pound-mass/(foot-hour)	2.419 088 E+00	4.133 789 E−01
centistoke	**metre^2/second (m^2/s)**	1.000 000*E−06	1.000 000*E+06
	centipoise/(gram/centimetre^3)	1.000 000*E+00	1.000 000*E+00
poise	**pascal-second (Pa·s)**	1.000 000*E−01	1.000 000*E+01
pound-mass/(foot-second)	**pascal-second (Pa·s)**	1.488 164 E+00	6.719 689 E−01
pound-mass/(foot-hour)	**pascal-second (Pa·s)**	4.133 789 E−04	2.419 088 E+03
pound-force-second/foot^2	**pascal-second (Pa·s)**	4.788 026 E+01	2.088 543 E−02
VOLUME			
acre-foot	**metre^3 (m^3)**	1.233 482 E+03	8.107 131 E−04
	foot^3	4.356 000*E+04	2.295 684 E−05
	barrel	7.758 368 E+03	1.288 931 E−04
barrel	**metre^3 (m^3)**	1.589 873 E−01	6.289 811 E+00
	foot^3	5.614 583 E+00	1.781 076 E−01
	gallon	4.200 000*E+01	2.380 952 E−02
foot^3	**metre^3 (m^3)**	2.831 685 E−02	3.531 466 E+01
	inch^3	1.728 000 E+03	5.787 037 E−04
	gallon	7.480 520 E+00	1.336 805 E−01
gallon	**metre^3 (m^3)**	3.785 412 E−03	2.641 720 E+02
	inch^3	2.310 001 E+02	4.329 003 E−03
litre	**metre^3 (m^3)**	1.000 000*E−03	1.000 000*E+03
VOLUMETRIC RATE			
barrel/day	**metre^3/sec (m^3/s)**	1.840 131 E−06	5.434 396 E+05
	metre^3/hour (m^3/h)	6.624 472 E−03	1.509 554 E+02
	metre^3/day (m^3/d)	1.589 873 E−01	6.289 810 E+00
	centimetre^3/second	1.840 131 E+00	5.434 396 E−01
	foot^3/minute	3.899 016 E−03	2.564 750 E+02
	gallon/minute	2.916 667 E−02	3.428 571 E+01
foot^3/minute	**metre^3/sec (m^3/s)**	4.719 474 E−04	2.118 880 E+03
foot^3/second	**metre^3/sec (m^3/s)**	2.831 685 E−02	3.531 466 E+01
gallon/minute	**metre^3/sec (m^3/s)**	6.309 020 E−05	1.585 032 E+04

TABLE A.5—AUXILIARY PERMEABILITY CONVERSIONS.

To Convert From	To	Multiply by	Inverse
md	darcy	1.000 000*E−03	1.000 000*E+03
	metre² (m²)	9.869 23 E−16	1.013 25 E+15
	centimetre² (cm²)	9.869 23 E−12	1.013 25 E+11
	micrometre² (μm^2)	9.869 23 E−04	1.013 25 E+03
	$\frac{(cm^3/s)\ cp}{cm^2\ (atm/cm)}$	1.000 000* E−03	1.000 000* E+03
	$\frac{(cm^3/s)\ cp}{cm^2[(dyne/cm^2)/cm]}$	9.869 23 E−10	1.013 25 E+09
	$\frac{(ft^3/s)\ cp}{ft^2\ (psi/ft)}$	7.324 41 E−08	1.365 30 E+07
	$\frac{(ft^3/s)\ cp}{cm^2[(cm\ water)/cm]}$	3.417 80 E−11	2.925 85 E+10
	$\frac{(B/D)\ cp}{ft^2\ (psi/ft)}$	1.127 12 E−03	8.872 17 E+02
	$\frac{(gal/min)\ cp}{ft^2\ [(ft\ water)/ft]}$	1.425 15 E−05	7.016 81 E+04
	ft^2	1.062 32 E−14	9.413 40 E+13

*Conversion factor is exact; all following digits are zero.

TABLE A.6—TEMPERATURE SCALE CONVERSIONS.*

To Convert	To	Solve
degree Fahrenheit	kelvin	$T_K = (T_F + 459.67)/1.8$
degree Rankine	kelvin	$T_K = T_R/1.8$
degree Fahrenheit	degree Rankine	$T_R = T_F + 459.67$
degree Fahrenheit	degree Celsius	$T_C = (T_F - 32)/1.8$
degree Celsius	kelvin	$T_K = T_C + 273.15$

*The SI standard, the kelvin (K), is *defined* so the triple point of water is 273.16 K *exactly*. The SI temperature symbol is written K, without a degree symbol. The cgs (and common) temperature unit is the degree Celsius, °C; the common oilfield unit is the degree Fahrenheit, °F.

TABLE A.8—RELATIONSHIP OF COMMON GROUNDWATER AND OILFIELD QUANTITIES.

A consistent-unit system is assumed. Variable definitions for each system are given in Table A.7.

Groundwater Quantity		Oilfield Quantity
Coefficient of permeability	$= P = K$	$= \frac{k}{\mu}\left(\frac{\rho g}{g_c}\right)$
Transmissivity	$= T = Km$	$= \frac{kh}{\mu}\left(\frac{\rho g}{g_c}\right)$
Coefficient of storage	$= S$	$= \phi c_t h \left(\frac{\rho g}{g_c}\right)$
Drawdown	$= s$	$= \frac{p_i - p}{(\rho g/g_c)}$
Head	$= h$	$= \frac{p}{(\rho g/g_c)}$
Dimensionless drawdown	$= W(1/4\alpha)$	$= 2p_D(t_D)$

TABLE A.7—COMPARISON OF UNITS AND EQUATIONS IN VARIOUS UNIT SYSTEMS.*

Oilfield Units	SI Units	Preferred API Standard SI Units	cgs Units*	Groundwater Units
q — production rate, STB/D	m^3/s	dm^3/s	cm^3/s	Q — production rate, gal/min
h — formation thickness, ft	m	m	cm	m — formation thickness, ft
k — permeability, md	m^2	μm^2	darcy	—
μ — viscosity, cp	$Pa \cdot s$	$Pa \cdot s$	cp	—
k/μ — mobility, md/cp	$m^2/(Pa \cdot s)$	$\mu m^2/(Pa \cdot s)$	darcy/cp	P or K — coefficient of permeability, gal/day ft²**
kh/μ — mobility-thickness product, md ft/cp	$m^3/(Pa \cdot s)$	$m(\mu m^2)/(Pa \cdot s)$	darcy · cm/cp	T — coefficient of transmissivity, gal/(day ft)**
Δp — pressure difference, psi	Pa	kPa	atm	s — drawdown, ft of water, >0 for pressure drawdown**
p — pressure, psi	Pa	kPa	atm	h — head of water, ft of water
r — radius, ft	m	m	cm	r — radius, ft
t — time, hours	s	h	s	t — time, days
ϕ — porosity, fraction				—
c_t — total system compressibility, psi^{-1}	Pa^{-1}	kPa^{-1}	atm^{-1}	—
$\phi c_t h$ — porosity-compressibility-thickness product, ft psi^{-1}	$m \cdot Pa^{-1}$	$m \cdot kPa^{-1}$	$cm \cdot atm^{-1}$	S — coefficient of storage, fraction**

DIMENSIONLESS TIME

$$t_D = \frac{0.000263679\,kt}{\phi\mu c_t r_w^2} \qquad t_D = \frac{kt}{\phi\mu c_t r_w^2} \qquad t_D = 3.6 \times 10^{-6}\,\frac{kt}{\phi\mu c_t r_w^2} \qquad t_D = \frac{kt}{\phi\mu c_t r_w^2} \qquad \alpha = 0.1336805\,\frac{Tt}{Sr_w^2}$$

DARCY'S LAW FOR INCOMPRESSIBLE, RADIAL FLOW

$$q = \frac{0.00708188\,kh(p_e - p_w)}{B\mu \ln(r_e/r_w)} \qquad q = 2\pi\,\frac{kh(p_e - p_w)}{B\mu \ln(r_e/r_w)} \qquad q = \frac{2\pi \times 10^{-6}\,kh(p_e - p_w)}{B\mu \ln(r_e/r_w)} \qquad q = 2\pi\,\frac{kh(p_e - p_w)}{B\mu \ln(r_e/r_w)} \qquad Q = \frac{0.00436332\,T(h_e - h_w)}{\ln(r_e/r_w)}$$

DIFFUSIVITY EQUATION

$$\frac{\partial^2 p}{\partial r^2} + \frac{1}{r}\frac{\partial p}{\partial r} = \frac{1}{0.000263679}\,\frac{\phi\mu c_t}{k}\,\frac{\partial p}{\partial t} \qquad \frac{\partial^2 p}{\partial r^2} + \frac{1}{r}\frac{\partial p}{\partial r} = \frac{\phi\mu c_t}{k}\,\frac{\partial p}{\partial t} \qquad \frac{\partial^2 p}{\partial r^2} + \frac{1}{r}\frac{\partial p}{\partial r} = \frac{1}{3.6 \times 10^{-6}}\,\frac{\phi\mu c_t}{k}\,\frac{\partial p}{\partial t} \qquad \frac{\partial^2 p}{\partial r^2} + \frac{1}{r}\frac{\partial p}{\partial r} = \frac{\phi\mu c_t}{k}\,\frac{\partial p}{\partial t} \qquad \frac{\partial^2 h}{\partial r^2} + \frac{1}{r}\frac{\partial h}{\partial r} = \frac{1}{0.1336805}\,\frac{S}{T}\,\frac{\partial h}{\partial t}$$

GENERALIZED TRANSIENT FLOW EQUATION

$$\Delta p = \frac{141.205\,qB\mu\,p_D(t_D)}{kh} \qquad \Delta p = \frac{qB\mu\,p_D(t_D)}{2\pi kh} \qquad \Delta p = 10^6\,\frac{qB\mu\,p_D(t_D)}{2\pi kh} \qquad \Delta p = \frac{1}{2\pi}\,\frac{qB\mu}{kh}\,p_D(t_D) \qquad s = 229.183\,\frac{Q}{T}\,p_D(\alpha)$$

SLOPE OF SEMILOG STRAIGHT LINE

$$m = 162.568\,\frac{qB\mu}{kh} \qquad m = 0.183234\,\frac{qB\mu}{kh} \qquad m = 1.83234 \times 10^5\,\frac{qB\mu}{kh} \qquad m = 0.183234\,\frac{qB\mu}{kh} \qquad M = 263.857\,\frac{Q}{T}$$

GENERALIZED SKIN-FACTOR EQUATION

$$s = 1.15129\left[\frac{p_{1hr} - p(\Delta t = 0)}{m} - \log\left(\frac{k}{\phi\mu c_t r_w^2}\right) + 3.227546\right] \qquad s = 1.15129\left[\frac{p_{1hr} - p(\Delta t = 0)}{m} - \log\left(\frac{k}{\phi\mu c_t r_w^2}\right) - 0.351378\right]$$

$$s = 1.15129\left[\frac{p_{1hr} - p(\Delta t = 0)}{m} - \log\left(\frac{k}{\phi\mu c_t r_w^2}\right) + 5.092319\right] \qquad s = 1.15129\left[\frac{p_{1hr} - p(\Delta t = 0)}{m} - \log\left(\frac{k}{\phi\mu c_t r_w^2}\right) - 0.351378\right]$$

$$\text{skin} = 1.15129\left[\frac{s_{1hr} - s(\Delta t = 0)}{M} - \log\left(\frac{T}{Sr_w^2}\right) + 0.522555\right]$$

*The cgs system is considered to be obsolete and is replaced by SI; cgs units are included only for comparison with published material. SI is a coherent system, so equations do not contain units conversion factors.

**See Table A.8.

Appendix B

Application of Superposition To Generate Dimensionless Pressures

B.1 Introduction

As indicated in Section 2.9 and by several authors,[1-9] the principle of superposition may be used to develop dimensionless pressure data for many finite and bounded systems. This appendix shows how to use superposition to form no-flow and constant-pressure boundaries, and closed systems. A method of "desuperposition" for changing existing dimensionless-pressures solutions to solutions for different systems is explained. Finally, a general equation for calculating pressures owing to variable production rates is derived.

B.2 Dimensionless Pressure Used

When using the principle of superposition, we must choose a dimensionless pressure, p_D, that applies for the system. Normally, superposition calculations are performed using dimensionless pressures for infinite-acting systems (even when the goal is to generate a closed system[4,6]), so the exponential-integral p_D, Eq. 2.5, is used. The exponential-integral p_D may be used when $r_D \geq 20$ and $t_D/r_D^2 \geq 0.5$ or when $t_D/r_D^2 \geq 25$. If neither of those restrictions is met, then Fig. C.1 must be used for the applicable r_D.

If superposition calculations are performed for a system that is not infinite-acting, the appropriate p_D from Appendix C must be used. In such a situation, there is no conceptual modification to the application of the superposition principle. However, p_D tables and figures for such systems often do not provide data for points other than at the well. Some useful p_D data are given in Appendix C and in Ref. 10.

B.3 Generating No-Flow and Constant-Pressure Boundaries

Fig. B.1 illustrates the method of images[3-6] when used to create a no-flow boundary in an infinite system. Well 1 operates at constant flow rate q, at distance L from a single impermeable boundary, represented by the y axis in Fig. B.1. The image well, Well 2 in Fig. B.1, at a distance $-L$ from the y axis mathematically generates the boundary. By applying superposition we can calculate the pressure at any point in the x-y plane of Fig. B.1:

$$p(t, x, y) = p_i - \frac{141.2\, qB\mu}{kh} \left[p_D(t_D, a_{D1}) + p_D(t_D, a_{D2}) \right]. \quad \ldots\ldots\ldots\ldots\ldots\ldots \text{(B.1)}$$

In Eq. B.1, the dimensionless distances a_{D1} and a_{D2} are calculated from

$$a_{D1} = \frac{a_1}{r_w} = \frac{1}{r_w} \sqrt{(x - L)^2 + y^2}, \quad \ldots\ldots\ldots\ldots \text{(B.2a)}$$

$$a_{D2} = \frac{a_2}{r_w} = \frac{1}{r_w} \sqrt{(x + L)^2 + y^2}, \quad \ldots\ldots\ldots\ldots \text{(B.2b)}$$

where r_w is the same for both wells. For an infinite system with $a_D > 20$, Eq. 2.5a applies.

$$p_D(t_D, a_D) = -\frac{1}{2} \text{Ei}\left(-\frac{a_D^2}{4t_D} \right), \quad \ldots\ldots\ldots\ldots \text{(B.3a)}$$

$$= -\frac{1}{2} \text{Ei}\left(-\frac{(x \pm L)^2 + y^2}{4r_w^2\, t_D} \right), \quad \ldots\ldots\ldots\ldots\ldots\ldots \text{(B.3b)}$$

$$= \frac{1}{2} \int_{\left[\frac{(x \pm L)^2 + y^2}{4r_w^2\, t_D}\right]}^{\infty} \frac{e^{-u}}{u}\, du. \quad \ldots\ldots\ldots\ldots \text{(B.3c)}$$

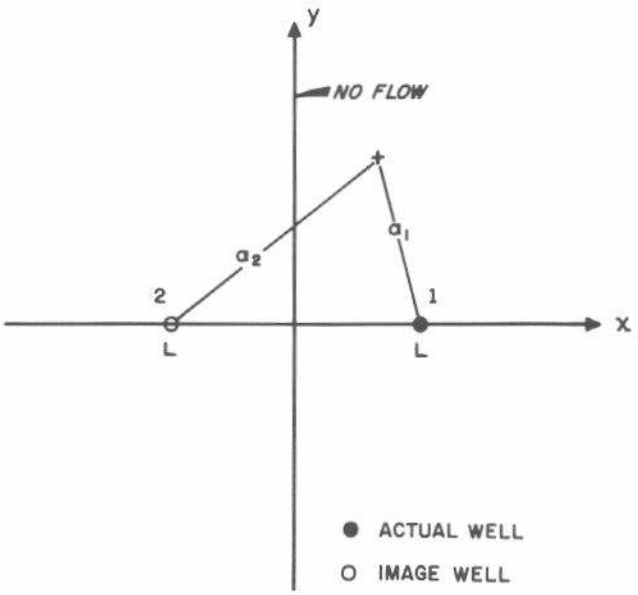

Fig. B.1 Image-well location for a no-flow boundary (sealing fault).

We wish to verify that no fluid flows across the impermeable barrier, the y axis. That is true if $(\partial p/\partial x)_{x=0} = 0$ at all points along the y axis. Differentiating Eq. B.1,

$$\frac{\partial p(t, x, y)}{\partial x} = \frac{-141.2\, qB\mu}{kh}\left[\frac{\partial p_D\,(t_D, a_{D1})}{\partial x} + \frac{\partial p_D\,(t_D, a_{D2})}{\partial x}\right]. \quad \text{(B.4)}$$

We wish to evaluate Eq. B.4 at $x = 0$ for arbitrary values of y. To do this we differentiate Eq. B.3c using Leibnitz's rule:[11]

$$\frac{\partial p_D\,(t_D, a_D)}{\partial x} = -\frac{(x \pm L)}{(x \pm L)^2 + y^2} \exp\left(-\frac{(x \pm L)^2 + y^2}{4r_w{}^2\, t_D}\right). \quad \text{(B.5)}$$

Eq. B.5 is substituted into Eq. B.4:

$$\frac{\partial p(t, x, y)}{\partial x} = \frac{141.2\, qB\mu}{kh}\left\{\left[\frac{x-L}{(x-L)^2 + y^2}\right] \exp\left(-\frac{(x-L)^2 + y^2}{4r_w{}^2\, t_D}\right) + \left[\frac{(x+L)}{(x+L)^2 + y^2}\right] \exp\left(-\frac{(x+L)^2 + y^2}{4r_w{}^2\, t_D}\right)\right\}, \quad \text{(B.6)}$$

which, when evaluated at $x = 0$, becomes

$$\frac{\partial p(t, 0, y)}{\partial x} = \frac{141.2\, qB\mu}{kh}\left(\frac{1}{L^2 + y^2}\right)\{-L + L\} \exp\left(-\frac{L^2 + y^2}{4r_w{}^2\, t_D}\right) = 0. \quad \text{(B.7)}$$

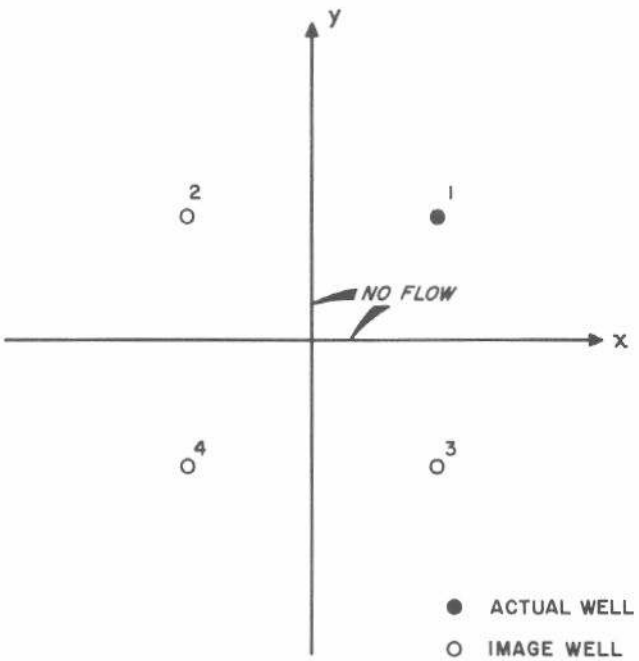

Fig. B.2 Image-well locations for two intersecting no-flow boundaries.

Since $(\partial p/\partial x)_{x=0} = 0$, we can see that an image of the operating well in the boundary creates a no-flow boundary. This is always true for straight-line boundaries no matter how many boundaries or how many wells there are. Some specific examples are given in Section B.4.

If the y axis in Fig. B.1 is to be a constant-pressure boundary, then the image well is an injection well with the same rate as the production well. In this case, superposition gives

$$p(t, x, y) = p_i - \frac{141.2\, qB\mu}{kh}\left[p_D(t_D, a_{D1}) - p_D(t_D, a_{D2})\right]. \quad \text{(B.8)}$$

Since

$$a_{D1} = a_{D2}, \quad \text{(B.9)}$$

at $x = 0$ for all y, then

$$p_D(t_D, a_{D1}) = p_D(t_D, a_{D2}), \quad \text{(B.10)}$$

and the pressure at all points along the boundary (y axis) is

$$p(t, 0, y) = p_i. \quad \text{(B.11)}$$

By using the method of images to form either no-flow or constant-pressure boundaries, one can generate dimensionless pressure solutions for many important situations.

B.4 Use of Method of Images To Generate Multiple Boundary and Closed Systems

Clearly, the method of images extends to systems with more than one no-flow barrier. Fig. B.2 shows a system with two no-flow barriers intersecting at right angles. Well 1 is located near the intersection of the two barriers. Well 2, the image of Well 1 in the y axis, prevents flow across that axis resulting from Well 1. Well 3, the image of Well 1 in the x axis, prevents flow across that axis owing to Well 1. Well 4 prevents flow across the x axis resulting from Well 2 and flow across the y axis resulting from Well 3. The method of images considers barriers to be of infinite length, so flow across any barrier caused by an *image* well must be prevented by other image wells, as demonstrated in Fig. B.2.

When barriers are formed by using images, pressure may be calculated at any point by superposition. Rather than write the equation for pressure change, we may write an equation for the dimensionless pressure at any point in the two-barrier system:

$$p_D(t_D, x_D, y_D) = p_D(t_D, a_{D1}) + p_D(t_D, a_{D2}) + p_D(t_D, a_{D3}) + p_D(t_D, a_{D4}), \quad \text{(B.12)}$$

where a_{D1} means the dimensionless distances from the point where the pressure is being calculated to Well 1, and so on, and x_D and y_D are dimensionless Cartesian coordinates. Their precise definition varies with the application; Refs. 6 and 10 use two practical definitions of those quantities. It is easy to verify that the four wells in Fig. B.2 do create the two intersecting no-flow barriers indicated.

In general, if there are more wells or more boundaries, the dimensionless pressure may be written

$$p_D(t_D, x_D, y_D) = \sum_{i=1}^{n} p_D(t_D, a_{Di}), \quad \ldots\ldots\ldots \text{(B.13)}$$

where the number of wells, n, includes all actual wells and all image wells.

Fig. B.3 shows a single well located between two parallel no-flow barriers and the image wells required to produce those barriers. Well a is the image of the actual well in Boundary A. Well b is the image of the actual well in Boundary B. Each image well would cause flow across the other boundary so additional image wells are required. Well (a)b is the image of Well a in Boundary B and is required to prevent Well a from causing fluid to flow across Boundary B. Well (b)a is required to prevent flow across Boundary A resulting from Well b. Some of the other image wells in Fig. B.3 are marked with a similar nomenclature to indicate the reason for each well. The line of image wells goes to infinity in both directions. The dimensionless pressure function for this system can be written

$$p_D(t_D, x_D, y_D) = \sum_{i=1}^{\infty} p_D(t_D, a_{Di}), \quad \ldots\ldots\ldots \text{(B.14)}$$

where a_{Di} is the dimensionless distance from Well i to x_D, y_D.

To obtain a closed system with a single well in it, add two horizontal no-flow boundaries to Fig. B.3 and image all the wells shown in Fig. B.3 in those two boundaries. Fig. B.4 shows the results — a single well in a closed rectangular drainage area. The image wells extend to infinity in all directions; the dimensionless pressure for the closed rectangular system is given by Eq. B.14. Although an infinite number of image wells is indicated, for calculation purposes it is usually only necessary to include several rows and columns of image wells before their contribution becomes negligible.

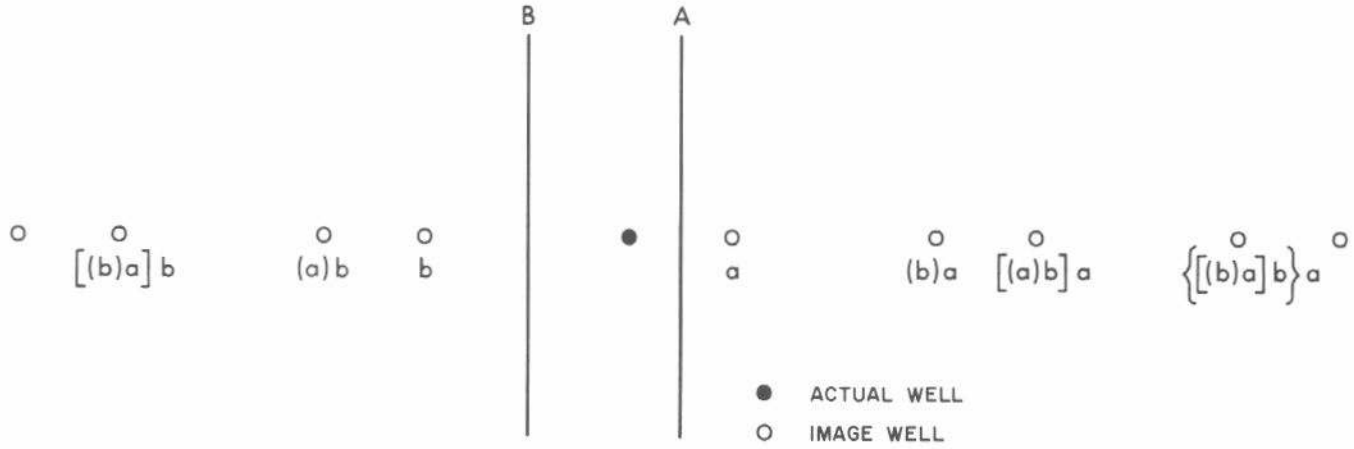

Fig. B.3 Image-well locations for two parallel no-flow boundaries.

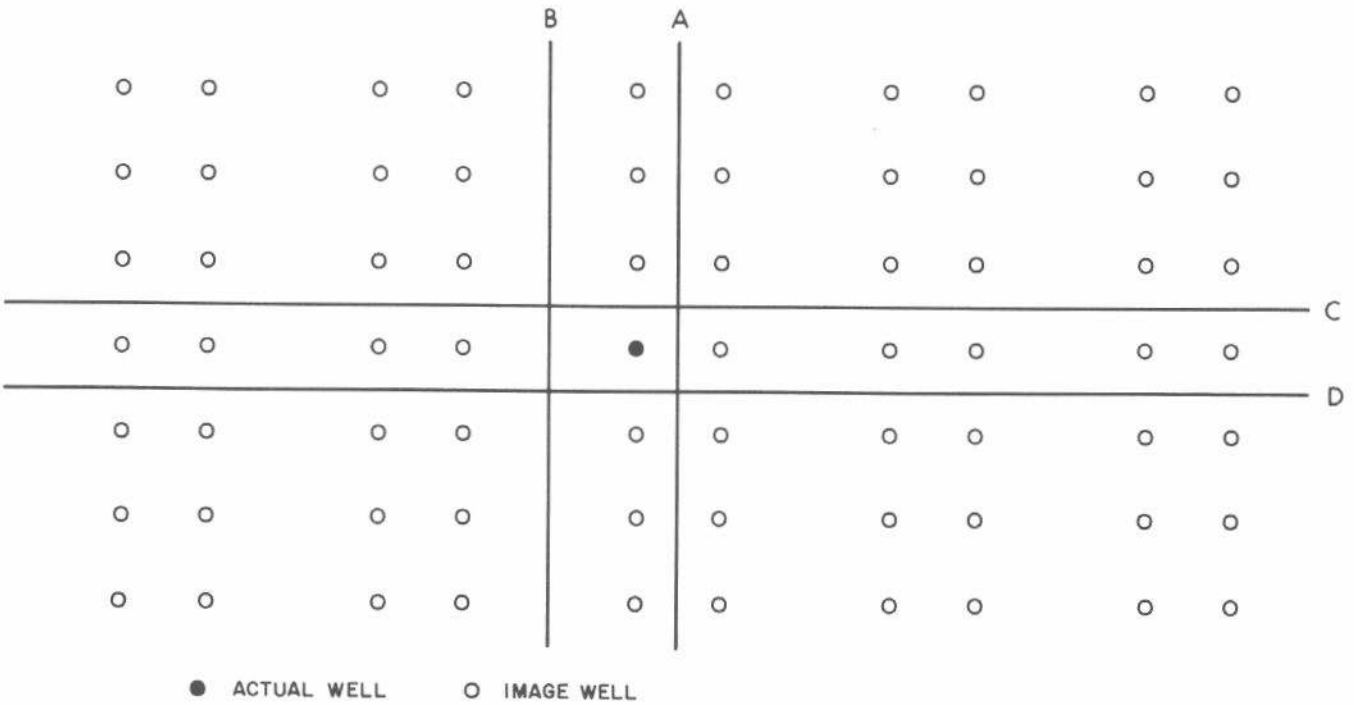

Fig. B.4 Image-well location for one well in a closed rectangle.

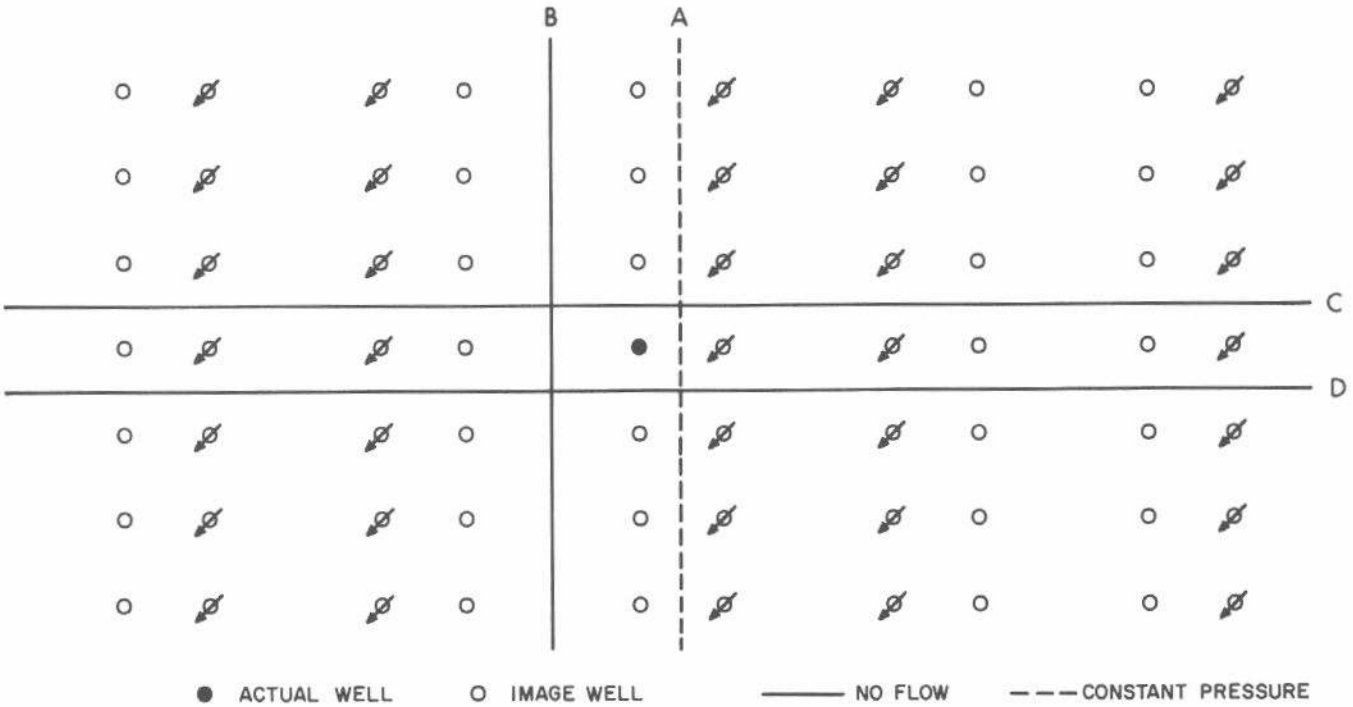

Fig. B.5 Image-well location for one well in a rectangle with three no-flow boundaries and one constant-pressure boundary.

To make one or more of the boundaries constant-pressure rather than no-flow, change some image production wells to injection wells.[6,9] Fig. B.5 shows the image-well array for the system of Fig. B.4 but with Boundary A at constant-pressure. Whether there are one, two, three, or four constant-pressure boundaries in a rectangular system, exactly one-half the image wells will be injectors and one-half will be producers. The location of each type of well depends on which boundaries are constant-pressure and which are no-flow. Ramey, Kumar, and Gulati[9] give several examples of systems with one or more constant-pressure boundaries and present a computer program for calculating p_D in such systems.

B.5 Superposition of Square Drainage Systems

Earlougher *et al.*[6] showed that a useful unit of superposition is a closed-square system with a single well located at its center (Fig. B.6). The dimensionless pressures at the well and at other locations within the square may be added together to obtain dimensionless pressures for systems with different well locations and different shapes. Fig. B.7 illustrates how two square systems are added to obtain a 2:1 rectangular system with the well at the center.[6] The open circles represent the well array for one square system; the closed circles show the well array for the second square system. The resulting well array creates a 2:1 rectangular drainage area with a well in the center as illustrated in Fig. B.7. As pointed out in Ref. 6, it is important to recognize that such superposition changes the area of the drainage system. That affects both the dimensionless time, t_{DA}, and the dimensionless pressure value *at the well* since p_D at a well in a closed drainage area depends on the value of $\sqrt{A}/r_w$. If p_D is desired at a well point for a system of different $\sqrt{A}/r_w$, it is necessary to make the correction

$$p_D\,(\sqrt{A}/r_w) = p_D\left(\left[\sqrt{A}/r_w\right]_{\text{table}}\right) + \ln\left[\frac{(\sqrt{A}/r_w)}{(\sqrt{A}/r_w)_{\text{table}}}\right], \quad \ldots\ldots\ldots \text{(B.15)}$$

where the p_D on the left-hand side of the equation is for the desired value of $\sqrt{A}/r_w$ and on the right-hand side is for the value given in a table or figure (such as Table C.2 or Fig. C.12) with a different value of $\sqrt{A}/r_w$. Additional informa-

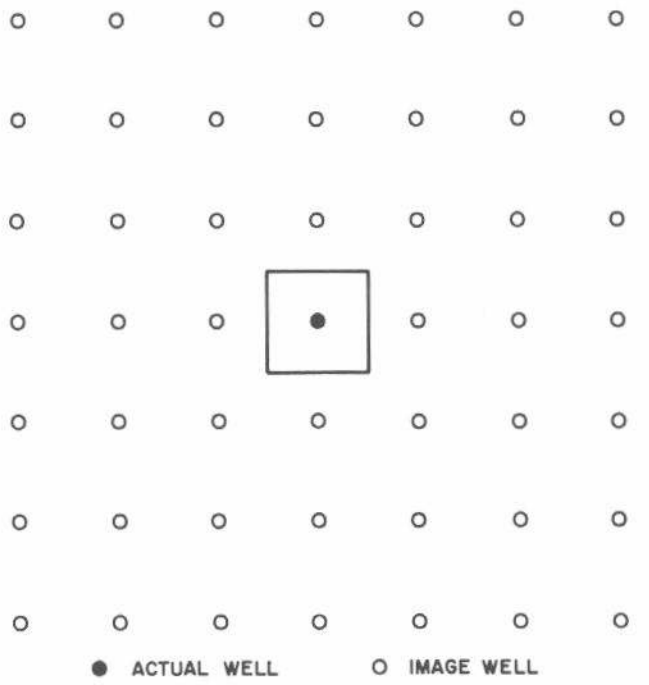

Fig. B.6 Image-well location for a single well in the center of a closed square.

tion and instructions for superposing square systems to obtain systems of other shapes are given in Ref. 6.

B.6 Desuperposition

Gringarten, Ramey, and Raghavan[7] and Chen and Brigham[8] have illustrated the concept of desuperposition for modifying known p_D values to p_D's for somewhat different systems. The approach may be used for any drainage shape and well location, although we illustrate it here only for a well in the center of a closed square. Suppose that we desire to compute p_D at a well in the center of a closed square for $C_D > 0$ and $s \neq 0$. Most p_D data for a closed-square system are for $C_D = 0$, $s = 0$, so those data are not what we need. However, we may use them to get the desired results by using

$$p_D(C_D, s, \square) = p_D(C_D = 0, s = 0, \square) - p_D(C_D = 0, s = 0, \infty) + p_D(C_D, s, \infty), \quad \ldots\ldots\ldots\ldots\ldots\ldots (B.16)$$

as illustrated in Fig. B.8. We start with p_D for the closed-square system with zero skin and zero wellbore storage as indicated in Part a of Fig. B.8. From this dimensionless pressure, the first term on the right-hand side of Eq. B.16, subtract p_D for a single well in an infinite system with zero skin and zero storage, the second term on the right-hand side of Eq. B.16. The result, shown in Part b of Fig. B.8, is an infinite array of wells with the well in the center of the square removed. Finally, add p_D for a single well in an infinite system with the desired wellbore storage coefficient and skin factor, the last term on the right-hand side of Eq. B.16, to obtain Part c of Fig. B.8. The theoretically correct dimensionless pressure is given by the right-hand side of Part d in Fig. B.8, where all the image wells have the desired skin factor and wellbore storage coefficient. However, since skin factors and wellbore storage coefficients have only a small influence[7] at points away from the well, the approximation is a good one.[8]

Gringarten, Ramey, and Raghavan[7] use this approach to estimate dimensionless pressure for closed fractured systems. Chen and Brigham[8] use the approach to generate dimensionless pressures and then pressure buildup curves for a single well with wellbore storage and skin in the center of a closed square. Dimensionless pressure for many other systems can be computed with the same approach.

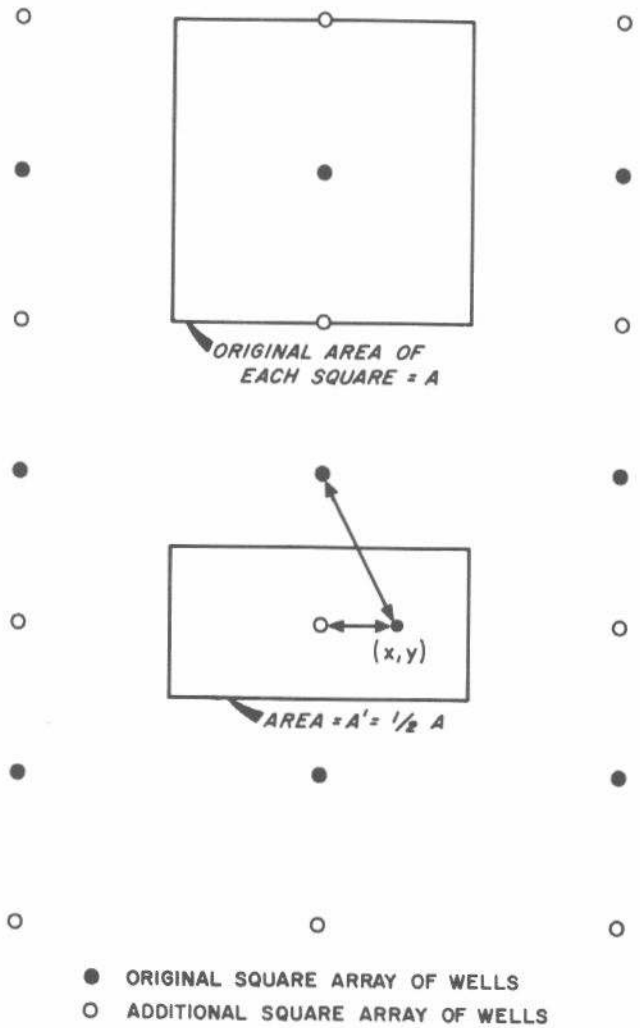

Fig. B.7 Superposition of two square arrays to form a 2:1 rectangle. After Earlougher *et al.*[6]

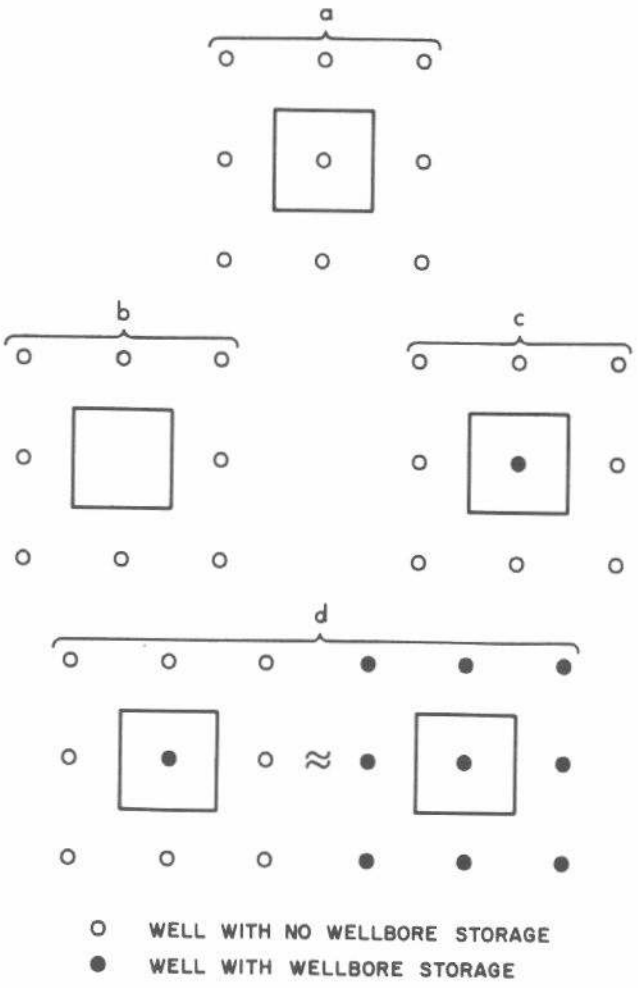

Fig. B.8 Desuperposition to approximate a single well with wellbore storage and skin in the center of a closed square. After Chen and Brigham.[8]

B.7 Superposition for Variable Rate

Fig. B.9 schematically shows a variable-rate history. In the nomenclature of that figure, production (or injection) starts at time 0; the rate remains constant at q_1 until time t_1, then changes to q_2 until time t_2, etc. Note that rate q_j ends at time t_j and that $t_0 = 0$. The last (and current rate) is always q_N. We may calculate the pressure at the well (or at any other point for which we know p_D) at any time during rate q_N by using the principle of superposition as indicated by Eq. 2.31. The pressure at the well is

$$p_{wf}(t) = p_i - \frac{141.2\,B\mu}{kh}\Big\{q_1\left[p_D(t_D) + s\right] + (q_2-q_1)\left[p_D(\left[t-t_1\right]_D) + s\right] + (q_3-q_2)\left[p_D(\left[t-t_2\right]_D) + s\right] + \ldots + (q_N-q_{N-1})\left[p_D(\left[t-t_{N-1}\right]_D) + s\right]\Big\}. \quad \ldots \text{(B.17)}$$

This may be rearranged to

$$p_{wf}(t) = p_i - \frac{141.2\,B\mu}{kh}\Big\{q_1\left[p_D(t_D) - p_D(\left[t-t_1\right]_D)\right] + q_2\left[p_D(\left[t-t_1\right]_D) - p_D(\left[t-t_2\right]_D)\right] + \ldots + q_{N-1}\left[p_D(\left[t-t_{N-2}\right]_D) - p_D(\left[t-t_{N-1}\right]_D)\right] + q_N\left[p_D(\left[t-t_{N-1}\right]_D) + s\right]\Big\}. \quad \ldots\ldots\ldots \text{(B.18)}$$

If the system is infinite-acting and if the logarithmic approximation of the exponential integral, Eq. 2.5b, applies, Eq. B.18 may be written

$$p_{wf}(t) = p_i - \frac{70.60\,B\mu}{kh}\Big\{q_1 \ln\left(\frac{t}{t-t_1}\right) + q_2 \ln\left(\frac{t-t_1}{t-t_2}\right) + \ldots + q_{N-1} \ln\left(\frac{t-t_{N-2}}{t-t_{N-1}}\right) + q_N\left[\ln(t-t_{N-1}) + \ln\left(\frac{k}{\phi\mu c_t r_w^{\,2}}\right) - 7.4316 + 2s\right]\Big\}, \quad \ldots \text{(B.19)}$$

or

$$p_{wf}(t) = p_i - \frac{162.6\,B\mu}{kh}\Big\{\sum_{j=1}^{N-1} q_j \log\left(\frac{t-t_{j-1}}{t-t_j}\right) + q_N\left[\log(t-t_{N-1}) + \log\left(\frac{k}{\phi\mu c_t r_w^{\,2}}\right) - 3.2275 + 0.86859\,s\right]\Big\}. \quad \ldots\ldots\ldots\ldots \text{(B.20)}$$

Eqs. B.17 through B.20 are convenient for estimating pressures resulting from multiple-rate histories. However, the form

$$\frac{p_i - p_{wf}(t)}{q_N} = \frac{162.6\,B\mu}{kh}\Big\{\sum_{j=1}^{N}\left[\left(\frac{q_j-q_{j-1}}{q_N}\right) \times \log(t-t_{j-1})\right] + \log\left(\frac{k}{\phi\mu c_t r_w^{\,2}}\right) - 3.2275 + 0.86859\,s\Big\}, \quad \ldots\ldots\ldots \text{(B.21)}$$

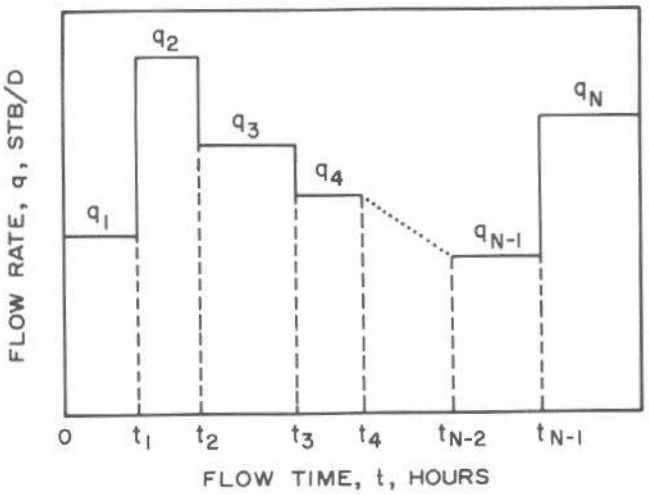

Fig. B.9 Schematic representation of a variable production-rate schedule.

which results from combining Eqs. B.17 and 2.5b, is more convenient for analyzing multiple-rate test data, as indicated in Section 4.2.

References

1. Matthews, C. S. and Russell, D. G.: *Pressure Buildup and Flow Tests in Wells*, Monograph Series, Society of Petroleum Engineers of AIME, Dallas (1967) **1.**
2. van Everdingen, A. F. and Hurst, W.: "The Application of the Laplace Transformation to Flow Problems in Reservoirs," *Trans.*, AIME (1949) **186,** 304-324.
3. Horner, D. R.: "Pressure Build-Up in Wells," *Proc.*, Third World Pet. Cong., The Hague (1951) Sec. II, 503-523. Also *Reprint Series, No. 9 — Pressure Analysis Methods*, Society of Petroleum Engineers of AIME, Dallas (1967) 25-43.
4. Matthews, C. S., Brons, F., and Hazebroek, P.: "A Method for Determination of Average Pressure in a Bounded Reservoir," *Trans.*, AIME (1954) **201,** 182-191. Also *Reprint Series, No. 9 — Pressure Analysis Methods*, Society of Petroleum Engineers of AIME, Dallas (1967) 51-60.
5. Collins, Royal Eugene: *Flow of Fluids Through Porous Materials*, Reinhold Publishing Corp., New York (1961) 109-113, 116-118.
6. Earlougher, Robert C., Jr., Ramey, H. J., Jr., Miller, F. G., and Mueller, T. D.: "Pressure Distributions in Rectangular Reservoirs," *J. Pet. Tech.* (Feb. 1968) 199-208; *Trans.*, AIME, **243.**
7. Gringarten, Alain C., Ramey, Henry J., Jr., and Raghavan, R.: "Unsteady-State Pressure Distributions Created by a Well With a Single Infinite-Conductivity Vertical Fracture," *Soc. Pet. Eng. J.* (Aug. 1974) 347-360; *Trans.*, AIME, **257.**
8. Chen, Hsiu-Kuo and Brigham, W. E.: "Pressure Buildup for a Well With Storage and Skin in a Closed Square," paper SPE 4890 presented at the SPE-AIME 44th Annual California Regional Meeting, San Francisco, April 4-5, 1974.
9. Ramey, Henry J., Jr., Kumar, Anil, and Gulati, Mohinder S.: *Gas Well Test Analysis Under Water-Drive Conditions*, AGA, Arlington, Va. (1973).
10. Earlougher, R. C., Jr., and Ramey, H. J., Jr.: "Interference Analysis in Bounded Systems," *J. Cdn. Pet. Tech.* (Oct.-Dec. 1973) 35-45.
11. Kaplan, Wilfred: *Advanced Calculus*, Addison Wesley Publishing Co., Inc., Reading, Mass. (1952) 220.

Appendix C

Dimensionless Pressure Solutions

C.1 Introduction

This appendix presents correlations of dimensionless pressure with dimensionless time for single-well systems producing at constant rate. Some data from the literature have been modified to be consistent with the nomenclature used in this monograph. We retain the definition of dimensionless pressure corresponding to

$$p_i - p = \Delta p = \frac{141.2\,qB\mu}{kh}\,p_D(t_D, \ldots) \quad \ldots\ldots \text{(C.1)}$$

Dimensionless time is usually based on wellbore radius,

$$t_D = \frac{0.0002637\,kt}{\phi\mu c_t r_w^2}, \quad \ldots\ldots\ldots\ldots\ldots \text{(C.2a)}$$

or based on drainage area,

$$t_{DA} = \frac{0.0002637\,kt}{\phi\mu c_t A} = t_D\left(\frac{r_w^2}{A}\right). \quad \ldots\ldots \text{(C.2b)}$$

We clearly indicate when it is convenient to base the dimensionless time on some other characteristic dimension.

C.2 Infinite Systems

No Wellbore Storage, No Skin

After wellbore storage effects are no longer important, the dimensionless pressure for infinite and infinite-acting systems is given by[1-4]

$$p_D = -\frac{1}{2}\,\mathrm{Ei}\left(-\frac{r_D^2}{4t_D}\right), \quad \ldots\ldots\ldots\ldots\ldots \text{(C.3)}$$

when ($r_D \geq 20$ and $t_D/r_D^2 \geq 0.5$) or when $t_D/r_D^2 \geq 25$. Dimensionless pressure values for smaller t_D and r_D are given in Fig. C.1 for a range of r_D and t_D; tabulated values for $r_D = 1$ are given by van Everdingen and Hurst.[5] The lowermost curve in Fig. C.1 ($r_D > 20$), which is the exponential-integral solution (Eq. C.3), is shown on an expanded scale in Fig. C.2.*

A simplification of Eq. C.3 and Figs. C.1 and C.2 applies when $t_D/r_D^2 > 100$ (or with less than 1-percent error when $t_D/r_D^2 > 10$):

$$p_D = \frac{1}{2}\left[\ln(t_D/r_D^2) + 0.80907\right]. \quad \ldots\ldots\ldots \text{(C.4)}$$

*See footnote on Page 24.

These dimensionless pressure solutions apply for a single undamaged well in an infinite-acting system with no wellbore storage. Damage or improvement may be included as indicated in Eq. 2.2.

Single Vertical Fracture, No Wellbore Storage

Figs. C.3* and C.4 give dimensionless pressure data for a vertically fractured well in an infinite-acting system. A single fracture of half-length x_f intersects the well. Two situations are shown:

1. The *uniform-flux fracture* is a first approximation to the behavior of a vertically fractured well.[6,7] Fluid enters the fracture at a uniform flow rate per unit area of fracture face so that there is a pressure drop in the fracture. The dimensionless pressure at the well for the uniform-flux fracture case is computed from[6,7]

$$p_D = \sqrt{\pi t_{Dxf}}\,\mathrm{erf}\left(\frac{1}{2\sqrt{t_{Dxf}}}\right) - \frac{1}{2}\,\mathrm{Ei}\left(\frac{-1}{4t_{Dxf}}\right), \quad \ldots \text{(C.5)}$$

where dimensionless time based on the half-fracture length is defined as

$$t_{Dxf} = t_D(r_w/x_f)^2 \quad \ldots\ldots\ldots\ldots\ldots\ldots\ldots \text{(C.6)}$$

When $t_{Dxf} > 10$, Eq. C.5 becomes[6,7]

$$p_D = \frac{1}{2}\left[\ln t_{Dxf} + 2.80907\right], \quad \ldots\ldots\ldots\ldots \text{(C.7)}$$

with less than 1-percent error. For $t_{Dxf} < 0.1$, Eq. C.5 becomes[6,7]

$$p_D = \sqrt{\pi t_{Dxf}}, \quad \ldots\ldots\ldots\ldots\ldots\ldots\ldots \text{(C.8)}$$

indicating that at short times flow into the fracture is linear.

2. The *infinite-conductivity fracture* has infinite permeability and, therefore, uniform pressure throughout. The dimensionless well pressure for that case is given in Figs. C.3 and C.4, and may be computed from[6,7]

$$p_D = \frac{1}{2}\sqrt{\pi t_{Dxf}}\left[\mathrm{erf}\left(\frac{0.134}{\sqrt{t_{Dxf}}}\right) + \mathrm{erf}\left(\frac{0.866}{\sqrt{t_{Dxf}}}\right)\right] - 0.067\,\mathrm{Ei}\left(-\frac{0.018}{t_{Dxf}}\right) - 0.433\,\mathrm{Ei}\left(-\frac{0.750}{t_{Dxf}}\right). \quad \ldots\ldots\ldots\ldots\ldots\ldots\ldots \text{(C.9)}$$

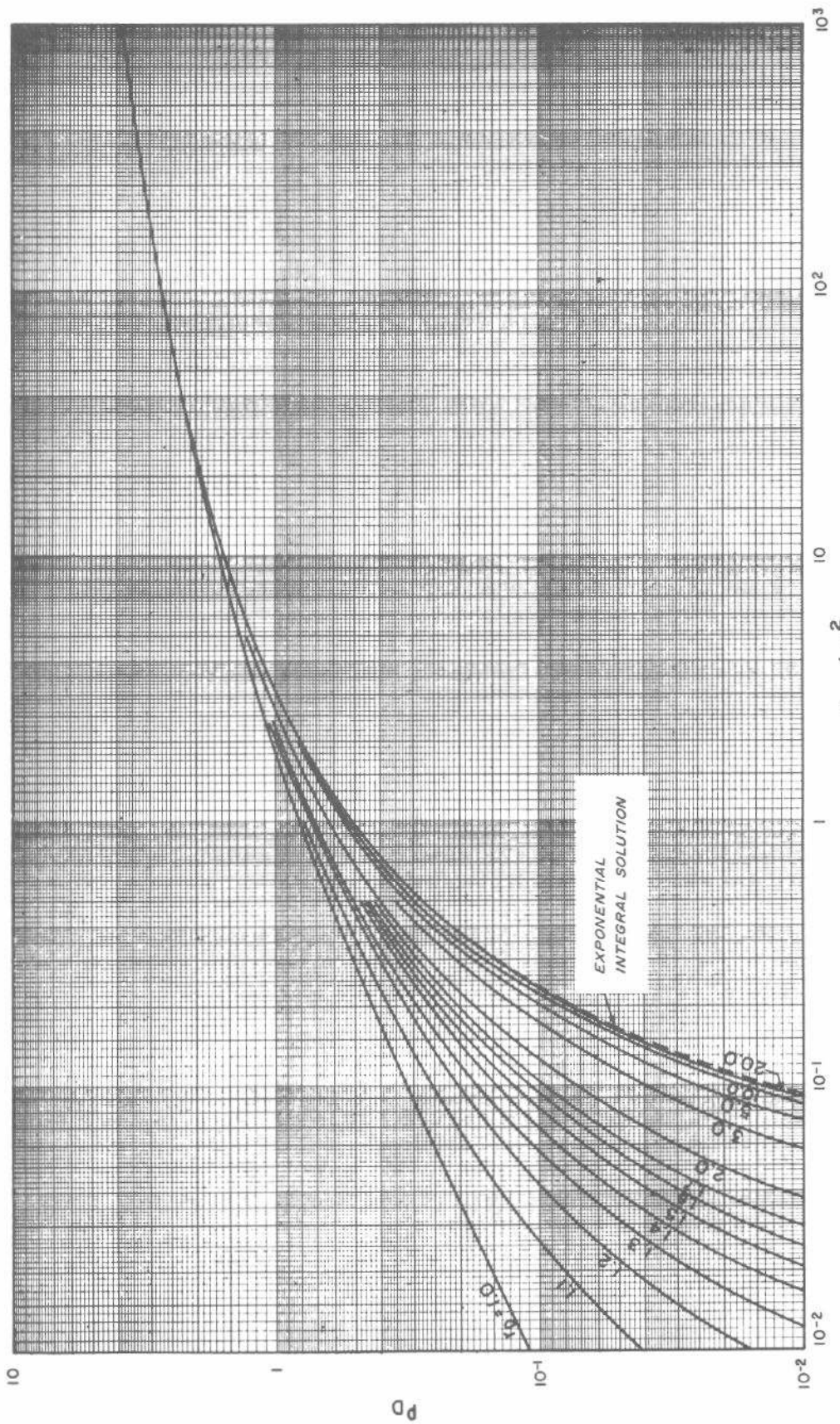

Fig. C.1 Dimensionless pressure for single well in an infinite system, small r_D, short time, no wellbore storage, no skin. After Mueller and Witherspoon.[4]

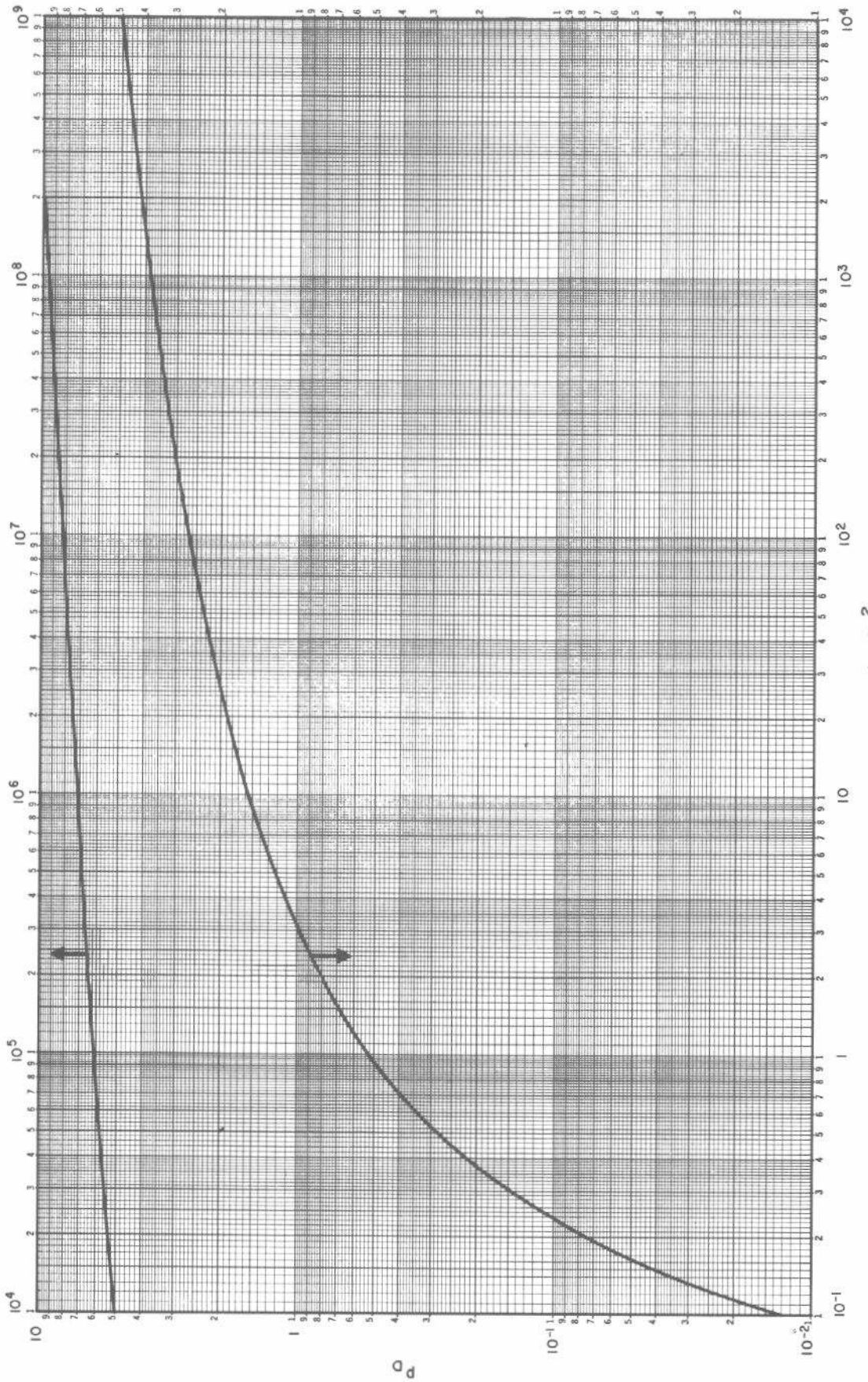

Fig. C.2 Dimensionless pressure for a single well in an infinite system, no wellbore storage, no skin. Exponential-integral solution.

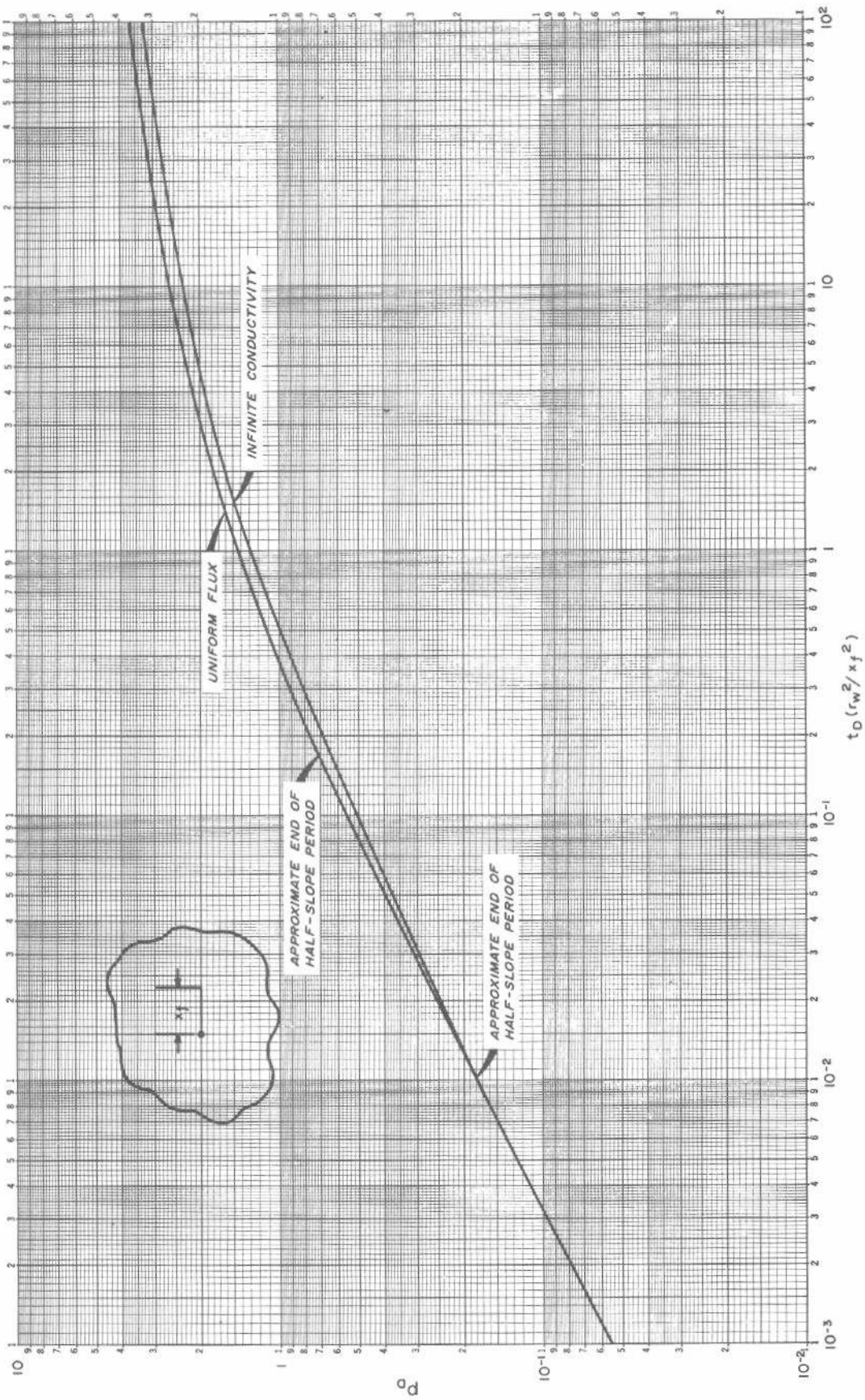

Fig. C.3 Dimensionless pressure for single, vertically fractured well in an infinite system, no wellbore storage. Log-log plot.
Data of Gringarten, Ramey, and Raghavan.[6,7]

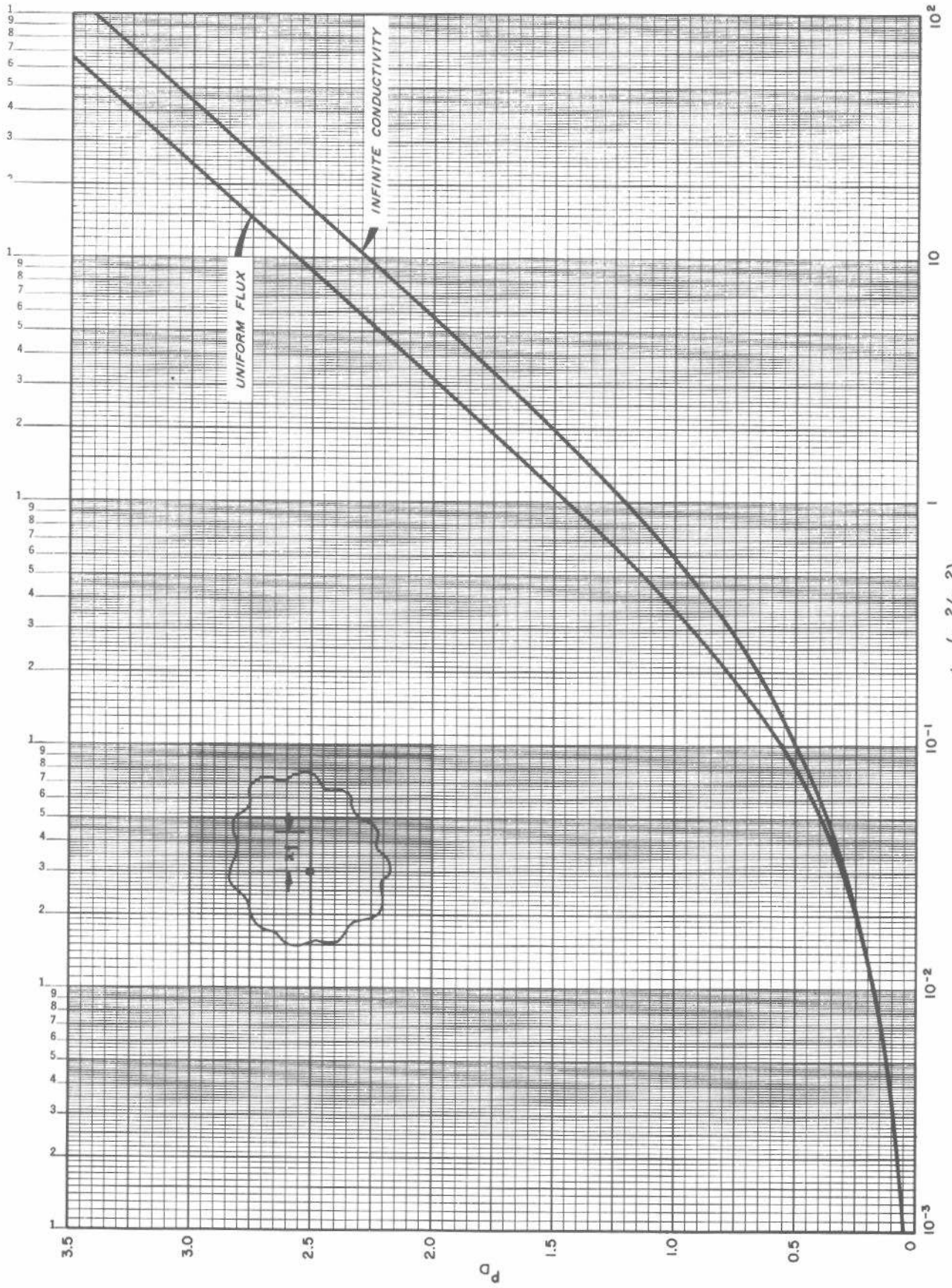

Fig. C.4 Dimensionless pressure for single, vertically fractured well in an infinite system, no wellbore storage. Semilog plot.
Data of Gringarten, Ramey, and Raghavan.[6,7]

When $t_{Dxf} > 10$, Eq. C.9 becomes[6,7]

$$p_D = \frac{1}{2}\left[\ln t_{Dxf} + 2.2000\right], \quad \text{(C.10)}$$

with less than 1-percent error. When t_{Dxf} is less than 0.01, Eq. C.8 applies.

An important feature of Fig. C.3 is the early-time slope of one-half cycle in pressure per cycle in time. Such a half-slope straight line on the log-log plot is often diagnostic of a vertically fractured well.

Gringarten, Ramey, and Raghavan[6,7] tabulate p_D values for the two types of vertical fractures.

Single Horizontal Fracture, No Wellbore Storage

Fig. C.5* shows p_D data at the well for an infinite system with a single horizontal fracture located at the formation midpoint. The dimensionless time used,

$$t_{Drf} = \frac{0.0002637\,kt}{\phi\mu c_t r_f^2} = t_D\left(\frac{r_w^2}{r_f^2}\right), \quad \text{(C.11)}$$

is based on the horizontal fracture radius, r_f. In Fig. C.5, dimensionless pressure is normalized by the parameter on the curves,

$$h_D = \frac{h}{r_f}\sqrt{\frac{k_r}{k_z}}, \quad \text{(C.12)}$$

where k_r and k_z are radial and vertical permeabilities, respectively. At short times and for large h_D, the curves in Fig. C.5 have a half-slope portion. It is apparent, however, that many horizontally fractured systems would not exhibit a half-slope straight line on the log-log plot. At low values of h_D, the curves in Fig. C.5 have a unit slope, like the unit slope caused by wellbore storage effects. There is *no wellbore storage effect* included in Fig. C.5, so the unit slope there is a result of the *fracture*, not the wellbore. Gringarten[8] and Ramey[9] tabulate p_D values for the horizontal-fracture case.

Wellbore Storage and Thin Skin Included

Fig. C.6* shows dimensionless pressure data for a single well in an infinite system with wellbore storage and skin effect included.[10] The dimensionless wellbore storage coefficient is

$$C_D = \frac{5.6146\,C}{2\pi\phi c_t h r_w^2}. \quad \text{(C.13)}$$

When $C_D > 0$, Fig. C.6 shows that the log-log plot has an early-time unit slope. At later times, the curves approach those for zero wellbore storage. Tabulated dimensionless pressure data are given by Agarwal, Al-Hussainy, and Ramey.[10] Although t_D in Fig. C.6 is based on r_w, generation of the negative skin solutions involved use of an apparent larger wellbore radius as defined by Eq. 2.11.

Wellbore Storage and Finite Skin Included

Fig. C.7* gives dimensionless pressure data for a single well in an infinite reservoir with wellbore storage and a finite skin effect.[11] Fig. 2.6 schematically illustrates the finite skin. The skin factor is calculated from

$$s = \left(\frac{k}{k_s} - 1\right)\ln(r_{sD}), \quad \text{(C.14)}$$

where

$$r_{sD} = r_s/r_w. \quad \text{(C.15)}$$

Wattenbarger and Ramey[11] provide tables of p_D vs t_D for the conditions of Fig. C.7.

Other Useful Type Curves

Fig. C.8* shows another relation between pressure and time for a single well with wellbore storage and skin effect in an infinite system.[12] The graph can be changed to a dimensionless pressure-dimensionless time basis by using equations given in Ref. 12. This type curve is particularly useful for curve matching and is not recommended for calculating pressure response. Its use is illustrated in Section 3.3.

Fig. C.9* is a type curve presented by McKinley[13] for a single well with wellbore storage, but no skin factor, in an infinite system. Fig. C.9 assumes

$$\frac{k}{\phi\mu c_t r_w^2} = 9.728 \times 10^6. \quad \text{(C.16)}$$

Although the figure is plotted on the basis of actual variables, it may be reduced to a dimensionless graph by using the definitions of C_D, t_D, and p_D with Eq. C.16. The main utility of Fig. C.9 is for type-curve matching of test data, not for calculating pressure response.

C.3 Closed Systems

All closed reservoir systems (that is, those with no-flow outer boundaries) have the transient behavior illustrated in Fig. 2.1. Within 1 percent,

$$p_D = \frac{1}{2}\left[\ln(t_{DA}) + \ln\left(\frac{A}{r_w^2}\right) + 0.80907\right], \quad \text{(C.17)}$$

if $0.000025 < t_{DA}$ and t_{DA} is less than the value in the "Use Infinite System Solution With Less Than 1% Error for t_{DA} <" column of Table C.1. At long times the system reaches pseudosteady state and[14]

$$p_D = 2\pi t_{DA} + \frac{1}{2}\ln\left(\frac{A}{r_w^2}\right) + \frac{1}{2}\ln\left(\frac{2.2458}{C_A}\right). \quad \text{(C.18)}$$

Eq. C.18 applies when t_{DA} exceeds the value in the "Less Than 1% Error for t_{DA} >" column of Table C.1. Values of C_A and of the last term on the right-hand side of Eq. C.18 are given in Table C.1 for many closed drainage shapes. Values of C_A are also given in Refs. 15 through 18 and in Table C.2.

Dimensionless pressure data *at the well* in closed reservoir systems are always given for a specific $\sqrt{A}/r_w$. If p_D is desired for a system of similar shape and geometry but with a different value of this parameter, it may be computed from[17]

$$(p_D)_{\text{desired}} = (p_D)_{\text{table}} + \ln\left[(\sqrt{A}/r_w)_{\text{desired}}/(\sqrt{A}/r_w)_{\text{table}}\right], \quad \text{(C.19)}$$

*See footnote on Page 24.

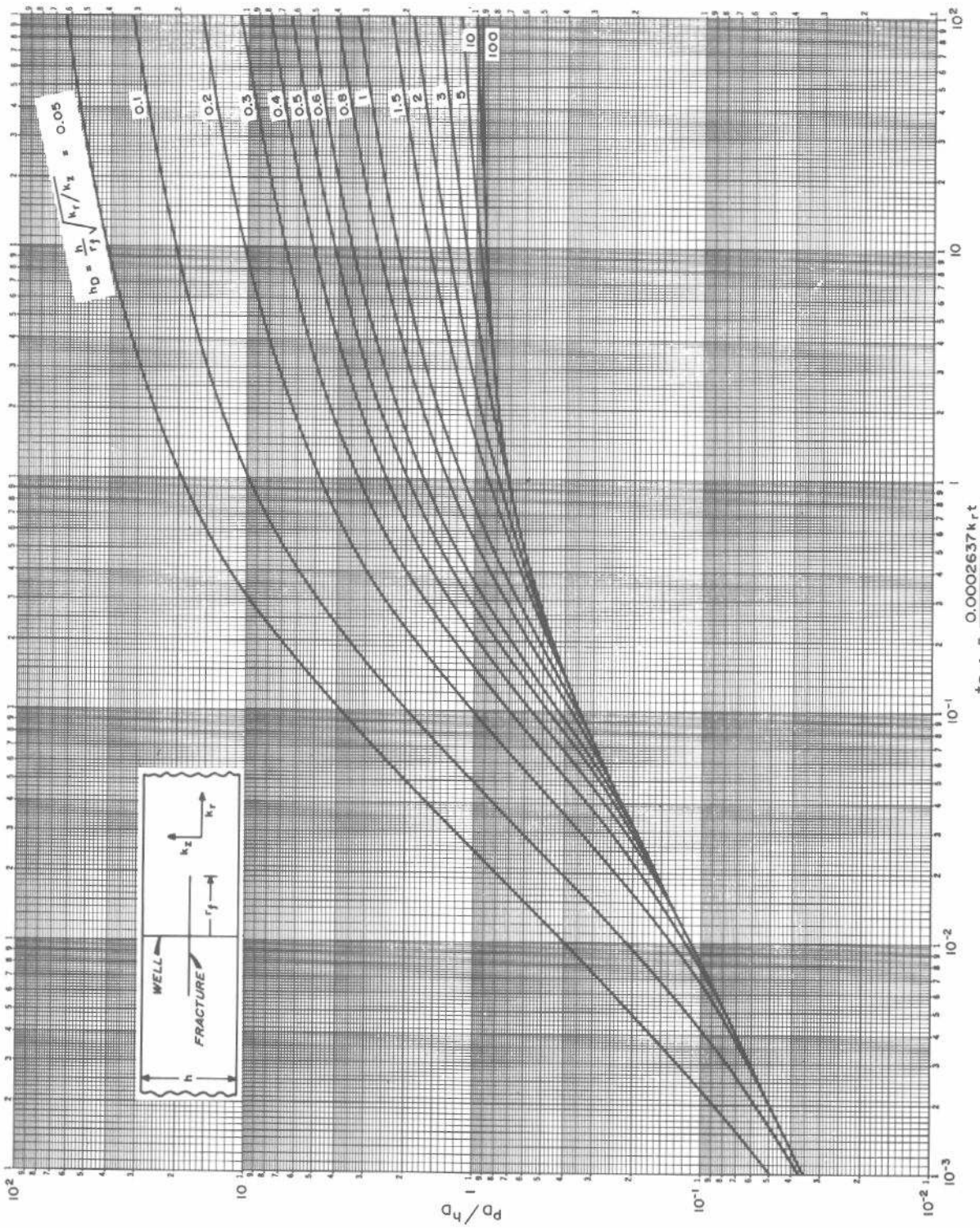

Fig. C.5 Dimensionless pressure for a single, horizontally fractured (uniform-flux) well in an infinite system, no wellbore storage. Fracture located in the center of the interval. After Gringarten, Ramey, and Raghavan.[6]

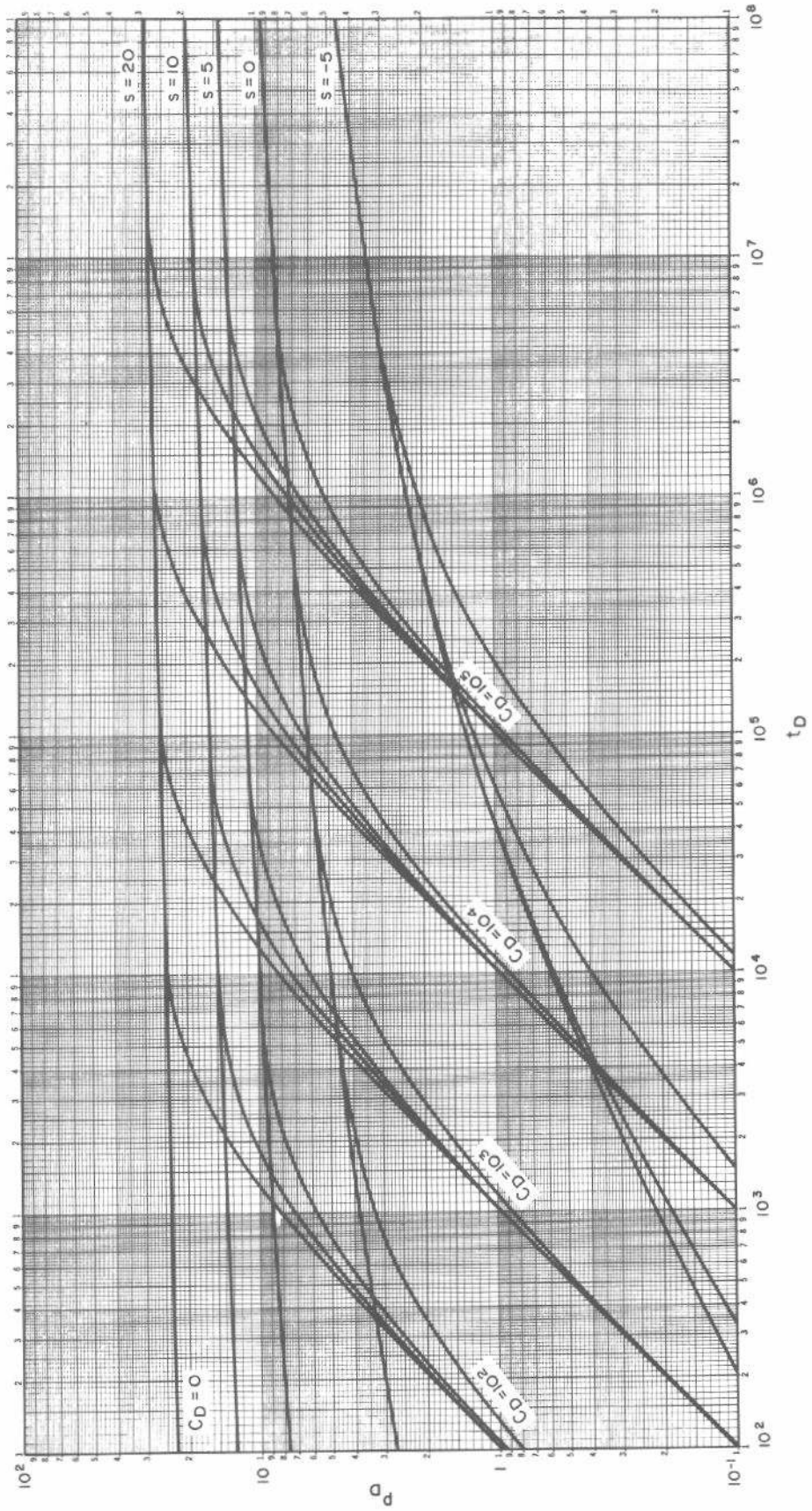

Fig. C.6 Dimensionless pressure for a single well in an infinite system, wellbore storage and skin included. After Agarwal, Al-Hussainy, and Ramey.[10] Graph courtesy H. J. Ramey, Jr.

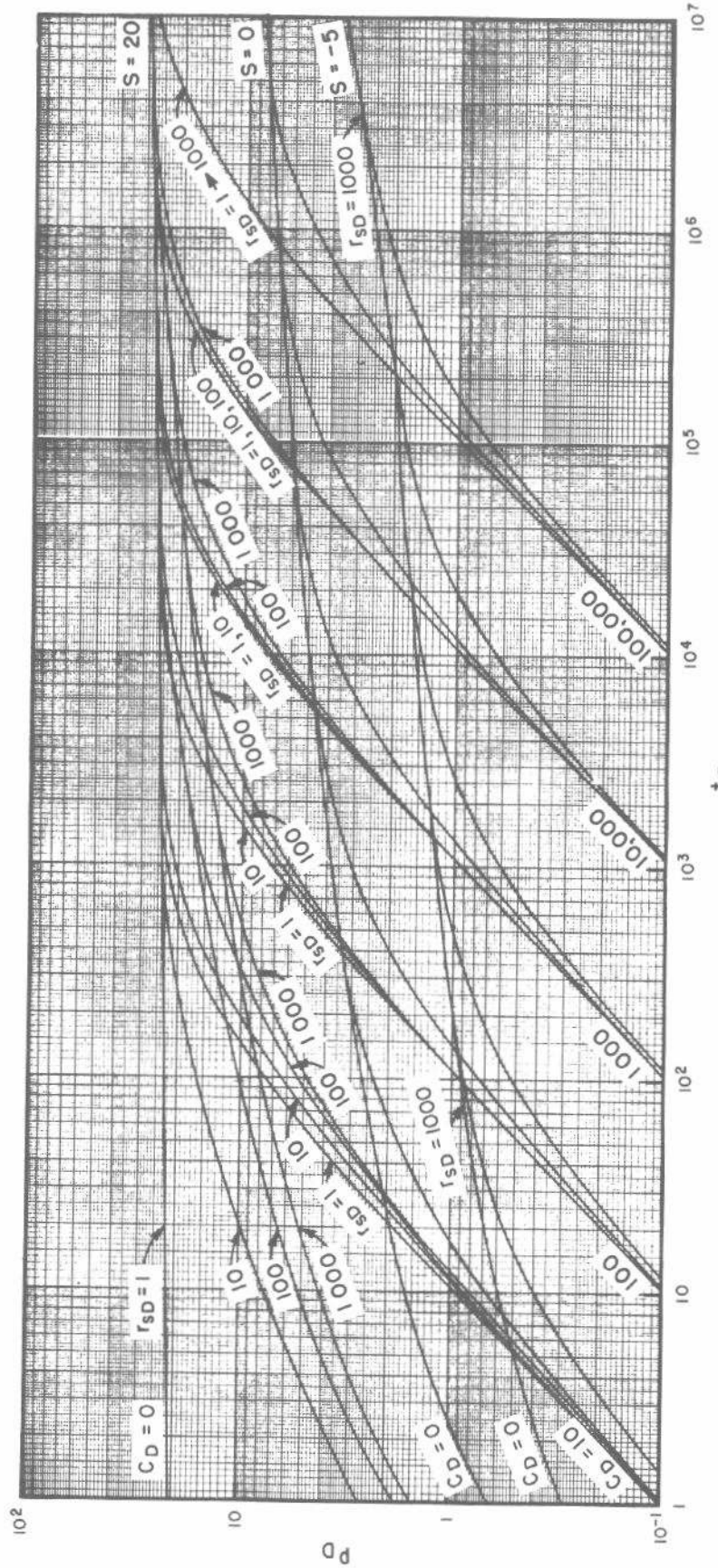

Fig. C.7 Dimensionless pressure for a single well in an infinite reservoir including wellbore storage and a finite skin (composite reservoir). After Wattenbarger and Ramey.[11] Graph courtesy H. J. Ramey, Jr.

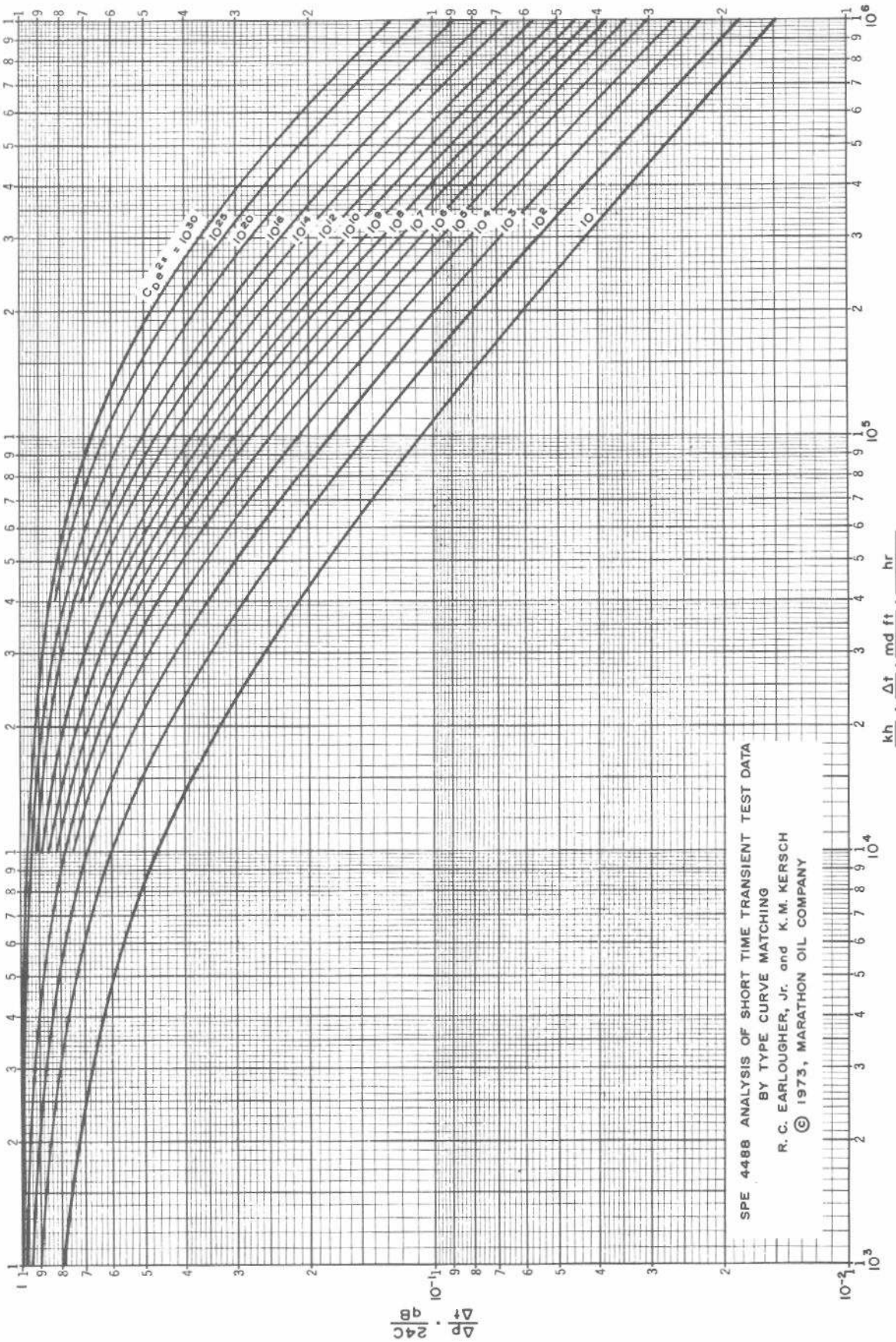

Fig. C.8 Type curve for a single well in an infinite system, wellbore storage and skin effects included. After Earlougher and Kersch.[12]
Reprinted by permission of Marathon Oil Co.

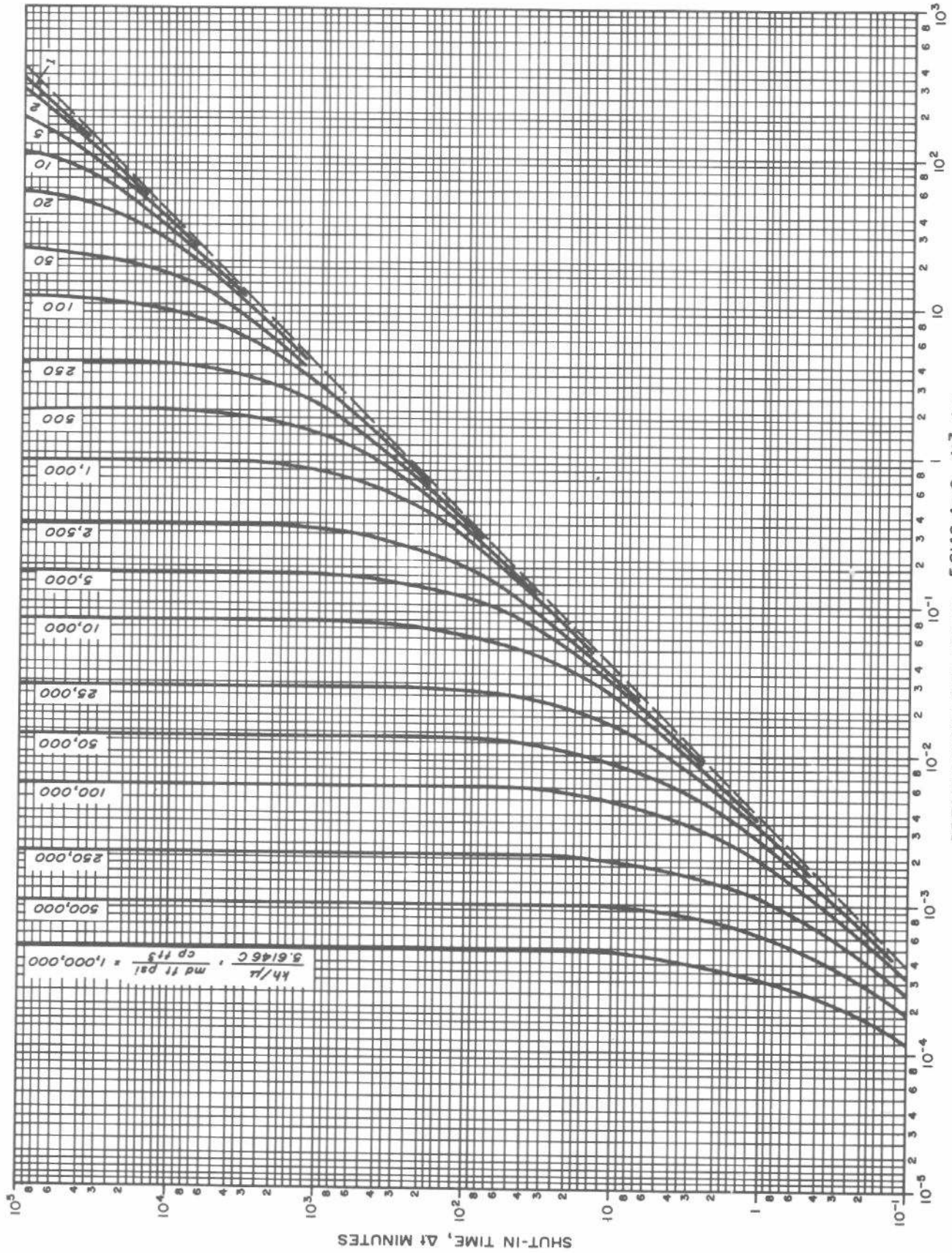

Fig. C.9 Type curve for a single well in an infinite system, wellbore storage included, no skin. After McKinley.[13]

TABLE C.1—SHAPE FACTORS FOR VARIOUS CLOSED SINGLE-WELL DRAINAGE AREAS.

IN BOUNDED RESERVOIRS	C_A	$\ln C_A$	$1/2 \ln\left(\frac{2.2458}{C_A}\right)$	EXACT FOR $t_{DA} >$	LESS THAN 1% ERROR FOR $t_{DA} >$	USE INFINITE SYSTEM SOLUTION WITH LESS THAN 1% ERROR FOR $t_{DA} <$
	31.62	3.4538	-1.3224	0.1	0.06	0.10
	31.6	3.4532	-1.3220	0.1	0.06	0.10
	27.6	3.3178	-1.2544	0.2	0.07	0.09
	27.1	3.2995	-1.2452	0.2	0.07	0.09
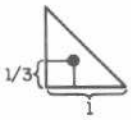	21.9	3.0865	-1.1387	0.4	0.12	0.08
	0.098	-2.3227	+1.5659	0.9	0.60	0.015
	30.8828	3.4302	-1.3106	0.1	0.05	0.09
	12.9851	2.5638	-0.8774	0.7	0.25	0.03
	4.5132	1.5070	-0.3490	0.6	0.30	0.025
	3.3351	1.2045	-0.1977	0.7	0.25	0.01
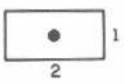	21.8369	3.0836	-1.1373	0.3	0.15	0.025
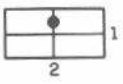	10.8374	2.3830	-0.7870	0.4	0.15	0.025
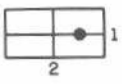	4.5141	1.5072	-0.3491	1.5	0.50	0.06
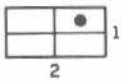	2.0769	0.7309	+0.0391	1.7	0.50	0.02
	3.1573	1.1497	-0.1703	0.4	0.15	0.005

TABLE C.1—CONT'D.

	C_A	$\ln C_A$	$1/2 \ln\left(\frac{2.2458}{C_A}\right)$	EXACT FOR $t_{DA}>$	LESS THAN 1% ERROR FOR $t_{DA}>$	USE INFINITE SYSTEM SOLUTION WITH LESS THAN 1% ERROR FOR $t_{DA}<$
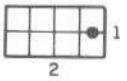	0.5813	-0.5425	+0.6758	2.0	0.60	0.02
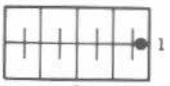	0.1109	-2.1991	+1.5041	3.0	0.60	0.005
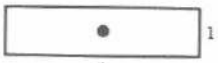	5.3790	1.6825	-0.4367	0.8	0.30	0.01
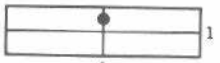	2.6896	0.9894	-0.0902	0.8	0.30	0.01
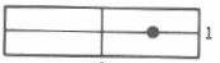	0.2318	-1.4619	+1.1355	4.0	2.00	0.03
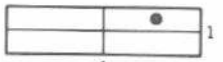	0.1155	-2.1585	+1.4838	4.0	2.00	0.01
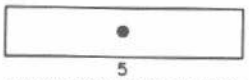	2.3606	0.8589	-0.0249	1.0	0.40	0.025
IN VERTICALLY-FRACTURED RESERVOIRS	USE $(x_e/x_f)^2$ IN PLACE OF A/r_w^2 FOR FRACTURED SYSTEMS					
 =x_f/x_e	2.6541	0.9761	-0.0835	0.175	0.08	CANNOT USE
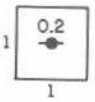	2.0348	0.7104	+0.0493	0.175	0.09	CANNOT USE
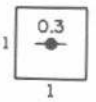	1.9986	0.6924	+0.0583	0.175	0.09	CANNOT USE
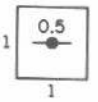	1.6620	0.5080	+0.1505	0.175	0.09	CANNOT USE
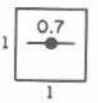	1.3127	0.2721	+0.2685	0.175	0.09	CANNOT USE
	0.7887	-0.2374	+0.5232	0.175	0.09	CANNOT USE
IN WATER-DRIVE RESERVOIRS						
	19.1	2.95	-1.07	—	—	—
IN RESERVOIRS OF UNKNOWN PRODUCTION CHARACTER						
	25.0	3.22	-1.20	—	—	—

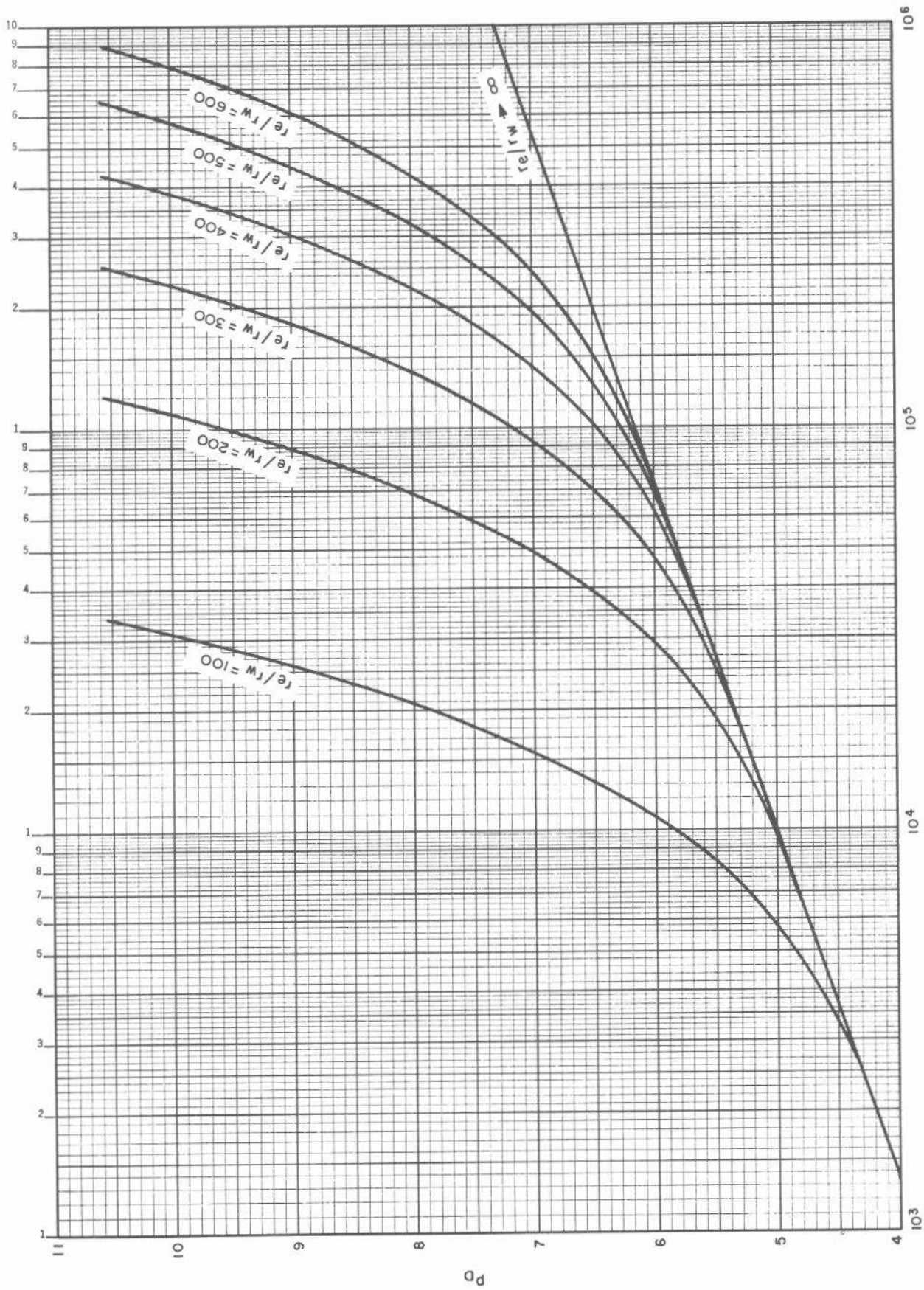

Fig. C.10A Dimensionless pressure for a well in the center of a closed circular reservoir, no wellbore storage, no skin. Calculated from Eq. C.20.

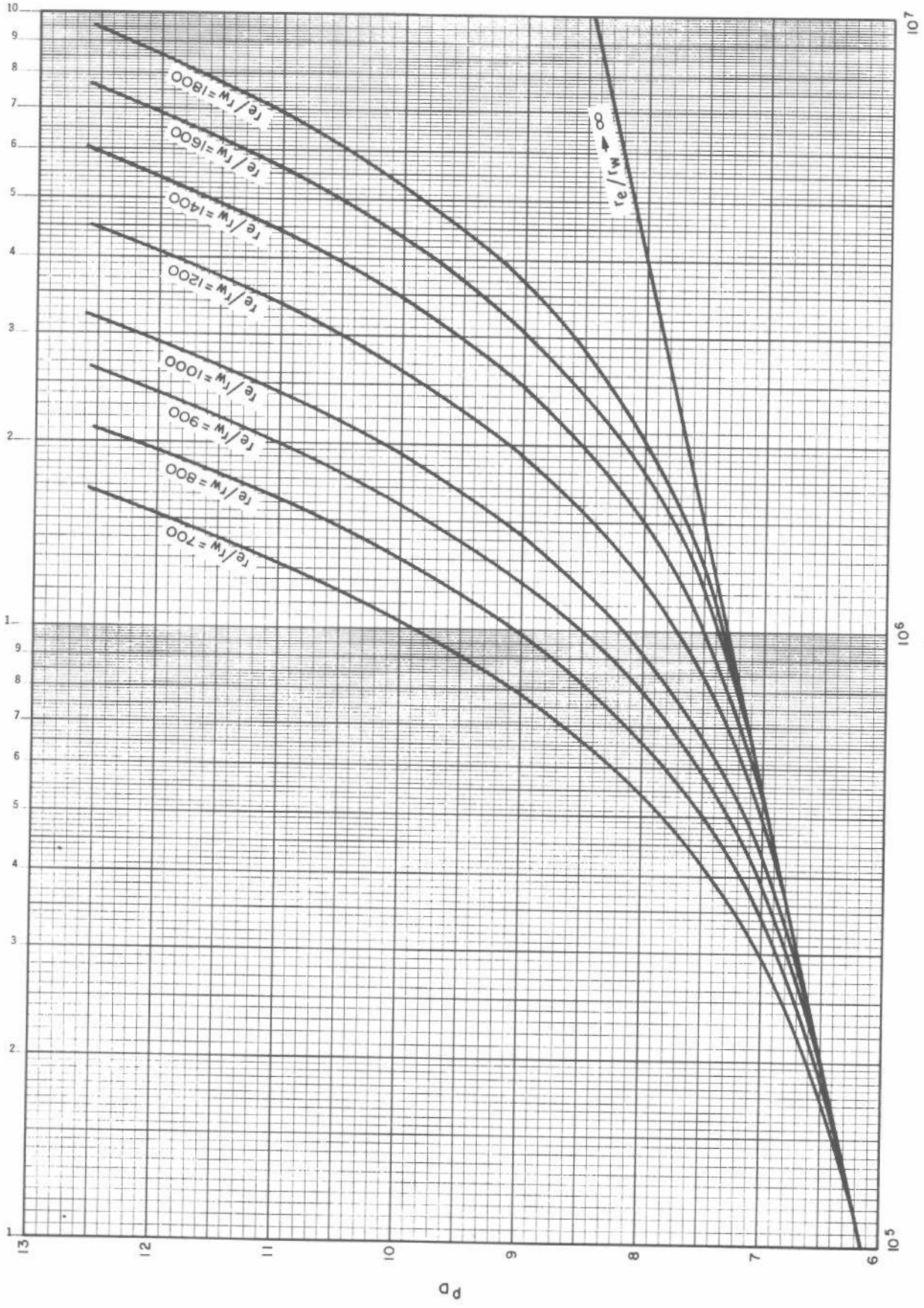

Fig. C.10B Dimensionless pressure for a well in the center of a closed circular reservoir, no wellbore storage, no skin. Calculated from Eq. C.20.

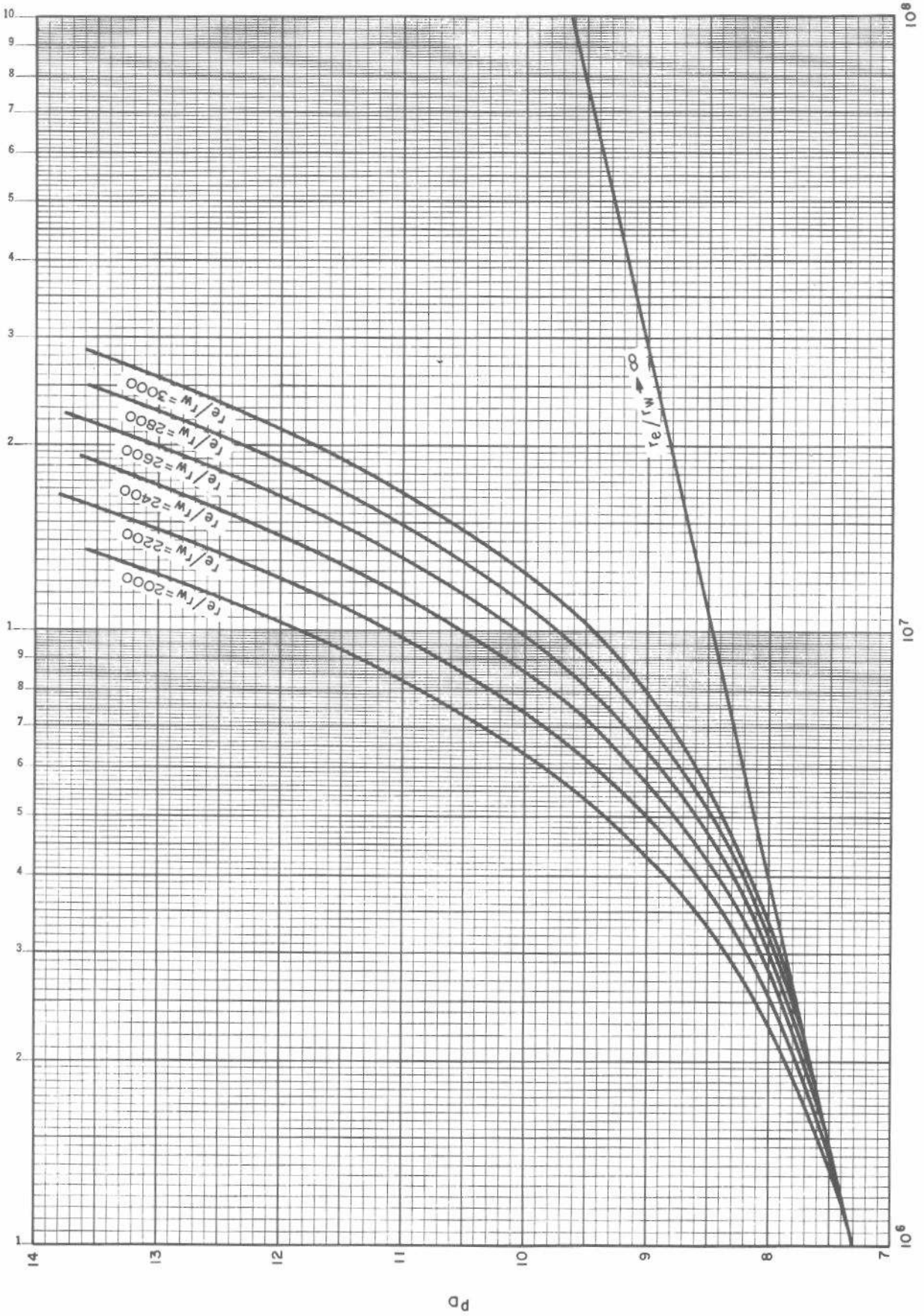

Fig. C.10C Dimensionless pressure for a well in the center of a closed circular reservoir, no wellbore storage, no skin. Calculated from Eq. C.20.

where

$(p_D)_{desired}$ = value of p_D at desired value of $\sqrt{A}/r_w$, and

$(p_D)_{table}$ = tabulated or plotted value of p_D using table or graph value of $\sqrt{A}/r_w$.

The quantity $\sqrt{A}/r_w$ affects the dimensionless pressure only at the well; values given at points away from the well are independent of this parameter.

Closed Circular Reservoir, No Wellbore Storage, No Skin

Figs. C.10A, C.10B, and C.10C show dimensionless pressure data for a well in the center of a closed circular reservoir with no wellbore storage and no skin. Skin effect may be included by using Eq. 2.2. The data in Fig. C.10 have been computed from[3]

$$p_D = -\frac{1}{2}\left\{\mathrm{Ei}\left(-\frac{1}{4t_D}\right) - \mathrm{Ei}\left(-\frac{1}{4t_{De}}\right) - 4t_{De}\exp\left(-1/4t_{De}\right)\right\}, \quad \text{(C.20)}$$

where the dimensionless time based on the external radius of the system is

$$t_{De} = \frac{0.0002637\,kt}{\phi\mu c_t r_e^2} = t_D\left(\frac{r_w^2}{r_e^2}\right). \quad \text{(C.21)}$$

Horner[3] points out that Eq. C.20 is "not even a mathematical solution of the basic flow equation," Eq. 2.1. However, it is an excellent approximation to the exact solution[3] (Ref. 3, Eq. XII, and Ref. 1, Eq. 2.36).

Closed-Square Reservoir, No Wellbore Storage, No Skin

Earlougher, Ramey, Miller, and Mueller[17] give dimensionless pressure data at several points in a closed-square drainage area with the well at the center of the system. Wellbore storage and skin effect are not included. Fig. C.11 schematically illustrates system geometry and the points for which p_D data are given. Figs. C.12A and C.12B show p_D at several points in the system. Table C.2 presents the data for this system.

Single-Well Rectangular Systems, No Wellbore Storage, No Skin

Figs. C.13 through C.16 present dimensionless pressure data at the well for a single well at various locations in various closed rectangular systems. Wellbore storage and skin factors are not included. Earlougher and Ramey[18] give tabular data for these figures; they also present p_D data for points away from the well.

The data in Figs. C.13 through C.16 are related to the data presented by Matthews, Brons, and Hazebroek[19] (Figs. 6.2 through 6.5) by[17]

$$p_D(t_{DA}) = 2\pi t_{DA} + \frac{1}{2}\left[\ln\left(t_{DA}\frac{A}{r_w^2}\right) + 0.80907 - p_{DMBH}(t_{DA})\right], \quad \text{(C.22)}$$

where

$$p_{DMBH} = \frac{kh\,(p^* - \bar{p})}{70.6\,qB\mu}. \quad \text{(C.23)}$$

Closed-Square Reservoir, Vertically Fractured Well, No Wellbore Storage

Fig. C.17* gives dimensionless pressure data for a single vertically fractured well (infinite-conductivity fracture case) in the center of a closed-square drainage region. Wellbore storage effects are not included. The data in Fig. C.17 are from Gringarten, Ramey, and Raghavan[6,7] and are considered to be slightly more accurate than other similar data.[20,21] As for the infinite, vertically fractured system, there is an initial half-slope straight line on the log-log plot; the duration of this line depends on the fracture length.

Fig. C.18* shows additional p_D data for a single, verti-

*See footnote on Page 24.

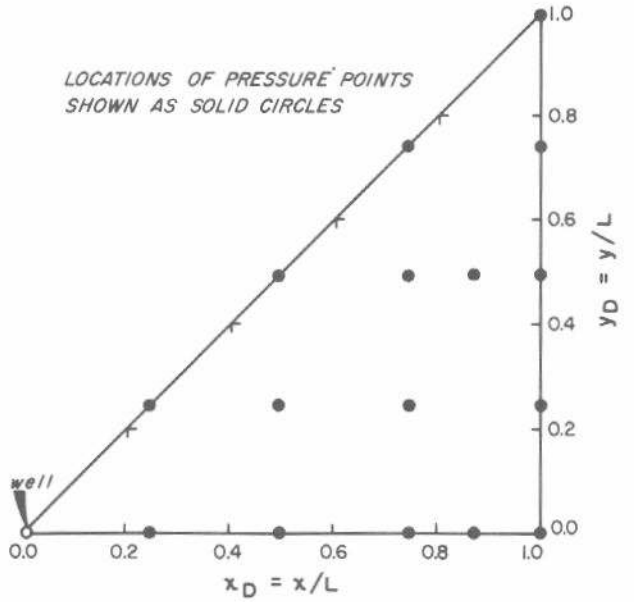

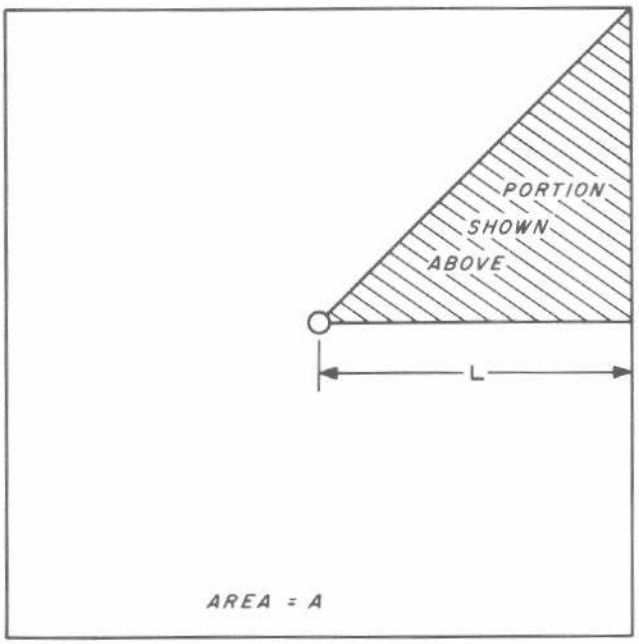

Fig. C.11 Well in the center of a closed-square system, well and pressure point location. After Earlougher, Ramey, Miller, and Mueller.[17]

cally fractured (infinite-conductivity) well in a closed-square drainage area. Wellbore storage is not included. Fig. C.18 may be more useful for type-curve matching than Fig. C.17 under some circumstances. Gringarten, Ramey, and Raghavan[6] give tabular p_D data for this case.

Fig. C.19* gives dimensionless pressure data for the systems of Figs. C.17 and C.18 but for a *uniform-flux* vertical fracture. Tabular data appear in Ref. 6. It is generally believed[6,7] that the uniform-flux fracture solution more closely approximates actual fractured systems than does the infinite-conductivity fracture solution.

*See footnote on Page 24.

A vertically fractured well in a closed system has the same general transient behavior as an unfractured well in a closed system. For the fractured well, the dimensionless pressure during the infinite-acting period is given by Eqs. C.5 and C.7 through C.10, depending on the fracture solution (infinite-conductivity or uniform-flux) and the time. Vertically fractured systems also exhibit pseudosteady-state behavior:

$$p_D = 2\pi t_{DA} + \frac{1}{2}\ln\left[\left(\frac{x_e}{x_f}\right)^2\right] + \frac{1}{2}\ln\left(\frac{2.2458}{C_A}\right). \quad \text{(C.24)}$$

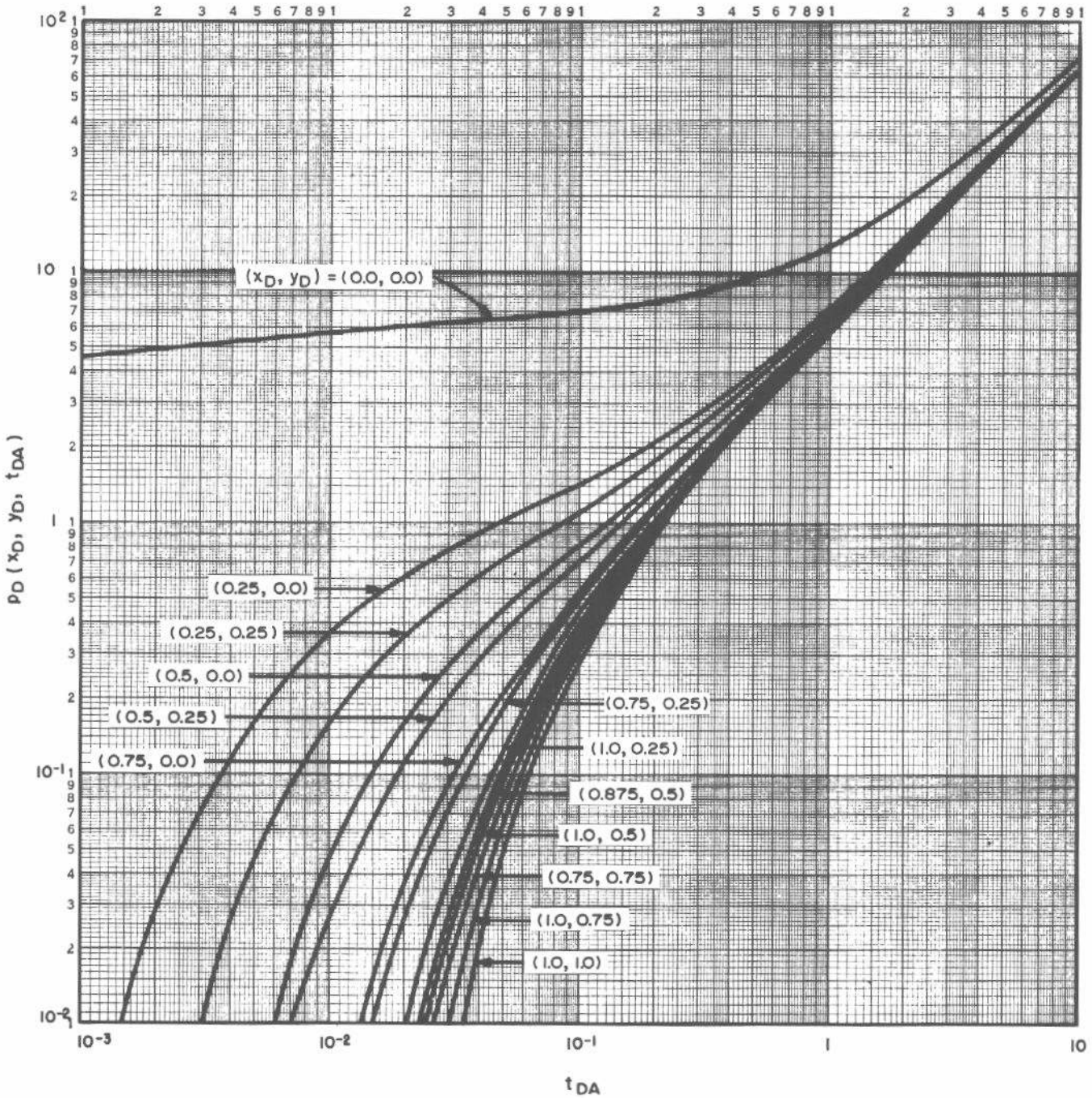

Fig. C.12A Dimensionless pressure at various points in a closed-square system with the well at the center, no wellbore storage, no skin, $\sqrt{A}/r_w = 2{,}000$. Log-log plot. See Fig. C.11 for point locations. After Earlougher, Ramey, Miller, and Mueller.[17]

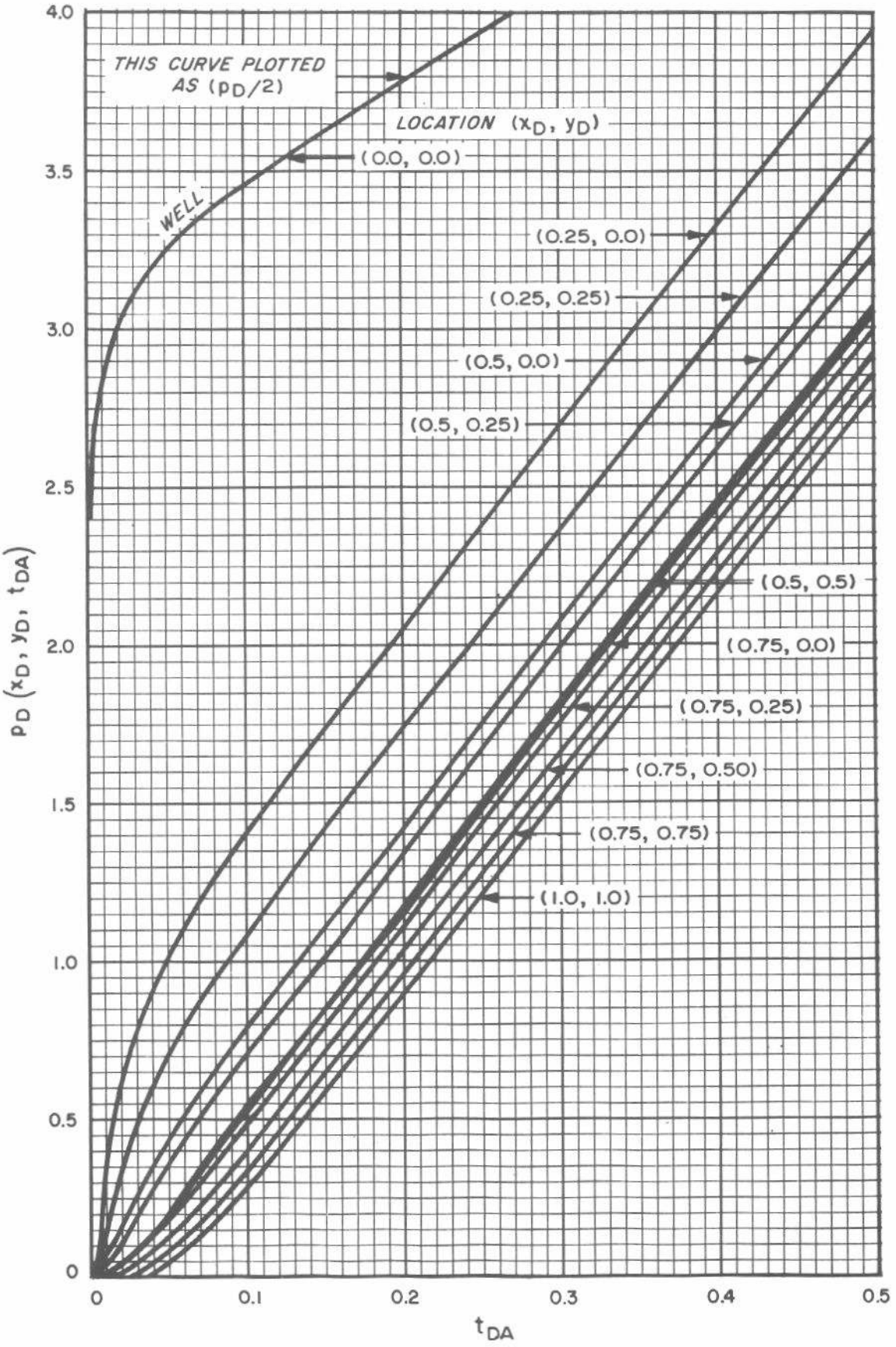

Fig. C.12B Dimensionless pressure at various points in a closed-square system with the well at the center, no wellbore storage, no skin, $\sqrt{A}/r_w = 2{,}000$. Coordinate plot. See Fig. C.11 for point locations. After Earlougher, Ramey, Miller, and Mueller.[17]

TABLE C.2—DIMENSIONLESS PRESSURE AT VARIOUS POINTS IN A CLOSED SQUARE WITH A WELL AT THE CENTER, NO WELLBORE STORAGE, NO SKIN. SEE FIG. C.11 FOR DEFINITION OF POINTS. $\sqrt{A}/r_w = 2{,}000$.
After Earlougher, Ramey, Miller, and Mueller.[17]

p_D

t_{DA}	x_D=0.000 y_D=0.000	x_D=0.250 y_D=0.000	x_D=0.250 y_D=0.250	x_D=0.500 y_D=0.000	x_D=0.500 y_D=0.250	x_D=0.500 y_D=0.500	x_D=0.750 y_D=0.000	x_D=0.750 y_D=0.250
0.0010	4.5516	0.0021	0.0000	0.0000	0.0000	0.0000	0.0000	0.0000
0.0015	4.7543	0.0109	0.0004	0.0000	0.0000	0.0000	0.0000	0.0000
0.0020	4.8981	0.0261	0.0021	0.0000	0.0000	0.0000	0.0000	0.0000
0.0025	5.0097	0.0456	0.0056	0.0001	0.0000	0.0000	0.0000	0.0000
0.0030	5.1009	0.0675	0.0109	0.0004	0.0001	0.0000	0.0000	0.0000
0.0040	5.2447	0.1141	0.0261	0.0021	0.0007	0.0000	0.0000	0.0000
0.0050	5.3563	0.1607	0.0456	0.0056	0.0021	0.0001	0.0001	0.0000
0.0060	5.4474	0.2053	0.0675	0.0109	0.0047	0.0004	0.0002	0.0001
0.0070	5.5245	0.2475	0.0906	0.0178	0.0085	0.0011	0.0006	0.0003
0.0080	5.5913	0.2871	0.1141	0.0261	0.0135	0.0021	0.0012	0.0007
0.0090	5.6502	0.3243	0.1376	0.0354	0.0194	0.0036	0.0021	0.0013
0.0100	5.7029	0.3592	0.1607	0.0456	0.0261	0.0056	0.0034	0.0021
0.0150	5.9056	0.5063	0.2676	0.1023	0.0675	0.0218	0.0154	0.0109
0.0200	6.0494	0.6211	0.3592	0.1607	0.1142	0.0456	0.0350	0.0266
0.0250	6.1610	0.7147	0.4379	0.2164	0.1609	0.0735	0.0597	0.0474
0.0300	6.2522	0.7939	0.5065	0.2685	0.2061	0.1032	0.0876	0.0716
0.0400	6.3965	0.9232	0.6224	0.3628	0.2906	0.1650	0.1485	0.1263
0.0500	6.5099	1.0279	0.7192	0.4470	0.3685	0.2276	0.2125	0.1854
0.0600	6.6050	1.1178	0.8041	0.5242	0.4415	0.2904	0.2772	0.2466
0.0700	6.6888	1.1983	0.8815	0.5968	0.5112	0.3532	0.3418	0.3086
0.0800	6.7654	1.2728	0.9539	0.6661	0.5786	0.4160	0.4061	0.3711
0.0900	6.8374	1.3434	1.0231	0.7334	0.6446	0.4788	0.4700	0.4338
0.1000	6.9063	1.4114	1.0902	0.7992	0.7095	0.5417	0.5336	0.4965
0.1500	7.2311	1.7347	1.4119	1.1186	1.0274	0.8558	0.8492	0.8106
0.2000	7.5468	2.0501	1.7271	1.4335	1.3421	1.1700	1.1636	1.1248
0.2500	7.8611	2.3644	2.0414	1.7478	1.6563	1.4841	1.4778	1.4390
0.3000	8.1753	2.6786	2.3556	2.0620	1.9705	1.7983	1.7919	1.7531
0.4000	8.8036	3.3069	2.9839	2.6903	2.5988	2.4266	2.4202	2.3814
0.5000	9.4320	3.9352	3.6122	3.3186	3.2271	3.0549	3.0486	3.0098
0.6000	10.0603	4.5636	4.2406	3.9469	3.8555	3.6833	3.6769	3.6381
0.7000	10.6886	5.1919	4.8689	4.5752	4.4838	4.3116	4.3052	4.2664
0.8000	11.3169	5.8202	5.4972	5.2036	5.1121	4.9399	4.9335	4.8947
0.9000	11.9452	6.4485	6.1255	5.8319	5.7404	5.5682	5.5618	5.5230
1.0000	12.5735	7.0768	6.7538	6.4602	6.3687	6.1965	6.1902	6.1513
2.0000	18.8567	13.3600	13.0370	12.7433	12.6519	12.4797	12.4733	12.4345
4.0000	31.4230	25.9263	25.6033	25.3097	25.2182	25.0460	25.0397	25.0009
8.0000	56.5557	51.0590	50.7360	50.4423	50.3509	50.1787	50.1723	50.1335
10.0000	69.1220	63.6253	63.3023	63.0087	62.9172	62.7450	62.7386	62.6999
C_A	30.8828	1.837×10^6	3.504×10^6	6.303×10^6	7.570×10^6	10.68×10^6	10.82×10^6	11.69×10^6
$\frac{1}{2} \ln\left(\frac{2.2458}{C_A}\right)$	-1.3106	-6.807	-7.130	-7.424	-7.515	-7.688	-7.694	-7.733

p_D

t_{DA}	x_D=0.750 y_D=0.500	x_D=0.750 y_D=0.750	x_D=0.875 y_D=0.000	x_D=0.875 y_D=0.500	x_D=1.000 y_D=0.000	x_D=1.000 y_D=0.250	x_D=1.000 y_D=0.500	x_D=1.000 y_D=0.750	x_D=1.000 y_D=1.000
0.0010	0.0000	0.0000	0.0000	0.0000	0.0000	0.0000	0.0000	0.0000	0.0000
0.0015	0.0000	0.0000	0.0000	0.0000	0.0000	0.0000	0.0000	0.0000	0.0000
0.0020	0.0000	0.0000	0.0000	0.0000	0.0000	0.0000	0.0000	0.0000	0.0000
0.0025	0.0000	0.0000	0.0000	0.0000	0.0000	0.0000	0.0000	0.0000	0.0000
0.0030	0.0000	0.0000	0.0000	0.0000	0.0000	0.0000	0.0000	0.0000	0.0000
0.0040	0.0000	0.0000	0.0000	0.0000	0.0000	0.0000	0.0000	0.0000	0.0000
0.0050	0.0000	0.0000	0.0000	0.0000	0.0000	0.0000	0.0000	0.0000	0.0000
0.0060	0.0000	0.0000	0.0000	0.0000	0.0000	0.0000	0.0000	0.0000	0.0000
0.0070	0.0000	0.0000	0.0001	0.0000	0.0000	0.0000	0.0000	0.0000	0.0000
0.0080	0.0001	0.0000	0.0002	0.0000	0.0000	0.0000	0.0000	0.0000	0.0000
0.0090	0.0003	0.0000	0.0004	0.0001	0.0001	0.0001	0.0000	0.0000	0.0000
0.0100	0.0005	0.0001	0.0008	0.0001	0.0003	0.0002	0.0000	0.0000	0.0000
0.0150	0.0040	0.0008	0.0055	0.0016	0.0031	0.0023	0.0009	0.0002	0.0001
0.0200	0.0121	0.0036	0.0164	0.0060	0.0111	0.0087	0.0042	0.0014	0.0005
0.0250	0.0245	0.0091	0.0329	0.0143	0.0249	0.0203	0.0112	0.0045	0.0023
0.0300	0.0404	0.0177	0.0539	0.0264	0.0436	0.0365	0.0219	0.0102	0.0062
0.0400	0.0805	0.0437	0.1050	0.0600	0.0913	0.0793	0.0532	0.0307	0.0223
0.0500	0.1281	0.0800	0.1628	0.1030	0.1469	0.1308	0.0947	0.0623	0.0498
0.0600	0.1807	0.1241	0.2237	0.1525	0.2065	0.1871	0.1431	0.1029	0.0872
0.0700	0.2366	0.1740	0.2859	0.2064	0.2678	0.2460	0.1962	0.1502	0.1321
0.0800	0.2948	0.2279	0.3486	0.2632	0.3299	0.3064	0.2525	0.2023	0.1826
0.0900	0.3546	0.2846	0.4114	0.3219	0.3925	0.3677	0.3109	0.2579	0.2369
0.1000	0.4153	0.3433	0.4744	0.3820	0.4551	0.4296	0.3708	0.3157	0.2939
0.1500	0.7257	0.6500	0.7888	0.6913	0.7692	0.7421	0.6797	0.6209	0.5976
0.2000	1.0393	0.9632	1.1030	1.0047	1.0834	1.0561	0.9931	0.9338	0.9103
0.2500	1.3534	1.2772	1.4172	1.3188	1.3975	1.3702	1.3071	1.2478	1.2243
0.3000	1.6676	1.5913	1.7313	1.6330	1.7117	1.6843	1.6213	1.5620	1.5384
0.4000	2.2959	2.2196	2.3597	2.2613	2.3400	2.3127	2.2496	2.1903	2.1667
0.5000	2.9242	2.8479	2.9880	2.8896	2.9683	2.9410	2.8779	2.8186	2.7950
0.6000	3.5525	3.4763	3.6163	3.5179	3.5966	3.5693	3.5062	3.4469	3.4233
0.7000	4.1808	4.1046	4.2446	4.1462	4.2249	4.1976	4.1346	4.0752	4.0517
0.8000	4.8092	4.7329	4.8729	4.7745	4.8533	4.8259	4.7629	4.7036	4.6800
0.9000	5.4375	5.3612	5.5012	5.4029	5.4816	5.4542	5.3912	5.3319	5.3083
1.0000	6.0658	5.9895	6.1296	6.0312	6.1099	6.0826	6.0195	5.9602	5.9366
2.0000	12.3490	12.2727	12.4127	12.3144	12.3930	12.3657	12.3027	12.2434	12.2198
4.0000	24.9153	24.8391	24.9791	24.8807	24.9594	24.9321	24.8690	24.8097	24.7861
8.0000	50.0480	49.9717	50.1117	50.0134	50.0921	50.0647	50.0017	49.9424	49.9188
10.0000	62.6143	62.5381	62.6781	62.5797	62.6584	62.6311	62.5680	62.5087	62.4851
C_A	13.87×10^6	16.16×10^6	12.21×10^6	14.87×10^6	12.70×10^6	13.41×10^6	15.22×10^6	17.14×10^6	18.96×10^6
$\frac{1}{2} \ln\left(\frac{2.2458}{C_A}\right)$	-7.818	-7.894	-7.754	-7.853	-7.774	-7.801	-7.865	-7.924	-7.974

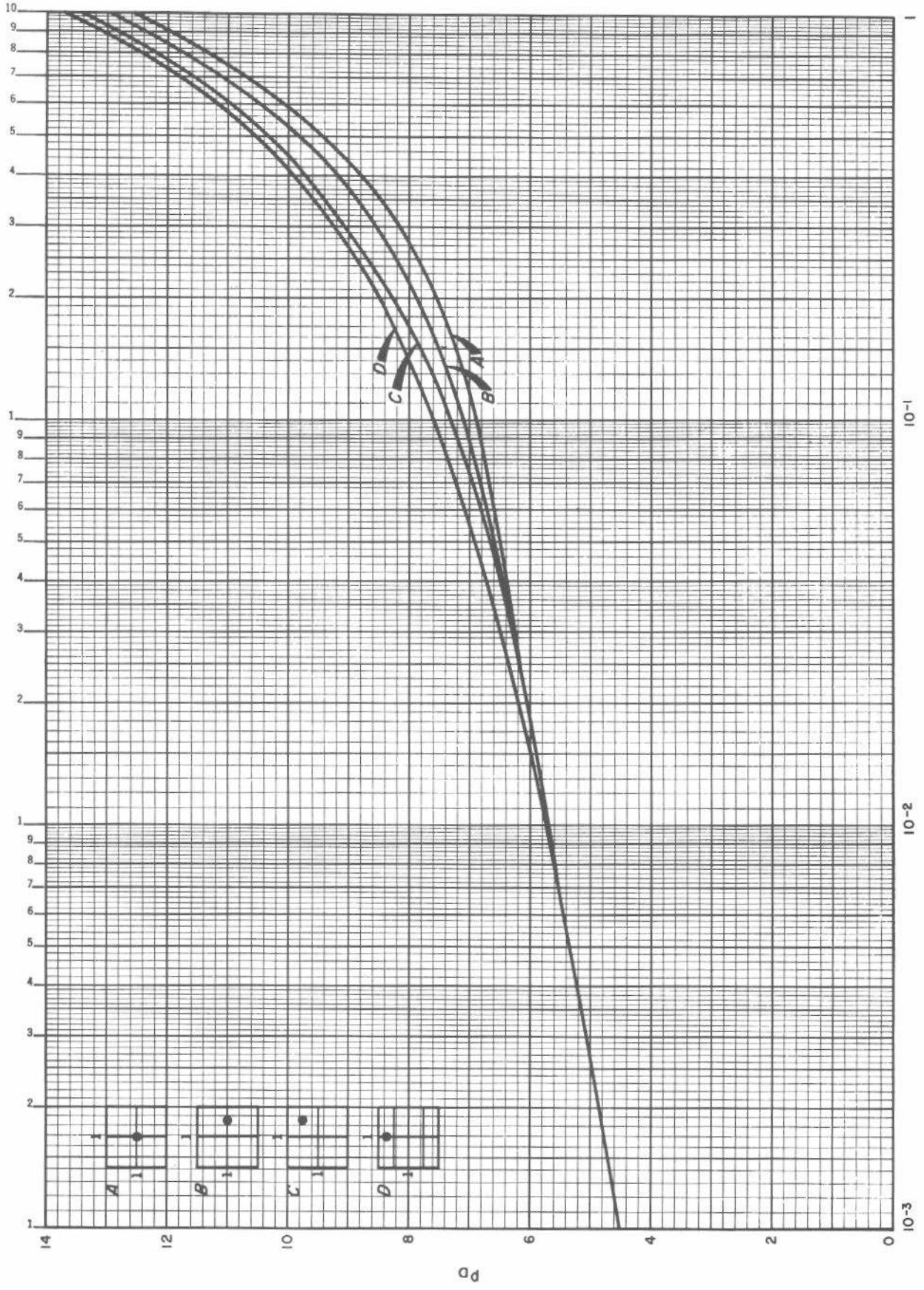

Fig. C.13 Dimensionless pressure for a single well in various closed rectangular systems, no wellbore storage, no skin, $\sqrt{A}/r_w = 2{,}000$. Data of Earlougher and Ramey.[18]

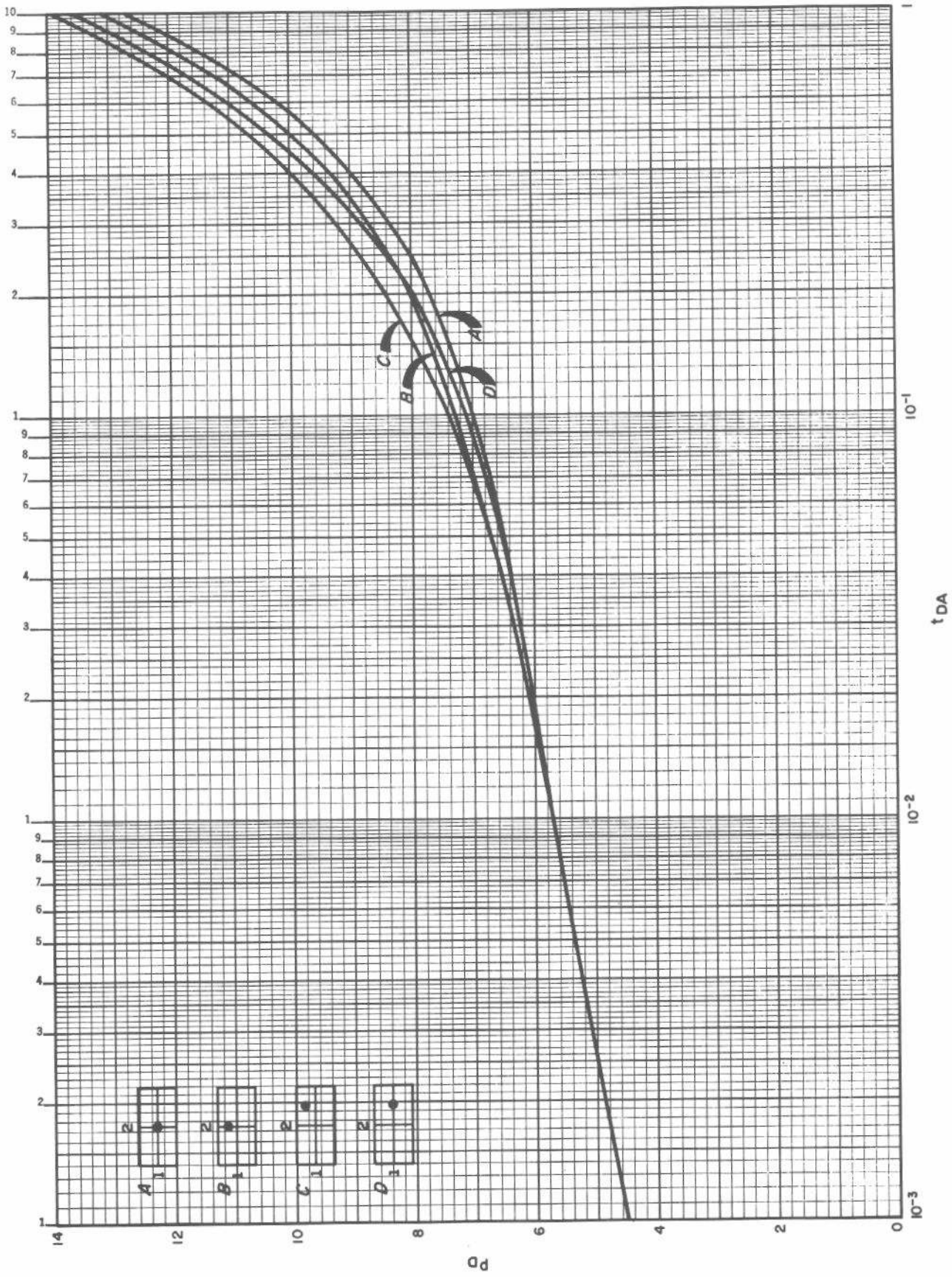

Fig. C.14 Dimensionless pressure for a single well in various closed rectangular systems, no wellbore storage, no skin, $\sqrt{A}/r_w = 2{,}000$. Data of Earlougher and Ramey.[18]

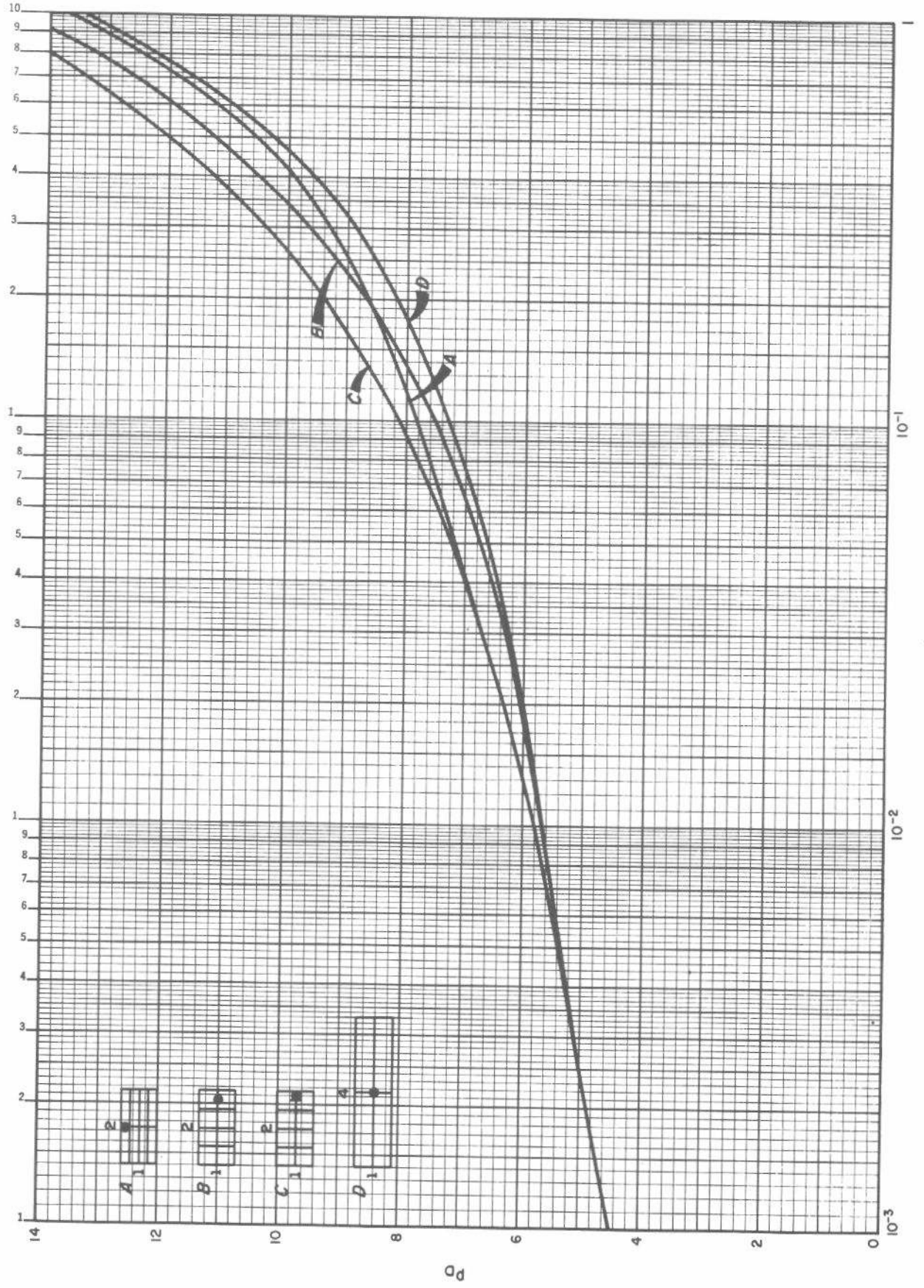

Fig. C.15 Dimensionless pressure for a single well in various closed rectangular systems, no wellbore storage, no skin, $\sqrt{A}/r_w = 2{,}000$. Data of Earlougher and Ramey.[18]

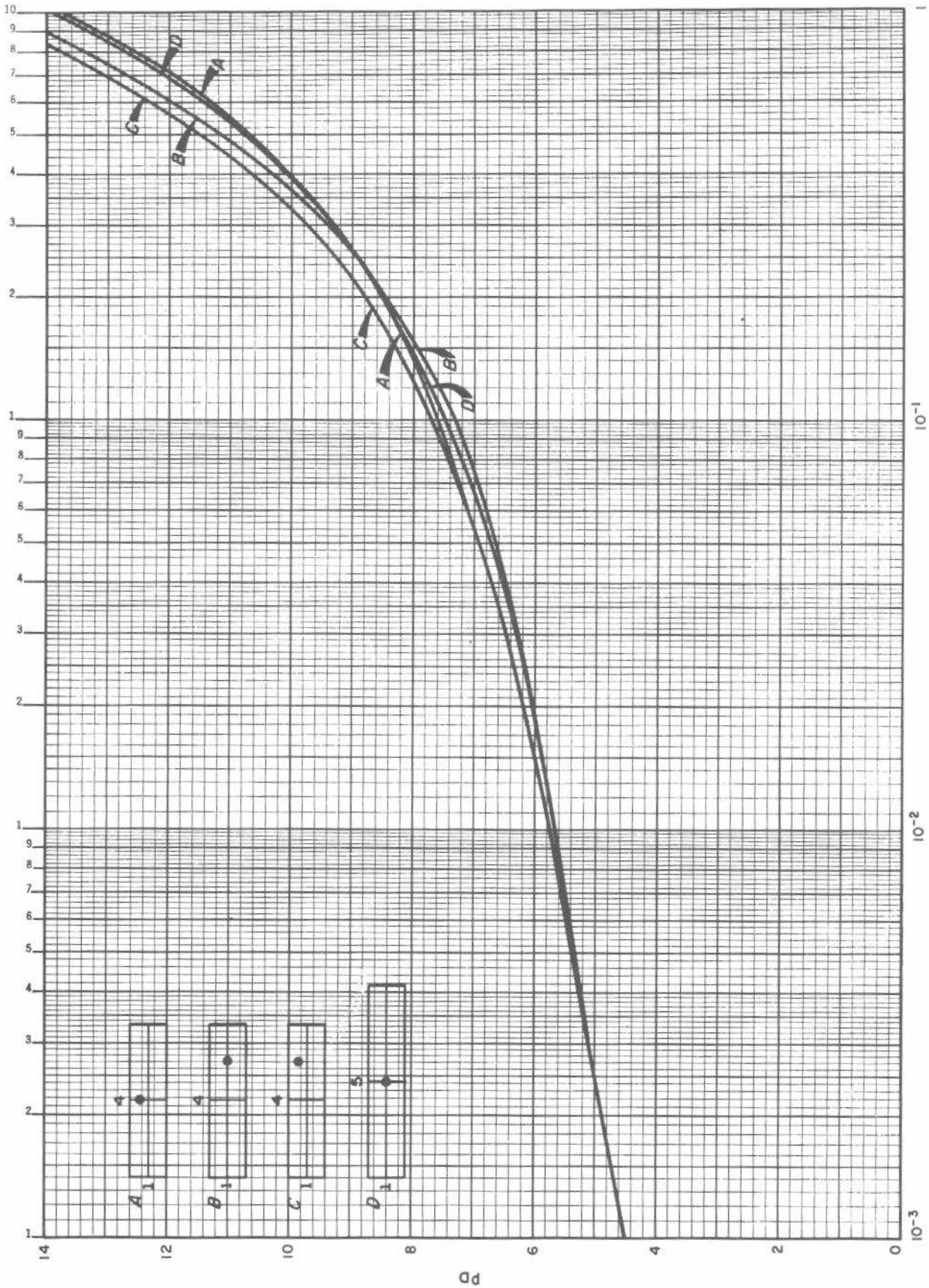

Fig. C.16 Dimensionless pressure for a single well in various closed rectangular systems, no wellbore storage, no skin, $\sqrt{A}/r_w = 2{,}000$. Data of Earlougher and Ramey.[18]

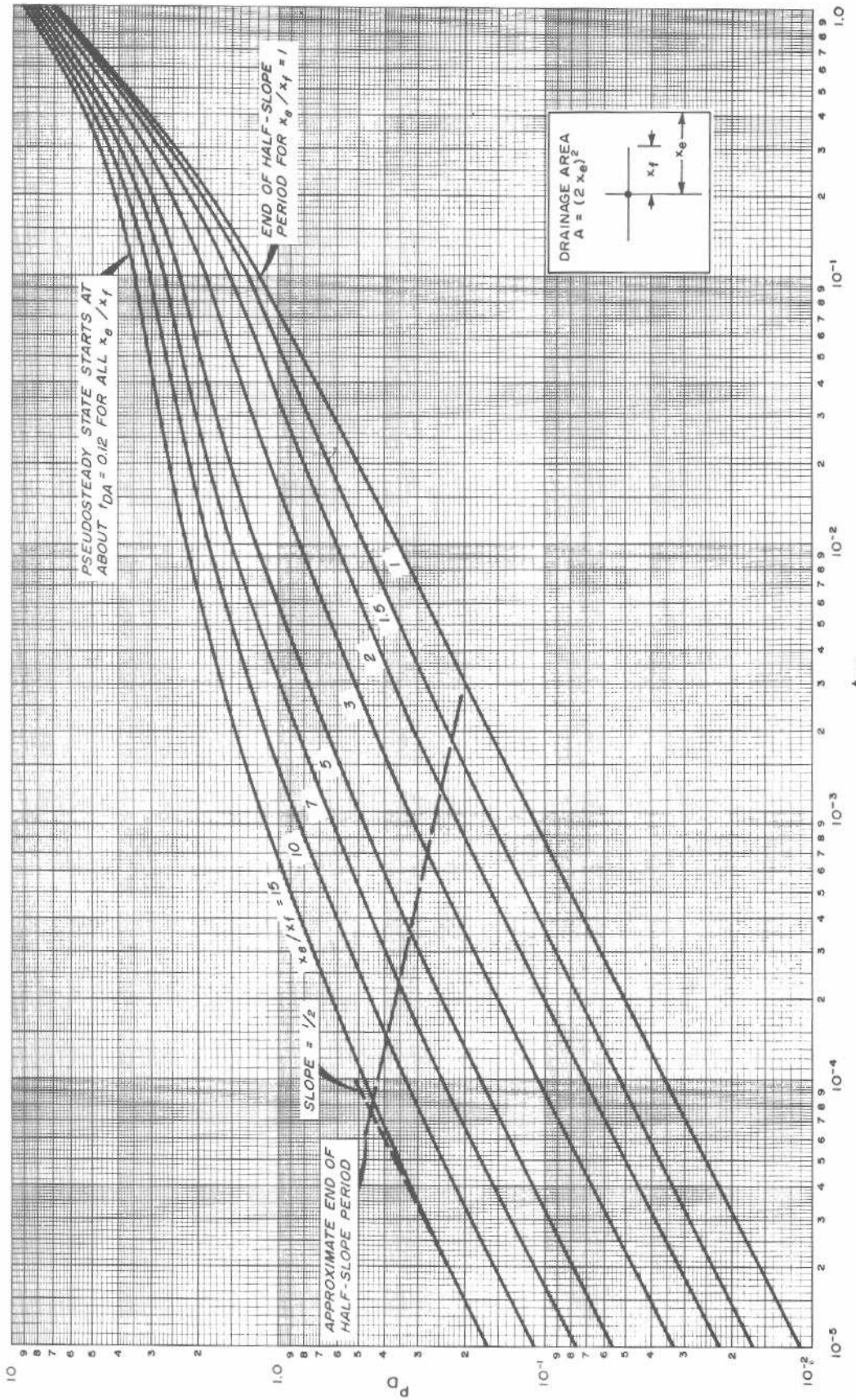

Fig. C.17 Dimensionless pressure for vertically fractured well in the center of a closed system, no wellbore storage, infinite-conductivity fracture. Data of Gringarten, Ramey, and Raghavan.[6,7] Graph courtesy H. J. Ramey, Jr.

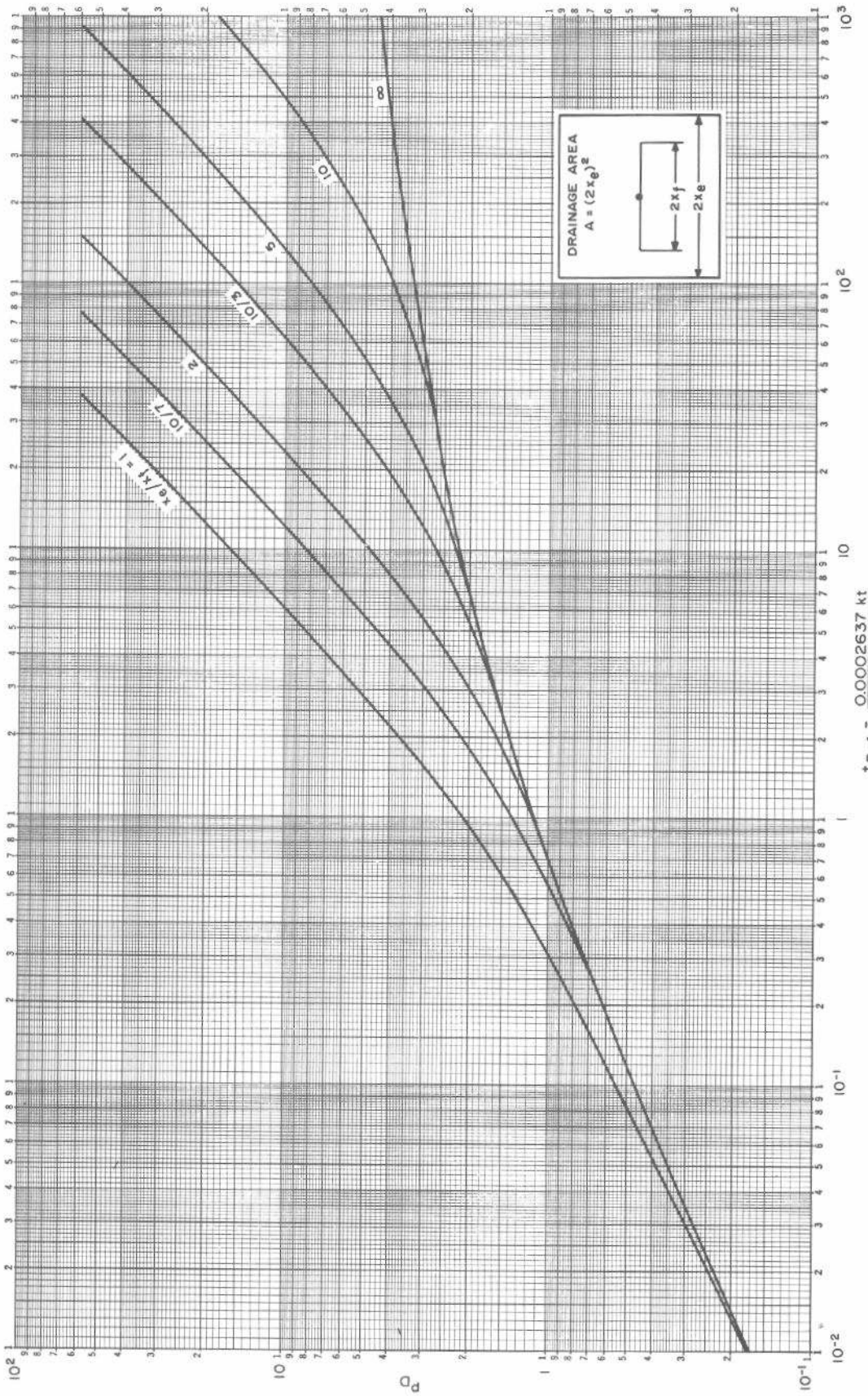

Fig. C.18 Dimensionless pressure for vertically fractured well in the center of a closed square, no wellbore storage, infinite-conductivity fracture. After Gringarten, Ramey, and Raghavan.[6,7]

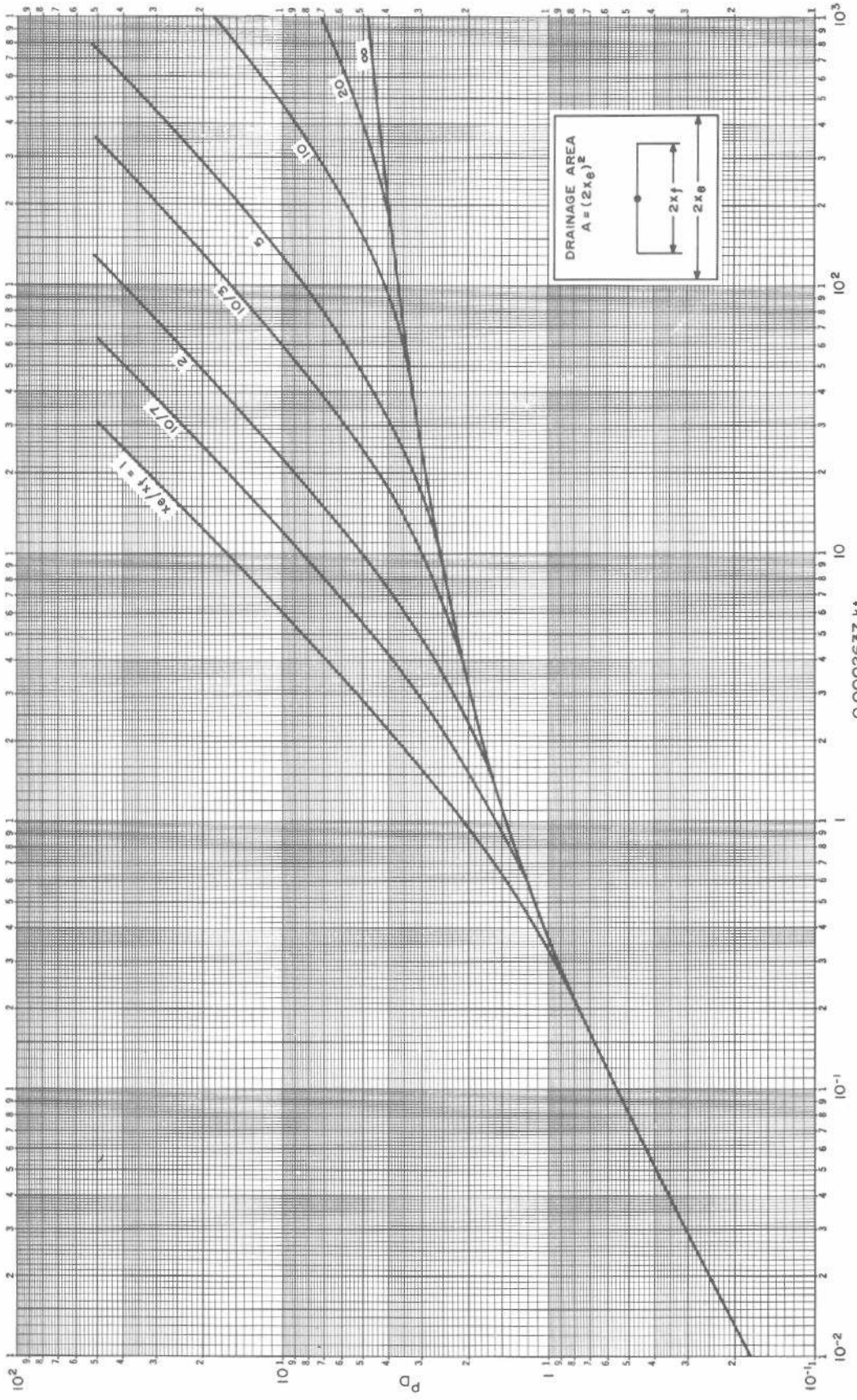

Fig. C.19 Dimensionless pressure for vertically fractured well in the center of a closed square, no wellbore storage, uniform-flux fracture. After Gringarten, Ramey and Raghavan.[6,7]

Eq. C.24 is Eq. C.18 with x_e/x_f substituted for $\sqrt{A}/r_w$. Shape factors for fractured systems based on this dimensional parameter are given in Table C.1.

C.4 Constant-Pressure Systems

Circular Reservoir, No Wellbore Storage, No Skin

Fig. C.20 shows p_D for a single well in the center of a circular reservoir with constant external pressure, no wellbore storage, and no skin. The system reaches true steady state when

$$t_D > 1.25\left(\frac{r_e^2}{r_w^2}\right), \quad \text{(C.25a)}$$

or

$$t_{DA} > 0.40 \quad \text{(C.25b)}$$

After that time the dimensionless pressure is given by Eq. 2.26a. Tabular data are presented by van Everdingen and Hurst.[5]

Rectangular Reservoirs, No Wellbore Storage, No Skin

Fig. C.21 gives dimensionless pressures for several square and rectangular systems with a single well and one or more boundaries at constant pressure. No wellbore storage or skin effects are included in Fig. C.21. Each system reaches steady state at some time. Ramey, Kumar, and Gulati[22] give additional information about steady state and

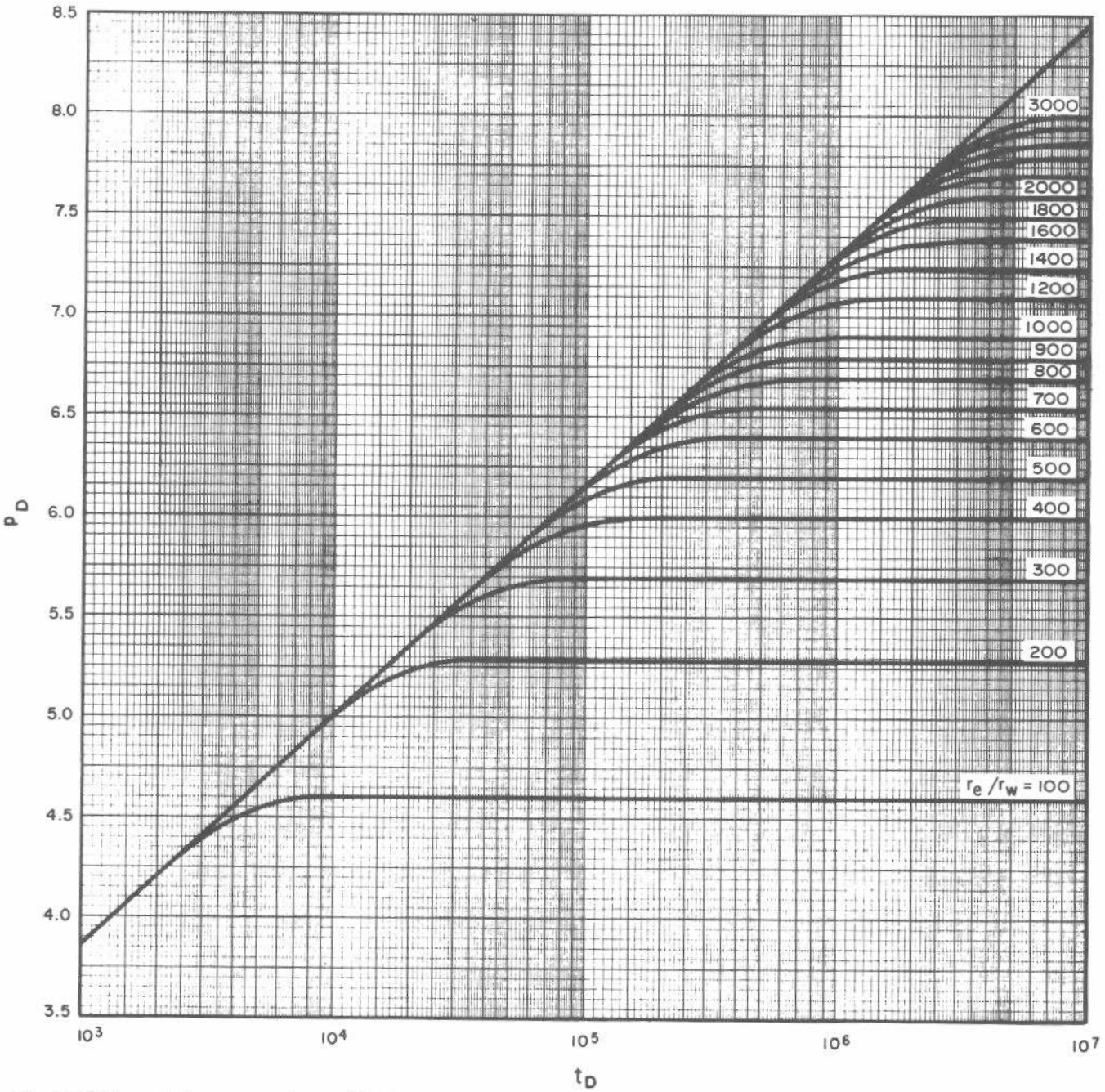

Fig. C.20 Dimensionless pressure for a well in the center of a closed circular reservoir with constant external pressure, no wellbore storage, no skin. After van Everdingen and Hurst.[5]

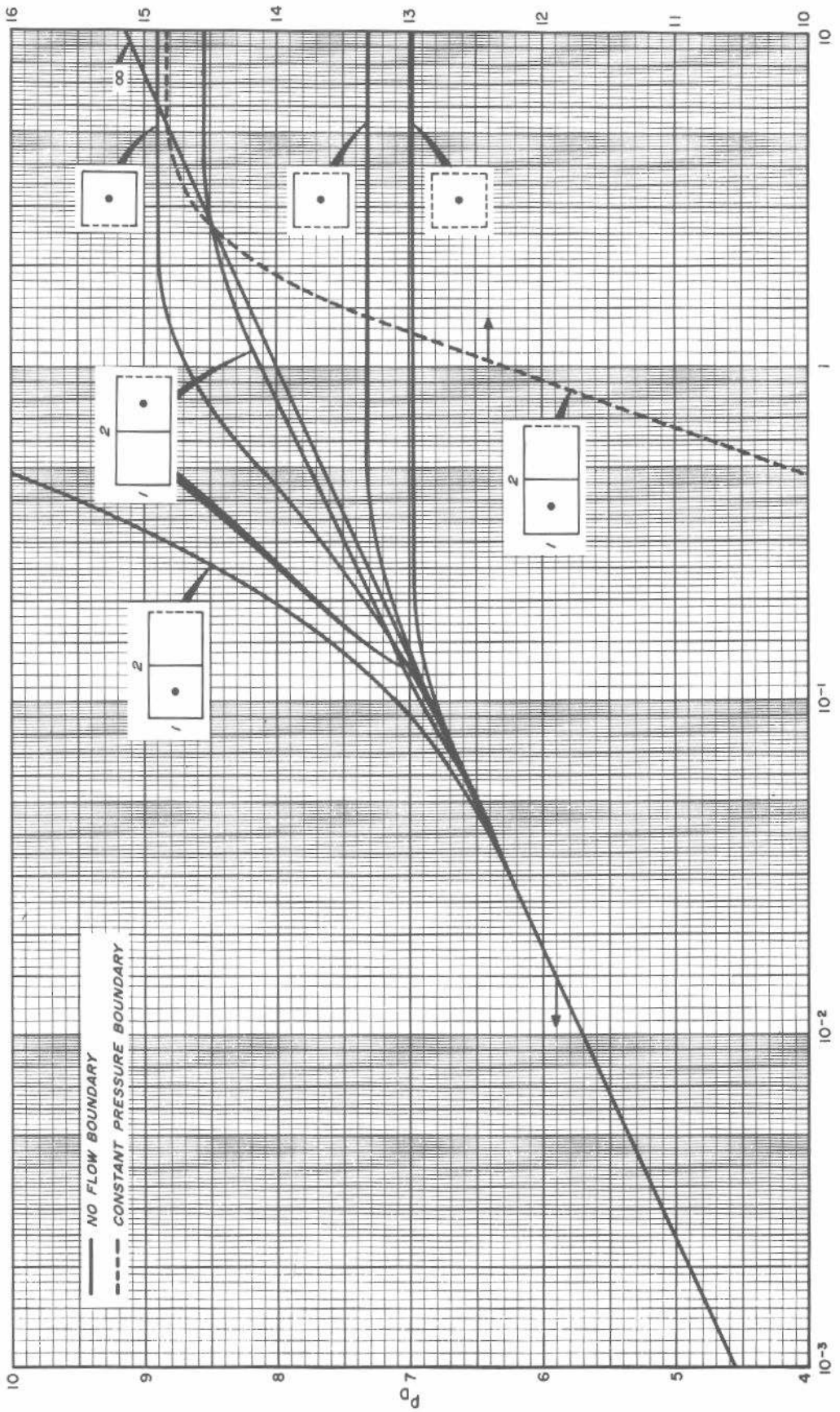

Fig. C.21 Dimensionless pressure for single wells in various rectangular shapes with one or more constant-pressure boundaries, no wellbore storage, no skin. Data of Ramey, Kumar, and Gulati.[22]

the time required to reach it. They also tabulate the p_D data of Fig. C.21.

In Fig. C.21, some systems show closed-system effects (even to the point of exhibiting pseudosteady-state behavior) before the effect of the constant-pressure boundary is felt. That is particularly clear for the 2:1 rectangle with the well located three-fourths of the length from the constant-pressure boundary.

References

1. Matthews, C. S. and Russell, D. G.: *Pressure Buildup and Flow Tests in Wells*, Monograph Series, Society of Petroleum Engineers of AIME, Dallas (1967) **1**, Chap. 2.
2. Theis, Charles V.: "The Relation Between the Lowering of the Piezometric Surface and the Rate and Duration of Discharge of a Well Using Ground-Water Storage," *Trans.*, AGU (1935) 519-524.
3. Horner, D. R.: "Pressure Build-Up in Wells," *Proc.*, Third World Pet. Cong., The Hague (1951) Sec. II, 503-523. Also *Reprint Series, No. 9 — Pressure Analysis Methods*, Society of Petroleum Engineers of AIME, Dallas (1967) 25-43.
4. Mueller, Thomas D. and Witherspoon, Paul A.: "Pressure Interference Effects Within Reservoirs and Aquifers," *J. Pet. Tech.* (April 1965) 471-474; *Trans.*, AIME, **234.**
5. van Everdingen, A. F. and Hurst, W.: "The Application of the Laplace Transformation to Flow Problems in Reservoirs," *Trans.*, AIME (1949) **186,** 305-324.
6. Gringarten, Alain C., Ramey, Henry J., Jr., and Raghavan, R.: "Pressure Analysis for Fractured Wells," paper SPE 4051 presented at the SPE-AIME 47th Annual Fall Meeting, San Antonio, Tex., Oct. 8-11, 1972.
7. Gringarten, Alain C., Ramey, Henry J., Jr., and Raghavan, R.: "Unsteady-State Pressure Distributions Created by a Well With a Single Infinite-Conductivity Vertical Fracture," *Soc. Pet. Eng. J.* (Aug. 1974) 347-360; *Trans.*, AIME, **257.**
8. Gringarten, Alain C.: "Unsteady-State Pressure Distributions Created by a Well With a Single Horizontal Fracture, Partial Penetration, or Restricted Flow Entry," PhD dissertation, Stanford U., Stanford, Calif. (1971) 106. (Order No. 71-23,512, University Microfilms, P.O. Box 1764, Ann Arbor, Mich. 48106.)
9. Gringarten, Alain C. and Ramey, Henry J., Jr.: "Unsteady-State Pressure Distributions Created by a Well With a Single Horizontal Fracture, Partial Penetration, or Restricted Entry," *Soc. Pet. Eng. J.* (Aug. 1974) 413-426; *Trans.*, AIME, **257.**
10. Agarwal, Ram G., Al-Hussainy, Rafi, and Ramey, H. J., Jr.: "An Investigation of Wellbore Storage and Skin Effect in Unsteady Liquid Flow: I. Analytical Treatment," *Soc. Pet. Eng. J.* (Sept. 1970) 279-290; *Trans.*, AIME, **249.**
11. Wattenbarger, Robert A. and Ramey, H. J., Jr.: "An Investigation of Wellbore Storage and Skin Effect in Unsteady Liquid Flow: II. Finite Difference Treatment," *Soc. Pet. Eng. J.* (Sept. 1970) 291-297; *Trans.*, AIME, **249.**
12. Earlougher, Robert C., Jr., and Kersch, Keith M.: "Analysis of Short-Time Transient Test Data by Type-Curve Matching," *J. Pet. Tech.* (July 1974) 793-800; *Trans.*, AIME, **257.**
13. McKinley, R. M.: "Wellbore Transmissibility From Afterflow-Dominated Pressure Buildup Data," *J. Pet. Tech.* (July 1971) 863-872; *Trans.*, AIME, **251.**
14. Ramey, H. J., Jr., and Cobb, William M.: "A General Buildup Theory for a Well in a Closed Drainage Area," *J. Pet. Tech.* (Dec. 1971) 1493-1505; *Trans.*, AIME, **251.**
15. Brons, F. and Miller, W. C.: "A Simple Method for Correcting Spot Pressure Readings," *J. Pet. Tech.* (Aug. 1961) 803-805; *Trans.*, AIME, **222.**
16. Dietz, D. N.: "Determination of Average Reservoir Pressure From Build-Up Surveys," *J. Pet. Tech.* (Aug. 1965) 955-959; *Trans.*, AIME, **234.**
17. Earlougher, Robert C., Jr., Ramey, H. J., Jr., Miller, F. G., and Mueller, T. D.: "Pressure Distributions in Rectangular Reservoirs," *J. Pet. Tech.* (Feb. 1968) 199-208; *Trans.*, AIME, **243.**
18. Earlougher, R. C., Jr., and Ramey, H. J., Jr.: "Interference Analysis in Bounded Systems," *J. Cdn. Pet. Tech.* (Oct.-Dec. 1973) 33-45.
19. Matthews, C. S., Brons, F., and Hazebroek, P.: "A Method for Determination of Average Pressure in a Bounded Reservoir," *Trans.*, AIME (1954) **201,** 182-191. Also *Reprint Series, No. 9 — Pressure Analysis Methods*, Society of Petroleum Engineers of AIME, Dallas (1967) 51-60.
20. Russell, D. G. and Truitt, N. E.: "Transient Pressure Behavior in Vertically Fractured Reservoirs," *J. Pet. Tech.* (Oct. 1964) 1159-1170; *Trans.*, AIME, **231.** Also *Reprint Series, No. 9 — Pressure Analysis Methods*, Society of Petroleum Engineers of AIME, Dallas (1967) 149-160.
21. Raghavan, R., Cady, Gilbert V., and Ramey, Henry J., Jr.: "Well-Test Analysis for Vertically Fractured Wells," *J. Pet. Tech.* (Aug. 1972) 1014-1020; *Trans.*, AIME, **253.**
22. Ramey, Henry J., Jr., Kumar, Anil, and Gulati, Mohinder S.: *Gas Well Test Analysis Under Water-Drive Conditions*, AGA, Arlington, Va. (1973).

Appendix D

Rock and Fluid Property Correlations

D.1 Introduction

This appendix provides information useful for estimating fluid and rock properties needed when analyzing transient-test pressure data. We believe that the correlations presented are among the most reliable presently available, although they are only a small sample of those available. The correlations may be used when necessary, but laboratory data measured on representative samples taken from the reservoir are always superior to general correlations and should be used whenever possible.

D.2 PVT Properties

This section presents correlations of pressure-volume-temperature (PVT) relations for reservoir fluids. The information can be used when laboratory data are not available. However, to ensure the best possible reservoir engineering and transient-test results, laboratory data should be obtained and used. It is both poor economics and poor engineering to resist obtaining good laboratory data simply because correlations are available.

Table D.1 gives physical properties of methane through decane and some other compounds commonly associated with petroleum reservoirs. More complete data are given in Ref. 1. Such information can be used to estimate some of the properties of hydrocarbon mixtures.

The pseudocritical temperature, T_{pc}, and pressure, p_{pc}, of a mixture are used in many correlations and equations in this appendix. If mixture composition is known, those quantities may be estimated from

$$T_{pc} = \sum_{i=1}^{N} y_i T_{ci}, \quad \ldots\ldots\ldots\ldots\ldots\ldots\ldots\ldots\ldots\ldots (D.1)$$

and

$$p_{pc} = \sum_{i=1}^{N} y_i p_{ci}, \quad \ldots\ldots\ldots\ldots\ldots\ldots\ldots\ldots\ldots\ldots (D.2)$$

where

N = number of components in the mixture
y_i = mole fraction of Component i
T_{ci} = critical temperature of Component i, °R
p_{ci} = critical pressure of Component i, psia.

If the system composition is not known, Figs. D.1 through D.3 may be used to estimate T_{pc} and p_{pc}. Fig. D.1 provides a way to estimate those quantities for undersaturated oil at reservoir pressure; the oil specific gravity corrected to 60 °F (the value normally reported) is used. If the API gravity is reported at other than 60 °F, it may be corrected to 60 °F

TABLE D.1—PHYSICAL PROPERTIES OF HYDROCARBONS AND ASSOCIATED COMPOUNDS.

Constituent	Molecular Weight	Normal Boiling Point °F	Normal Boiling Point °R	Liquid Density (lb_m/cu ft)	Gas Density at 60 °F, 1 atm (lb_m/cu ft)	Critical Temperature (°R)	Critical Pressure (psia)
Methane, CH_4	16.04	−258.7	201	18.72*	0.04235	344	673
Ethane, C_2H_6	30.07	−127.5	332	23.34*	0.07986	550	712
Propane, C_3H_8	44.09	−43.8	416	31.68**	0.1180	666	617
iso-butane, C_4H_{10}	58.12	10.9	471	35.14**	0.1577	735	528
n-butane, C_4H_{10}	58.12	31.1	491	36.47**	0.1581	766	551
iso-pentane, C_5H_{12}	72.15	82.1	542	38.99	—	830	483
n-pentane, C_5H_{12}	72.15	96.9	557	39.39	—	847	485
n-hexane, C_6H_{14}	86.17	155.7	615	41.43	—	914	435
n-heptane, C_7H_{16}	100.20	209.2	669	42.94	—	972	397
n-octane, C_8H_{18}	114.22	258.1	718	44.10	—	1,025	362
n-nonane, C_9H_{20}	128.25	303.3	763	45.03	—	1,073	335
n-decane, $C_{10}H_{22}$	142.28	345.2	805	45.81	—	1,115	313
Nitrogen, N_2	28.02	−320.4	140	—	0.0739	227	492
Air (O_2 + N_2)	29	−317.7	142	—	0.0764	239	547
Carbon dioxide, CO_2	44.01	−109.3	351	68.70	0.117	548	1,073
Hydrogen sulfide, H_2S	34.08	−76.5	383	87.73	0.0904	673	1,306
Water	18.02	212	672	62.40	—	1,365	3,206

*Apparent density in liquid phase.
**Density at saturation pressure.

using the technique described in Ref. 4. (In Ref. 4, Table 5 is used for hydrometer measurements at other than 60 °F; Table 7 allows correction of volume at a given temperature to volume at 60 °F.) Fig. D.2 applies to bubble-point liquids, again using the specific gravity corrected to 60 °F. The bubble-point pressure at 60 °F should be determined in the laboratory.* Fig. D.3 applies to condensate well fluids and natural gases; knowledge of the gas gravity is required to use Fig. D.3.

T_{pc} and p_{pc} are normally used to estimate the pseudoreduced temperature and pressure:

$$T_{pr} = \frac{T}{T_{pc}}, \quad \ldots\ldots\ldots\ldots\ldots\ldots\ldots\ldots\ldots\ldots \text{(D.3)}$$

and

$$p_{pr} = \frac{p}{p_{pc}}, \quad \ldots\ldots\ldots\ldots\ldots\ldots\ldots\ldots\ldots\ldots \text{(D.4)}$$

where

T = temperature of interest, °R
p = pressure of interest, psia.

Note in Eqs. D.1 through D.4 that temperature must be absolute temperature and pressure must be absolute pressure.

Since many correlations in this appendix use specific gravity or API gravity, it is worthwhile to restate the relationship between those two quantities:

$$°\text{API} = \frac{141.5}{\gamma} - 131.5. \quad \ldots\ldots\ldots\ldots\ldots\ldots\ldots\ldots \text{(D.5)}$$

In Eq. D.5, the specific gravity, γ, must be corrected to 60 °F and atmospheric pressure.

Figs. D.4 through D.6 are Standing's[5] correlations for properties of mixtures of hydrocarbon gases and liquids. Examples of their use are shown in the figures. Standing's correlations are based mainly on the properties of California crude oils. Cronquist[6] gives correlations that may be useful for Gulf Coast oils.

Fig. D.7 is the well known chart of real gas deviation factor for natural gases. Pseudoreduced properties may be estimated from Eqs. D.1 through D.4.

*If only the value at reservoir temperature is known, Fig. D.5 may be used to estimate the 60 °F value by going vertically upward from the bubble-point pressure to reservoir temperature, horizontally left to 60 °F, and vertically downward to the estimated bubble-point pressure.

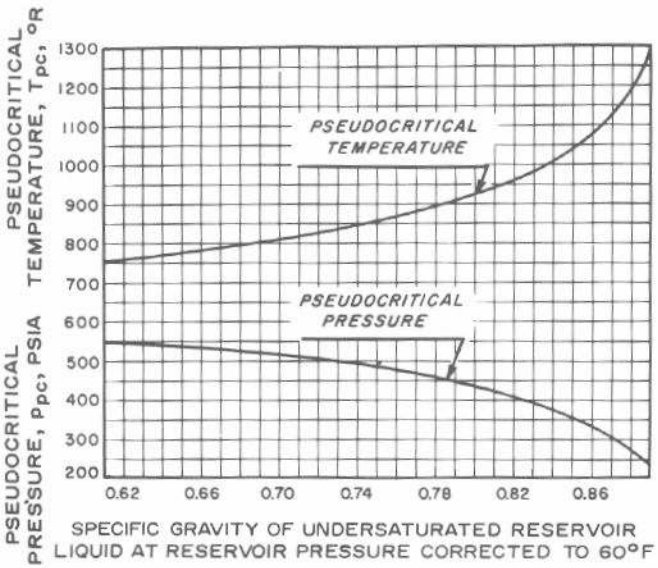

Fig. D.1 Approximate correlation of liquid pseudocritical pressure and temperature with specific gravity. After Trube.[2]

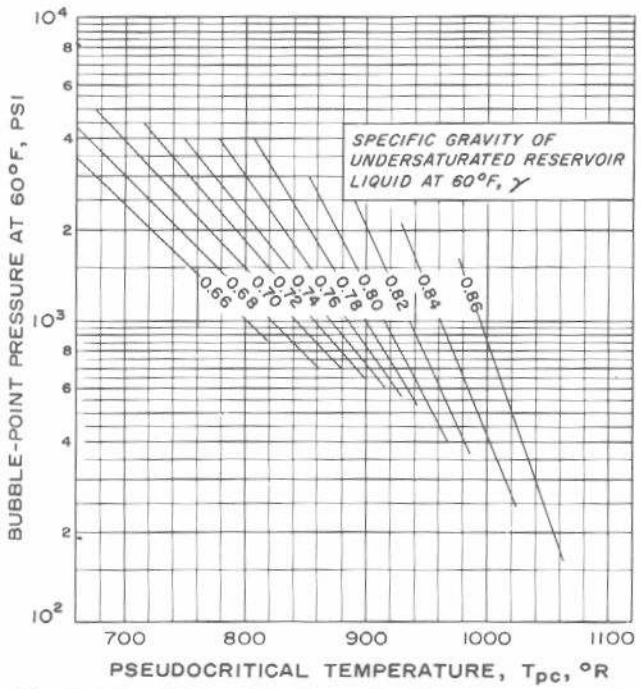

Fig. D.2 Correlation of liquid pseudocritical temperature with specific gravity and bubble point. After Trube.[2]

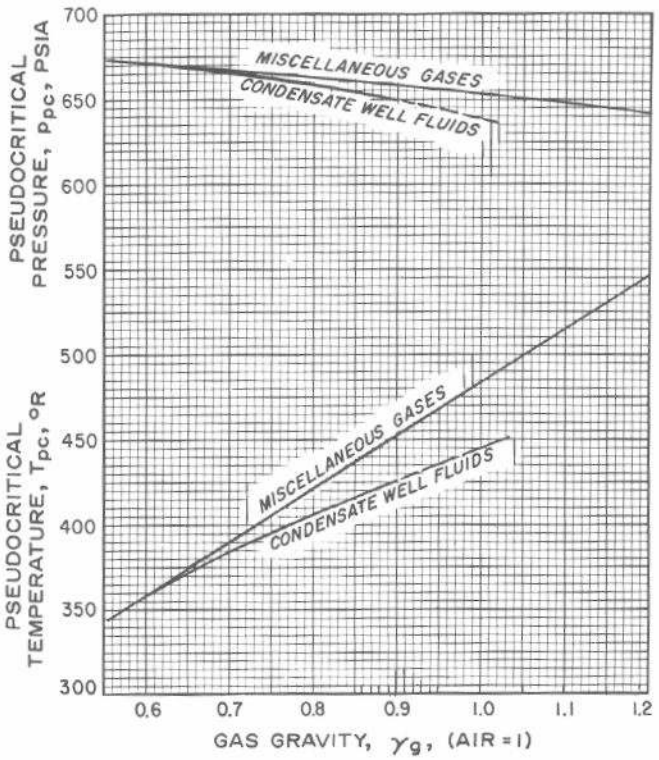

Fig. D.3 Correlation of pseudocritical properties of condensate well fluids and miscellaneous natural gas with fluid gravity. After Brown *et al.*[3]

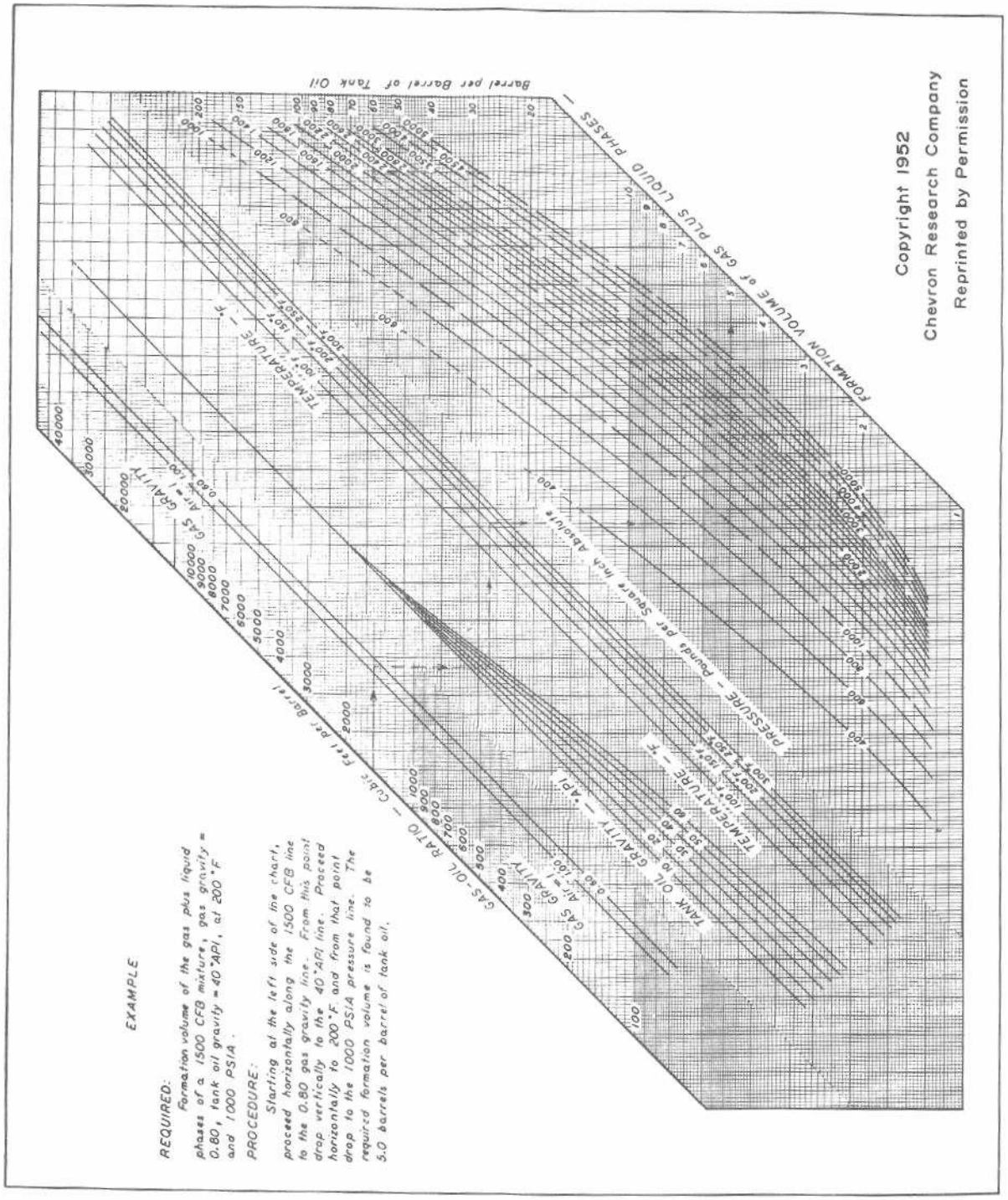

Fig. D.4 Properties of natural mixtures of hydrocarbon gas and liquids, formation volume of gas plus liquid phase. After Standing.[5]

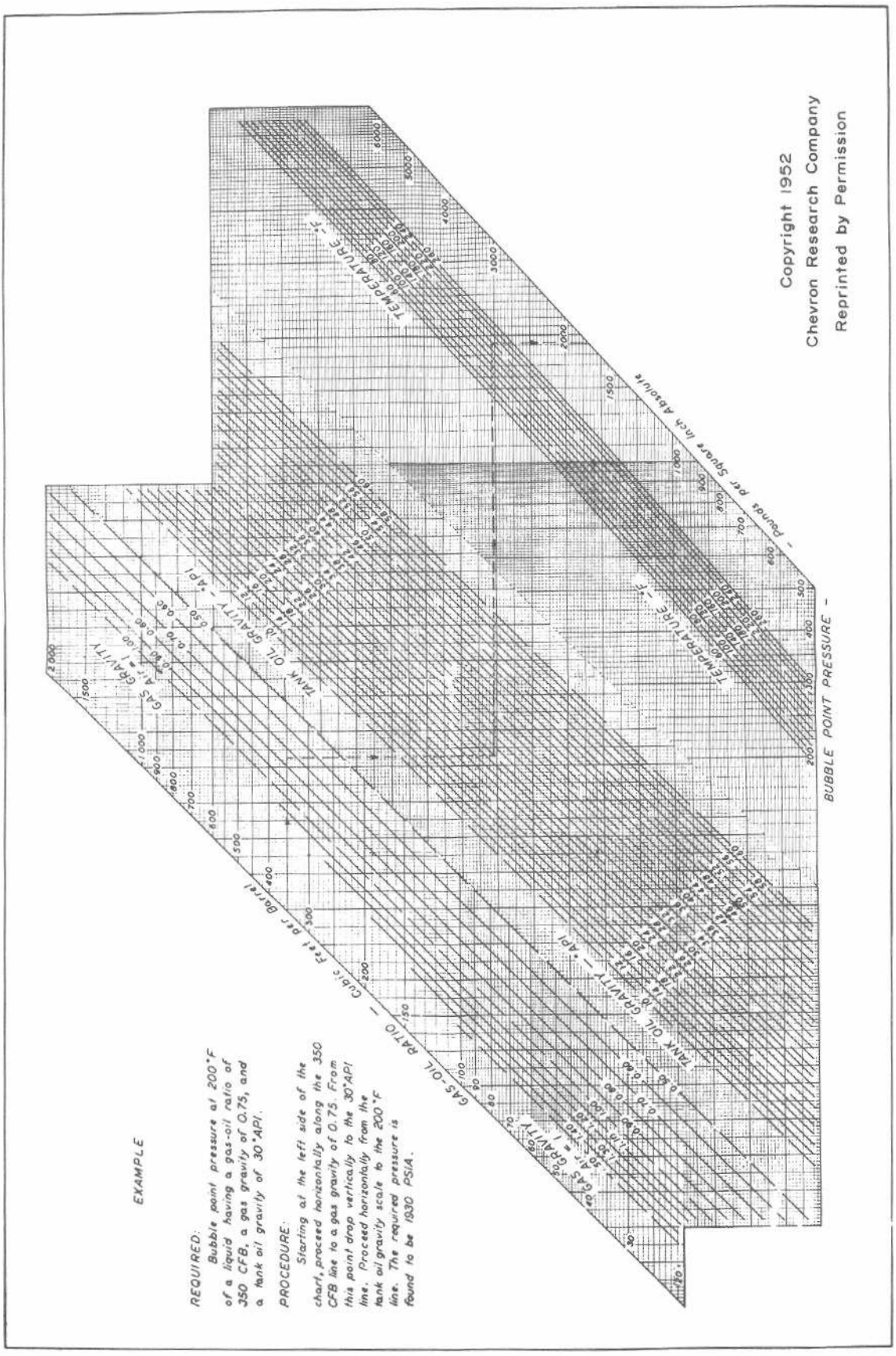

Fig. D.5 Properties of natural mixtures of hydrocarbon gas and liquids, bubble-point pressure. After Standing.[5]

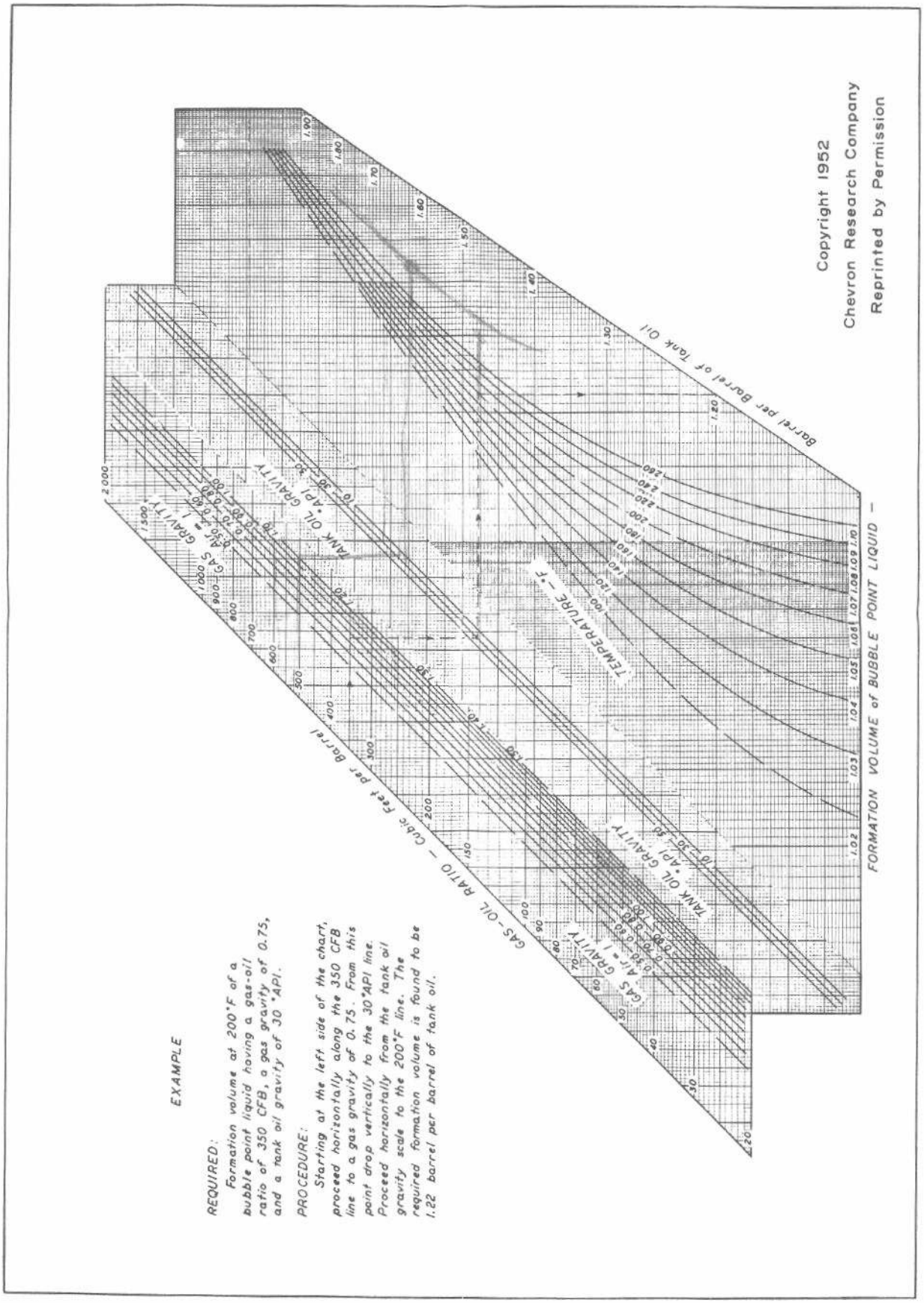

Fig. D.6 Properties of natural mixtures of hydrocarbon gas and liquids, formation volume of bubble-point liquids. After Standing.[5]

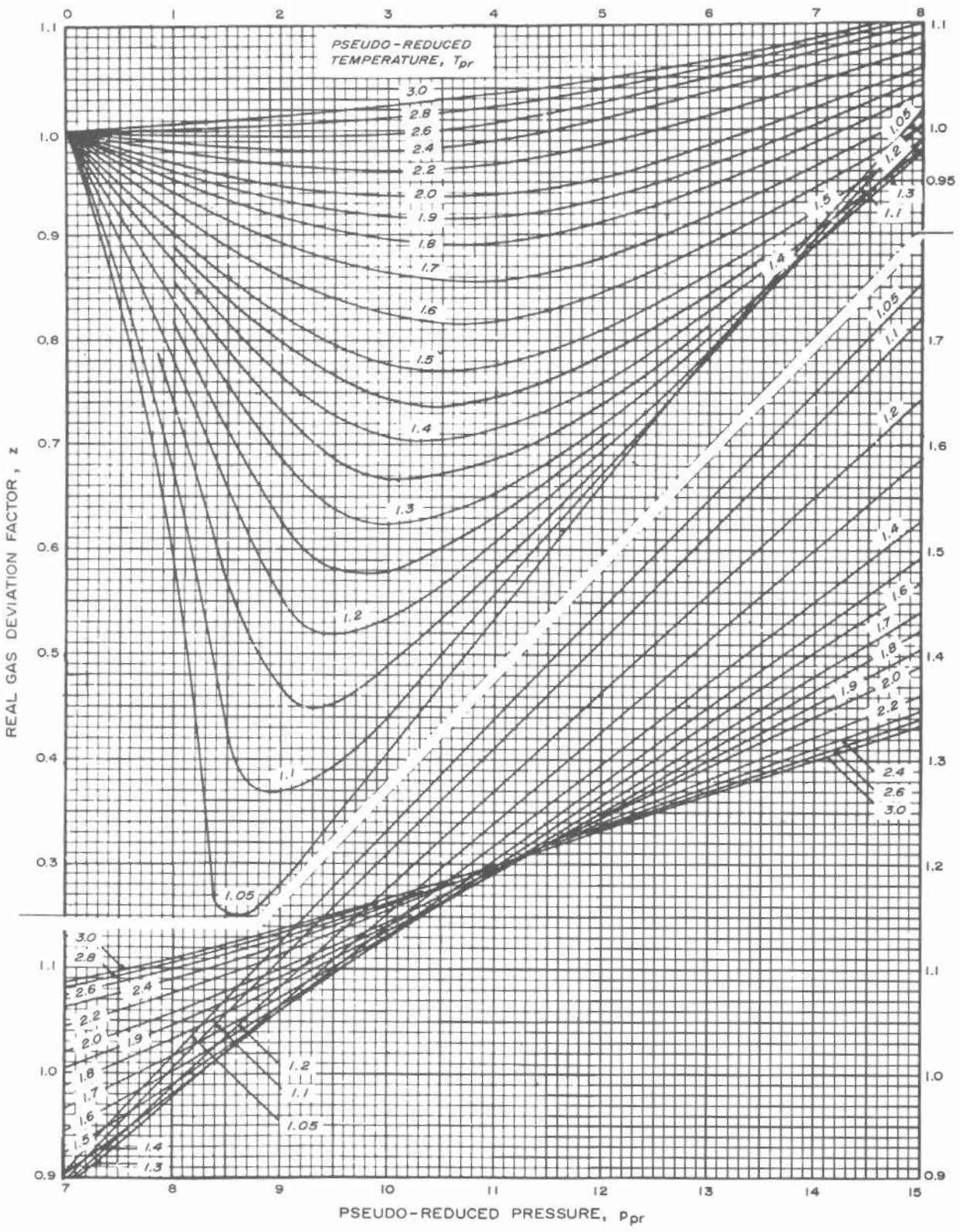

Fig. D.7 Real gas deviation factor for natural gases as a function of pseudoreduced pressure and temperature. After Standing and Katz.[7]

The gas formation volume factor may be estimated from

$$B_g = 5.039 \times 10^{-3} \frac{zT}{p}, \quad \ldots\ldots\ldots\ldots\ldots\ldots (D.6)$$

where z is from Fig. D.7.

The water formation volume factor, B_w, may be estimated from Fig. D.8.

D.3 Rock Pore-Volume Compressibility

The isothermal formation (rock, pore volume) compressibility is generally defined as

$$c_f = \frac{1}{V_p}\left(\frac{\partial V_p}{\partial p}\right)_T . \quad \ldots\ldots\ldots\ldots\ldots\ldots\ldots (D.7)$$

The subscript T indicates that the partial derivative is taken at constant temperature. All compressibilities used in this monograph are isothermal compressibilities; the subscript is frequently omitted. Formation compressibility is defined so that it is a positive number. Thus, Eq. D.7 indicates that as fluid pressure decreases, the pore volume decreases. That occurs because the confining lithostatic pressure is essentially constant while the reservoir is depleted, thus causing compression of the rock.

Several authors[9-11] have attempted to correlate formation compressibility with various physical parameters. The correlations of Hall[10] and van der Knaap[11] have been used extensively in the petroleum literature. Recently, Newman[9] has shown that those correlations do not apply to a very wide range of reservoir rocks. Fig. D.9 shows data for compressibility of limestone samples superimposed on both van der Knaap's and Hall's limestone correlations. In Fig. D.9, and in other figures in this section, the lithostatic pressure is defined as the pressure obtained by multiplying reservoir depth by 1 psi/ft.

Figs. D.10 through D.12 compare Newman's and other data with Hall's sandstone correlation. In preparing the three figures, Newman used the following definitions:[9]

1. Consolidated samples consisted of hard rocks (thin edges could not be broken off by hand).
2. Friable samples could be cut into cylinders but the edges could be broken off by hand.
3. Unconsolidated samples could fall apart under their own weight unless they had undergone special treatment, such as freezing.

As can be seen in the three figures, no correlation would provide a good description of the large suite of samples studied. It is apparent from Fig. D.11 that there is no correlation at all for the friable samples. Fig. D.12 indicates that if there is any correlation for unconsolidated samples, the trend may be opposite the trend for consolidated samples (Fig. D.10).

Unfortunately, Figs. D.9 through D.12 lead to only one conclusion: formation compressibility should be measured for the reservoir being studied. At best, correlations can be expected to give only order-of-magnitude estimates.

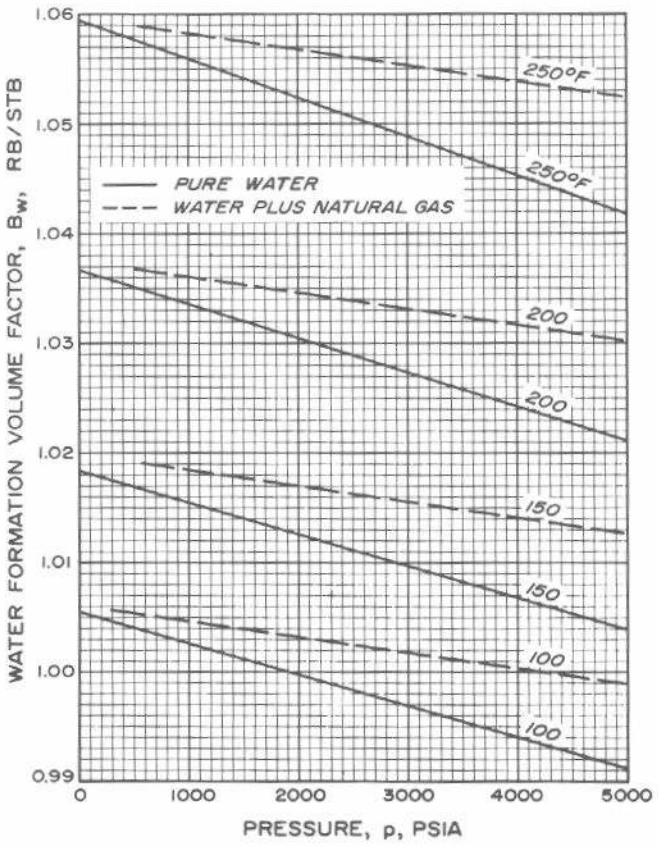

Fig. D.8 Formation volume factor of pure water and a mixture of natural gas and water. Data of Dodson and Standing.[8]

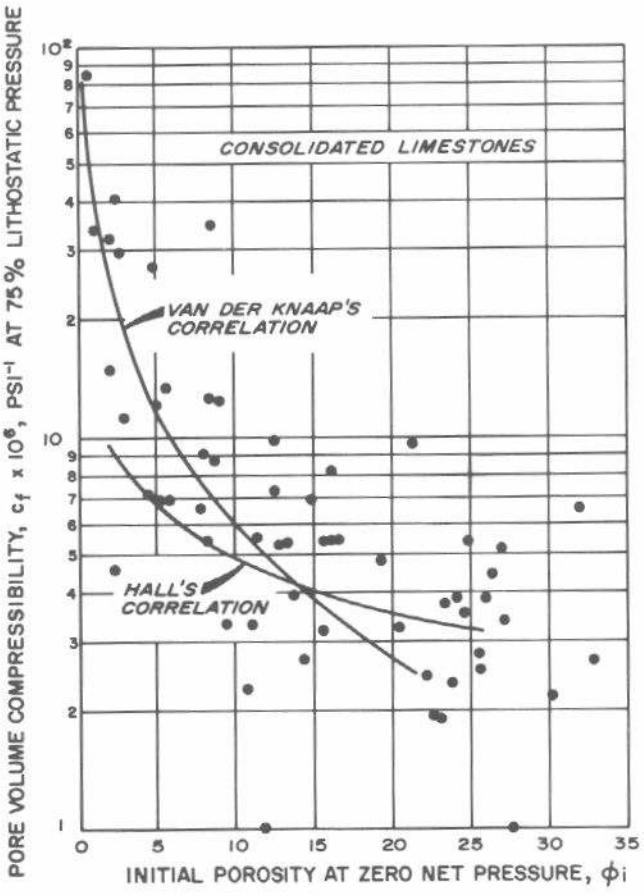

Fig. D.9 Pore-volume compressibility at 75-percent lithostatic pressure vs initial sample porosity for limestones. After Newman.[9]

D.4 Oil Compressibility

The isothermal compressibility of an undersaturated oil (oil above the bubble point) is defined as

$$c_o = -\frac{1}{V_o}\left(\frac{\partial V_o}{\partial p}\right)_T = \frac{1}{\rho_o}\left(\frac{\partial \rho_o}{\partial p}\right)_T = -\frac{1}{B_o}\left(\frac{\partial B_o}{\partial p}\right)_T . \quad \ldots\ldots\ldots\ldots\ldots\ldots\ldots\ldots (D.8)$$

Since the volume of an undersaturated liquid decreases as the pressure increases, c_o is positive.

Generally, oil compressibility should be computed from laboratory PVT data for the oil existing in the reservoir being studied. The final equality in Eq. D.8 is useful for calculating c_o from such data. In some reservoirs, c_o is essentially constant above the bubble point, while in others it varies with pressure.

If laboratory data are not available, Trube's[2] correlation for compressibility of an undersaturated oil (Fig. D.13) may be used. It is necessary to estimate T_{pr} and p_{pr} from Fig. D.1 or Fig. D.2. The pseudoreduced compressibility, c_{pr}, is read from Fig. D.13 and the oil compressibility is estimated from

$$c_o = \frac{c_{pr}}{p_{pc}} . \quad \ldots\ldots\ldots\ldots\ldots\ldots\ldots\ldots\ldots\ldots\ldots\ldots (D.9)$$

Below the bubble point, dissolved gas must be considered in computing compressibilities used in transient test and reservoir analysis. Thus, we define an *apparent* oil compressibility for the region below the bubble point where oil volume increases with pressure as a result of gas going into solution:

$$c_{oa} = -\frac{1}{B_o}\frac{\partial B_o}{\partial p} + \frac{B_g}{B_o}\frac{\partial R_s}{\partial p} . \quad \ldots\ldots\ldots\ldots\ldots\ldots\ldots (D.10)$$

Note that Eq. D.10 reduces to Eq. D.8 above the bubble point when R_s is constant with pressure. If available, laboratory data should be used to estimate c_{oa}; otherwise, correlations may be used with caution. When using correlations, the $\partial R_s/\partial p$ term in Eq. D.10 may be estimated from Fig. D.14 or from

$$\frac{\partial R_s}{\partial p} \simeq \frac{R_s}{(0.83p + 21.75)} . \quad \ldots\ldots\ldots\ldots\ldots\ldots\ldots\ldots (D.11)$$

Eq. D.11 and Fig. D.14 are from Ramey[12] and are based on Standing's data.[5] The gas formation volume factor may be estimated from Eq. D.6, where the z factor is estimated from Fig. D.7. The term $\partial B_o/\partial p$ in Eq. D.10 may be estimated from

$$\frac{\partial B_o}{\partial p} \simeq \frac{\partial R_s}{\partial p} \cdot \frac{\partial B_o}{\partial R_s} , \quad \ldots\ldots\ldots\ldots\ldots\ldots\ldots\ldots (D.12)$$

where the first term on the right-hand side is from Eq. D.11 or Fig. D.14 and the second term on the right-hand side is from Fig. D.15. Oil and gas gravities must be known to use

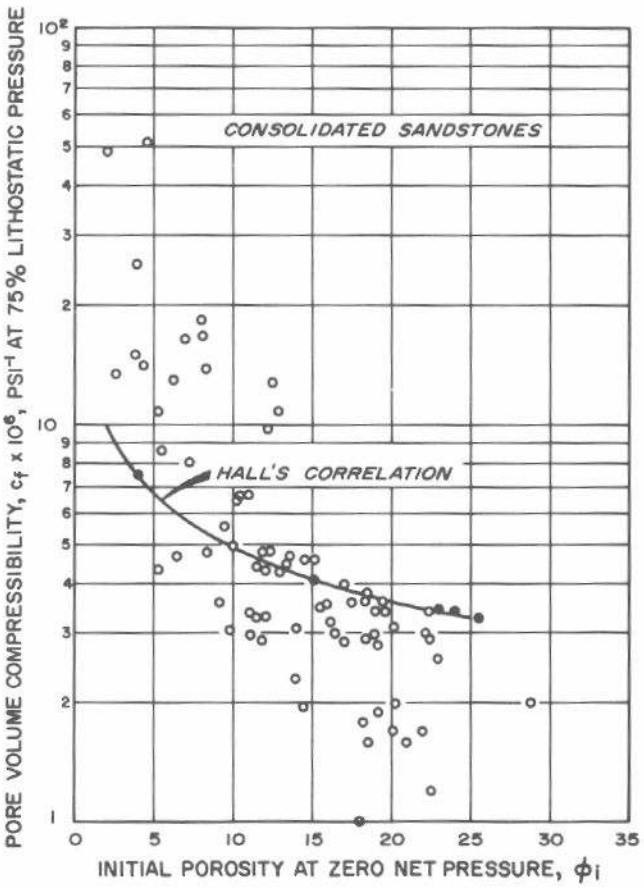

Fig. D.10 Pore-volume compressibility at 75-percent lithostatic pressure vs initial sample porosity for consolidated sandstones. After Newman.[9]

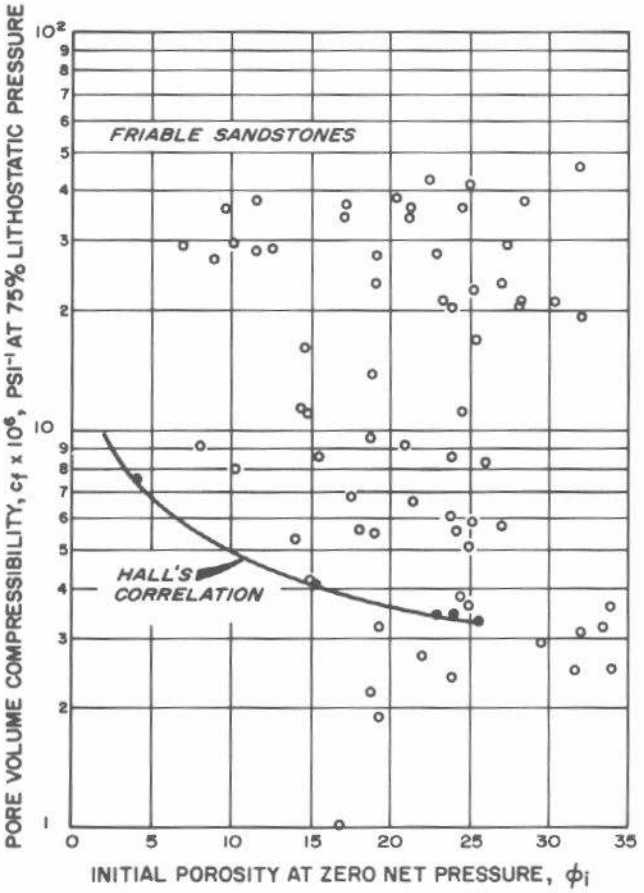

Fig. D.11 Pore-volume compressibility at 75-percent lithostatic pressure vs initial sample porosity for friable sandstones. After Newman.[9]

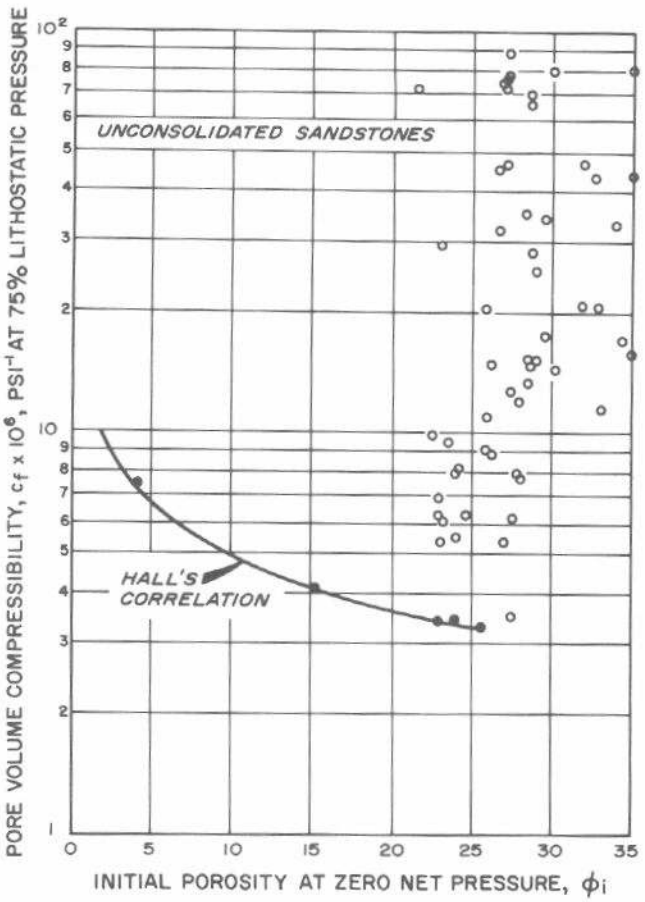

Fig. D.12 Pore-volume compressibility at 75-percent lithostatic pressure vs initial sample porosity for unconsolidated sandstones. After Newman.[9]

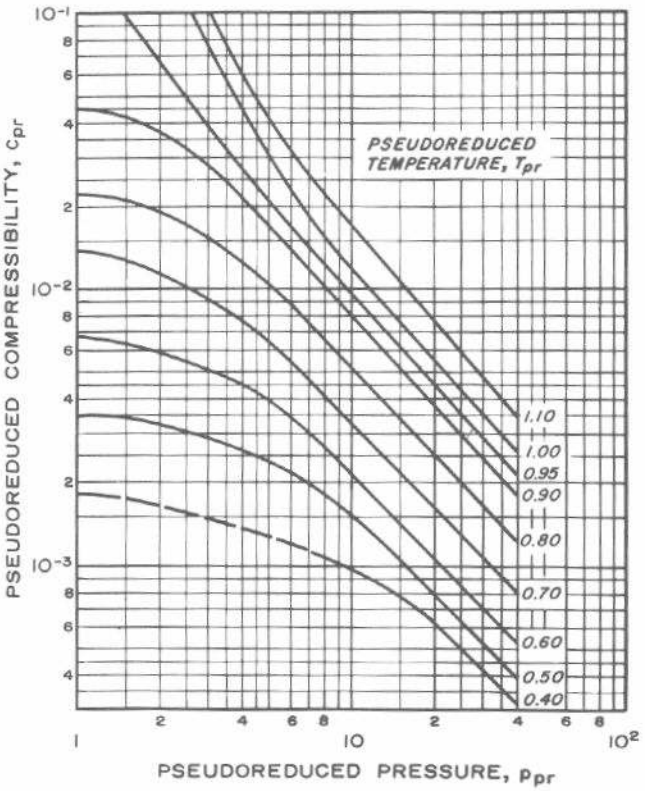

Fig. D.13 Correlation of pseudoreduced compressibility for an undersaturated oil. After Trube.[2]

Fig. D.15. The oil formation volume factor, B_o, may be estimated from Standing's correlation (Fig. D.6).

D.5 Water Compressibility

The water compressibility is defined analogously to the oil compressibility (Eq. D.8). The compressibility of water or brine *without* any solution gas is estimated from Figs. D.16 through D.19. Linear interpolation may be used for intermediate pressures and salinities.

To estimate the compressibility of undersaturated water or brine (that is, with solution gas), Long and Chierici[13] recommend using

$$c_w = (c_w)_{0,n}\left[1 + 0.0088 \times 10^{-Kn}(R_{sw})\right], \quad \ldots . \text{(D.13)}$$

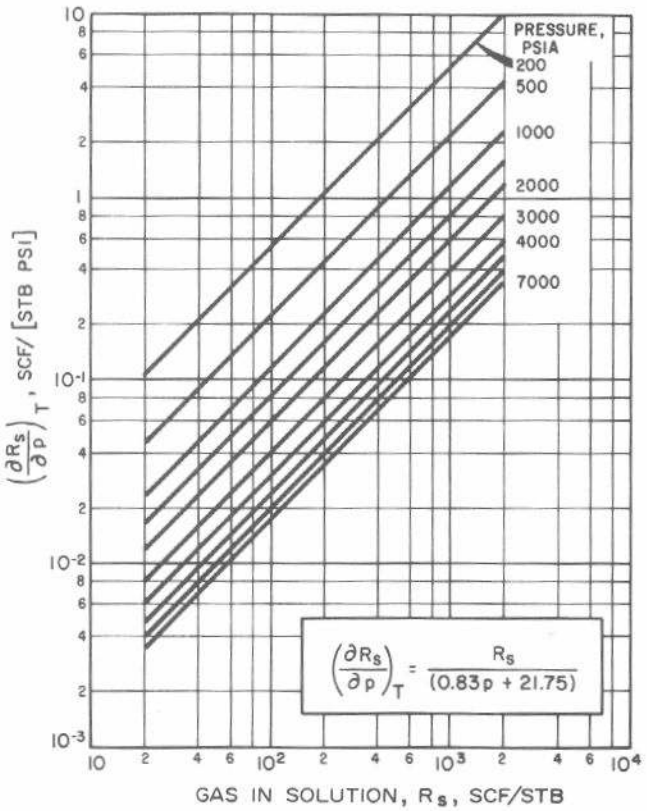

Fig. D.14 Change of gas in solution in oil with pressure vs gas in solution. After Ramey,[12] data of Standing.[5]

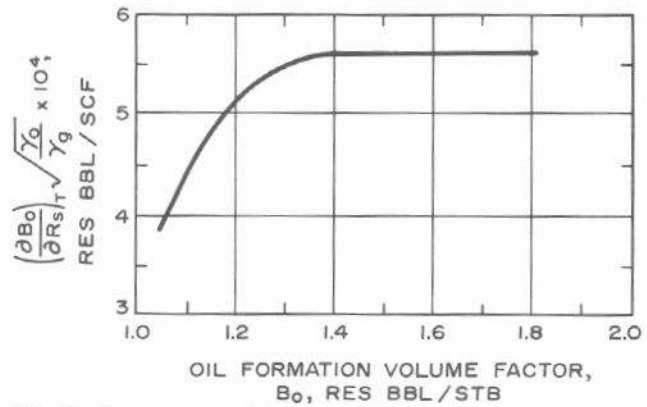

Fig. D.15 Change of oil formation volume factor with gas in solution vs oil formation volume factor. After Ramey.[12]

where

c_w = compressibility of an undersaturated brine containing solution gas and n gram-equivalents of dissolved solids, psi^{-1}

$(c_w)_{0,n}$ = compressibility of a *gas-free* brine containing n gram-equivalents of dissolved solids, psi^{-1}, from Figs. D.16 through D.19

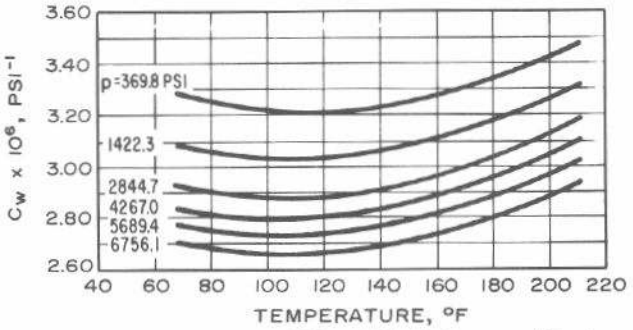

Fig. D.16 Average compressibility of distilled water. After Long and Chierici.[13]

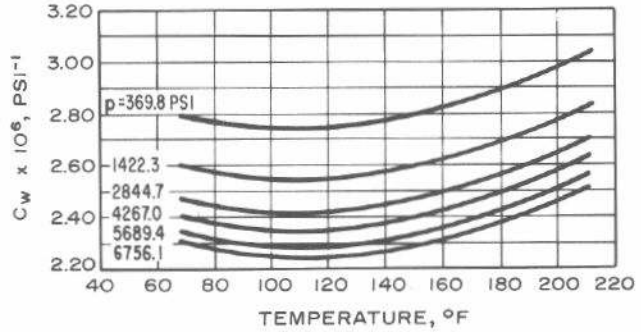

Fig. D.17 Average compressibility of 100,000-ppm NaCl in distilled water. After Long and Chierici.[13]

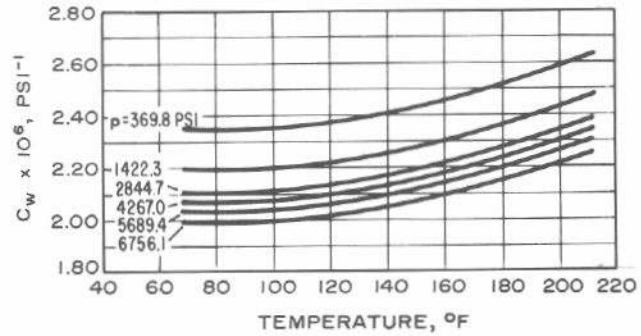

Fig. D.18 Average compressibility of 200,000-ppm NaCl in distilled water. After Long and Chierici.[13]

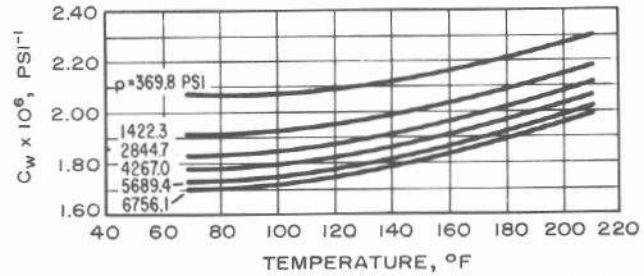

Fig. D.19 Average compressibility of 300,000-ppm NaCl in distilled water. After Long and Chierici.[13]

n = dissolved solids (ppm) ÷ 58,443, concentration of dissolved solids, gram-equivalents/liter

K = Secenov's coefficient, obtained at reservoir temperature from Fig. D.20

R_{sw} = gas solubility in distilled water at the required pressure and temperature, from Fig. D.21, scf/bbl.

An alternate approach to estimating the compressibility of undersaturated water is to use Fig. D.22 to estimate water compressibility at reservoir temperature, pressure, and solution gas-oil ratio. Fig. D.23 is used to estimate the solution gas-water ratio as a function of temperature, pressure, and salinity.

The apparent compressibility of water below the bubble point is given by

$$c_{wa} = -\frac{1}{B_w}\frac{\partial B_w}{\partial p} + \frac{B_g}{B_w}\frac{\partial R_{sw}}{\partial p} . \quad \ldots\ldots\ldots (D.14)$$

Again, it is best to compute c_{wa} from PVT analyses if they are available. However, since they seldom are, the use of

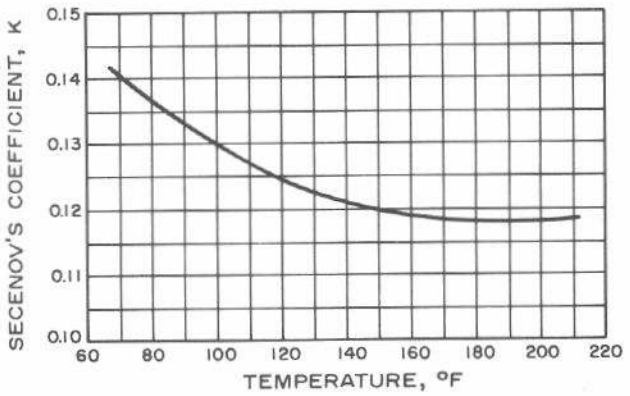

Fig. D.20 Secenov's coefficient for methane, for Eq. D.13. After Long and Chierici.[13]

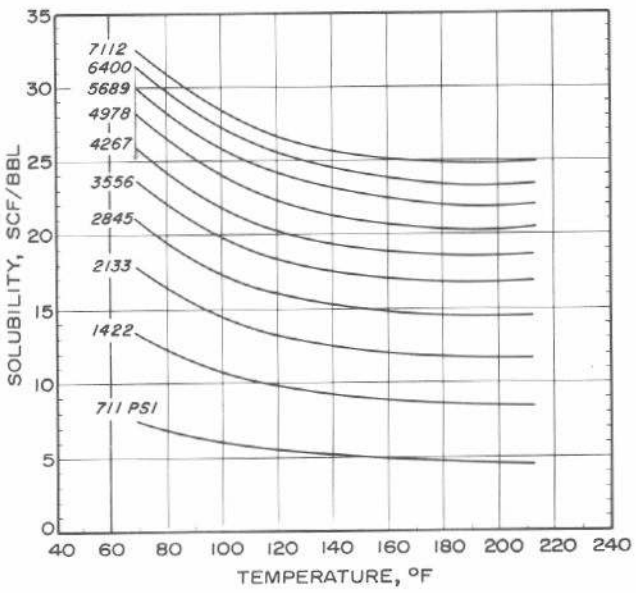

Fig. D.21 Solubility of methane in distilled water. After Long and Chierici.[13]

correlations is often required. The $\partial R_{sw}/\partial p$ term may be approximated from Fig. D.24, while B_w may be approximated from Fig. D.8. B_g is estimated with Eq. D.6. The first term on the right-hand side of Eq. D.14 must be estimated from Fig. D.22 or Eq. D.13.

D.6 Gas Compressibility

Isothermal gas compressibility is defined analogously to the oil compressibility (Eq. D.8). The gas equivalent of Eq. D.8 may be written using the real gas deviation factor, z:

$$c_g = \frac{1}{p} - \frac{1}{z}\left(\frac{\partial z}{\partial p}\right)_T \quad \text{..... (D.15a)}$$

If pseudoreduced pressures and temperatures are introduced into Eq. D.15a, the isothermal gas compressibility may be written as

$$c_g = \frac{1}{p_{pc}}\left[\frac{1}{p_{pr}} - \frac{1}{z}\left(\frac{\partial z}{\partial p_{pr}}\right)_{T_{pr}}\right] \quad \text{..... (D.15b)}$$

The z-factor chart, Fig. D.7, may be used directly to estimate the derivative term for Eq. D.15b.

Gas compressibility also may be estimated from the pseudoreduced-compressibility correlation shown in Figs. D.25 and D.26. The pseudoreduced compressibility is read

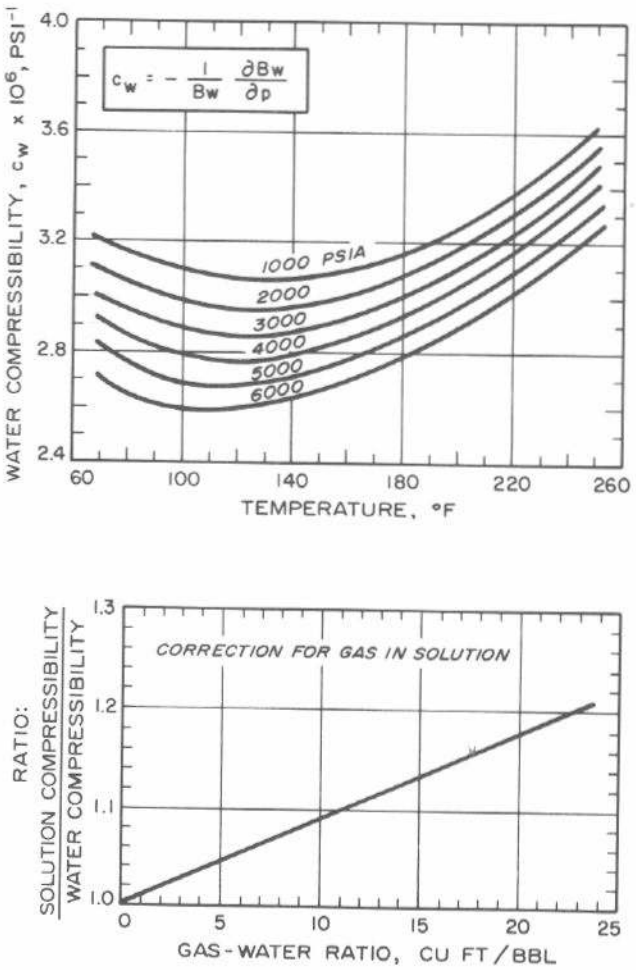

Fig. D.22 Effect of dissolved gas on water compressibility. After Dodson and Standing.[8]

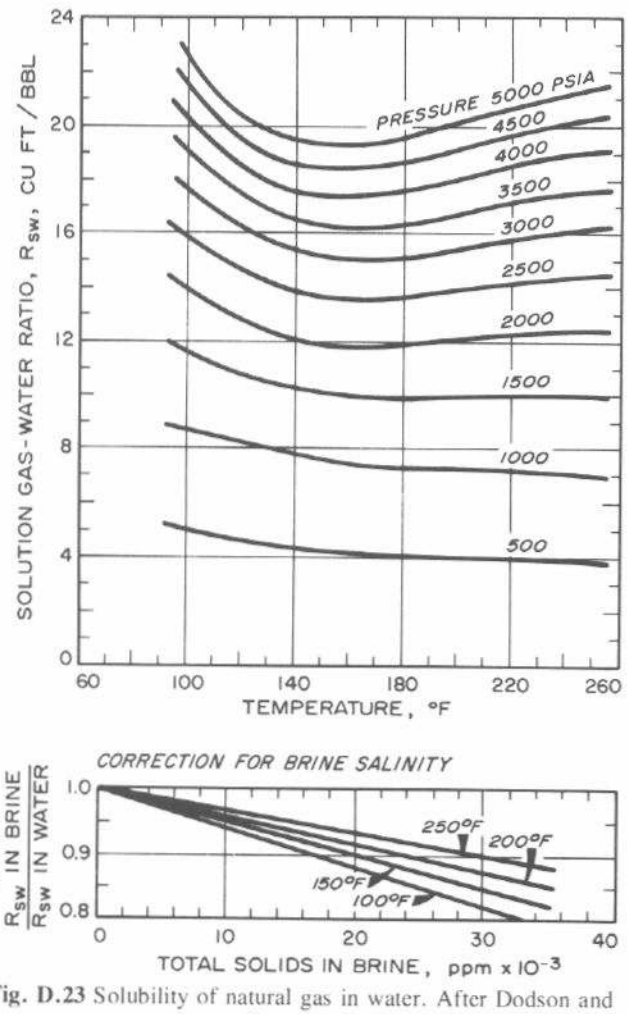

Fig. D.23 Solubility of natural gas in water. After Dodson and Standing.[8]

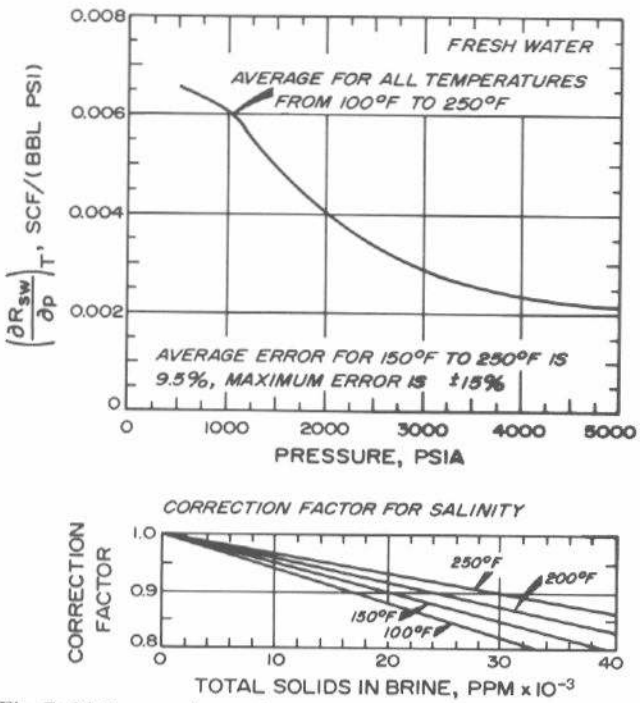

Fig. D.24 Change of natural gas in solution in formation water with pressure vs pressure. Multiply $(\partial R_{sw}/\partial p)_T$ by the correction factor to get result for brine. After Ramey,[12] data of Standing.[5]

from one of those figures and the gas compressibility is computed from

$$c_g = \frac{c_{pr}}{p_{pc}} . \quad \ldots\ldots\ldots\ldots\ldots\ldots\ldots\ldots\ldots\ldots (D.16)$$

D.7 Gas Viscosity

Fig. D.27 is one of the simplest hydrocarbon gas viscosity correlations available.[1] That figure gives gas viscosity as a function of gas gravity, pressure, and temperature. Its use is illustrated by the arrows. For a 0.7-gravity gas at 750 psia and 220 °F, viscosity is 0.0158 cp.

Carr, Kobayashi, and Burrows[15] present a method for estimating natural gas viscosity that is widely used. That method requires knowledge of the gas composition and of the viscosity of each component at atmospheric pressure and reservoir temperature. The viscosity of the mixture at atmospheric pressure is estimated from

$$\mu_{ga} = \frac{\sum_{i=1}^{N} y_i \mu_i \sqrt{M_i}}{\sum_{i=1}^{N} y_i \sqrt{M_i}} , \quad \ldots\ldots\ldots\ldots\ldots\ldots (D.17)$$

where

μ_{ga} = viscosity of the gas mixture at the desired temperature and *atmospheric* pressure, cp
y_i = mole fraction of the ith component
μ_i = viscosity of ith component at the desired temperature and *atmospheric* pressure, obtained from Fig. D.28
M_i = molecular weight of ith component (Table D.1)
N = number of components in the gas.

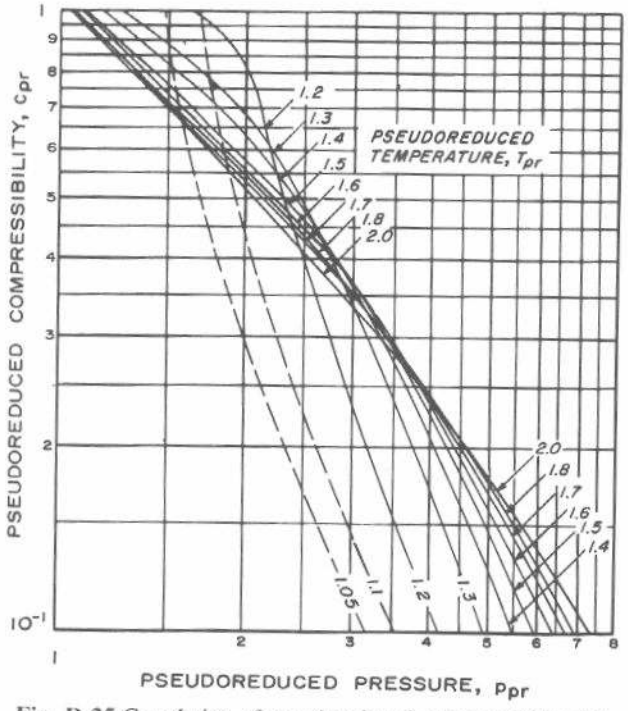

Fig. D.25 Correlation of pseudoreduced compressibility for natural gases. After Trube.[14]

Viscosity for many gaseous components is shown in Fig. D.28 at 1 atm and various temperatures. If the gas composition is not known, Fig. D.29 may be used with gas molecular weight to estimate the gas viscosity at reservoir temperature and atmospheric pressure. Molecular weight is related to gas gravity by

$$M \simeq 29\gamma. \quad \ldots\ldots\ldots\ldots\ldots\ldots\ldots\ldots\ldots\ldots (D.18)$$

The gas viscosity at reservoir pressure is estimated by determining the ratio μ_g/μ_{ga} at the appropriate temperature and pressure from Fig. D.30 or Fig. D.31. Then, that ratio is applied to μ_{ga} computed from Eq. D.17 or Fig. D.29. The pseudoreduced temperatures and pressures for use in Figs. D.30 and D.31 are estimated from Eqs. D.1 through D.4 or from Fig. D.3.

D.8 Oil Viscosity

Whenever possible, oil viscosity should be determined by laboratory measurements at reservoir temperature and pressure. Oil viscosity is usually reported in standard PVT analyses. If such laboratory data are not available, the Chew and Connally[16] correlation for viscosity of gas-saturated oil, Fig. D.32, may be used. Both solution gas-oil ratio and oil viscosity at reservoir temperature and atmospheric pressure must be known to use Fig. D.32. If the dead oil viscosity is not determined from laboratory data, it may be estimated from Fig. D.33.

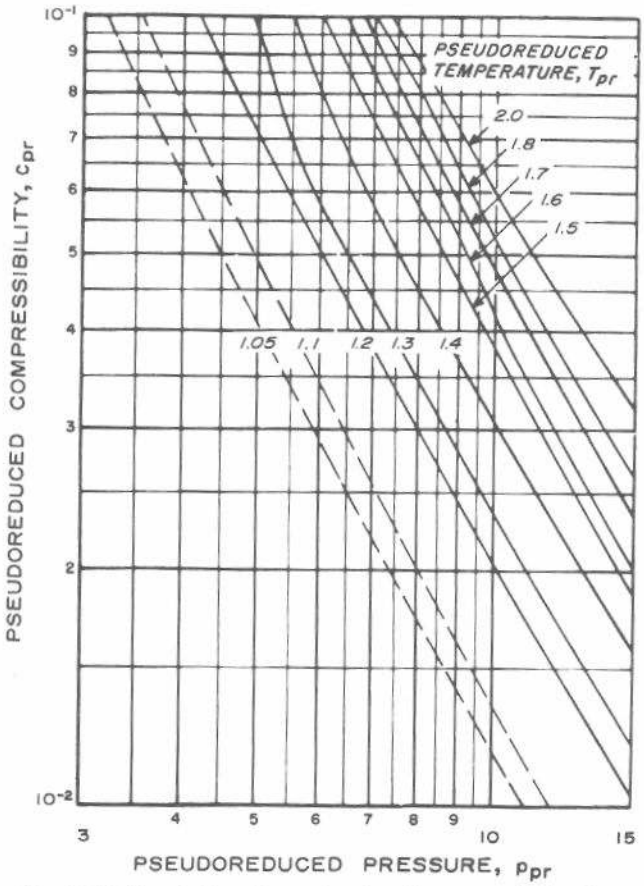

Fig. D.26 Correlation of pseudoreduced compressibility for natural gases. After Trube.[14]

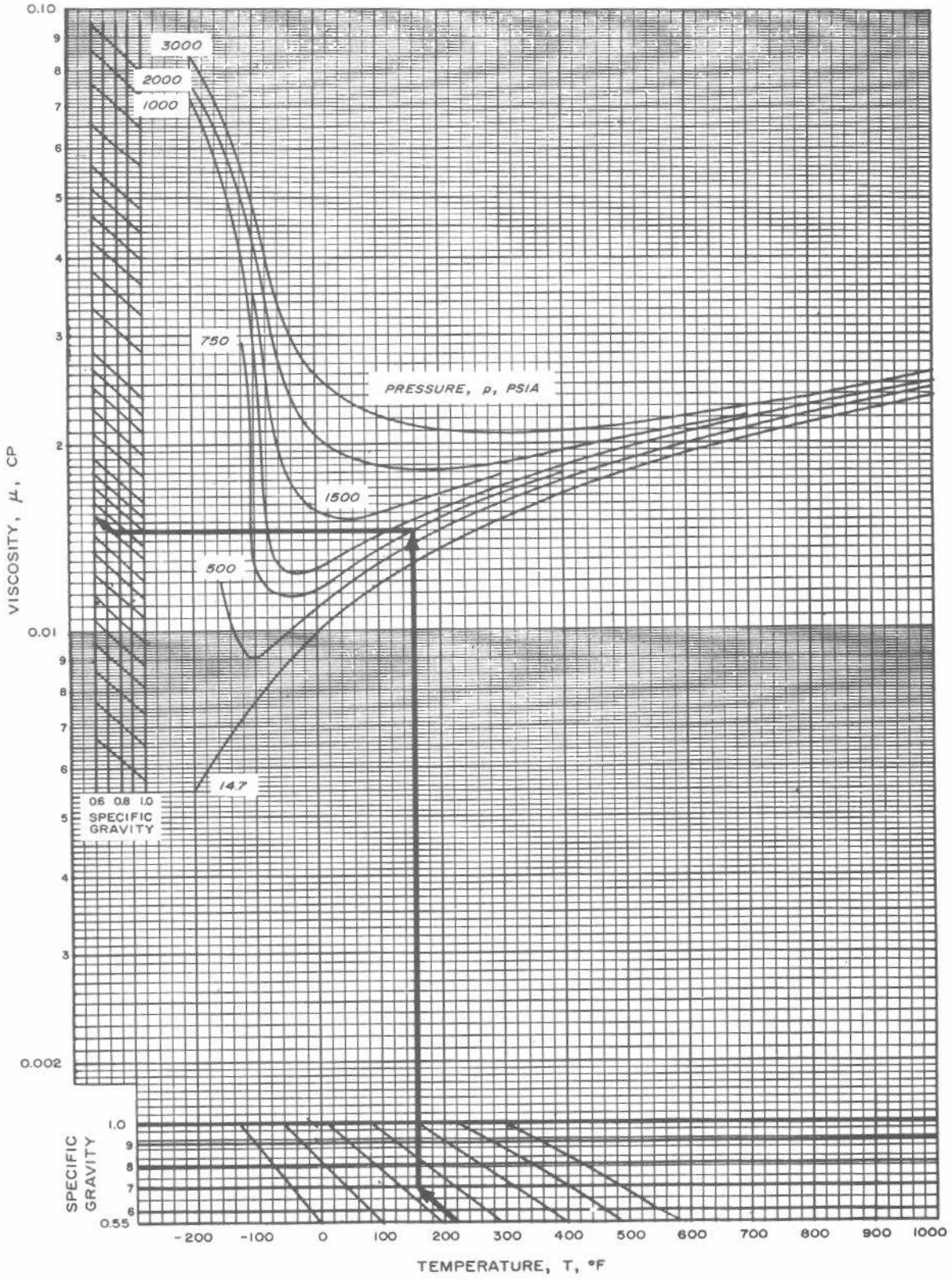

Fig. D.27 Viscosity of hydrocarbon gases.[1]

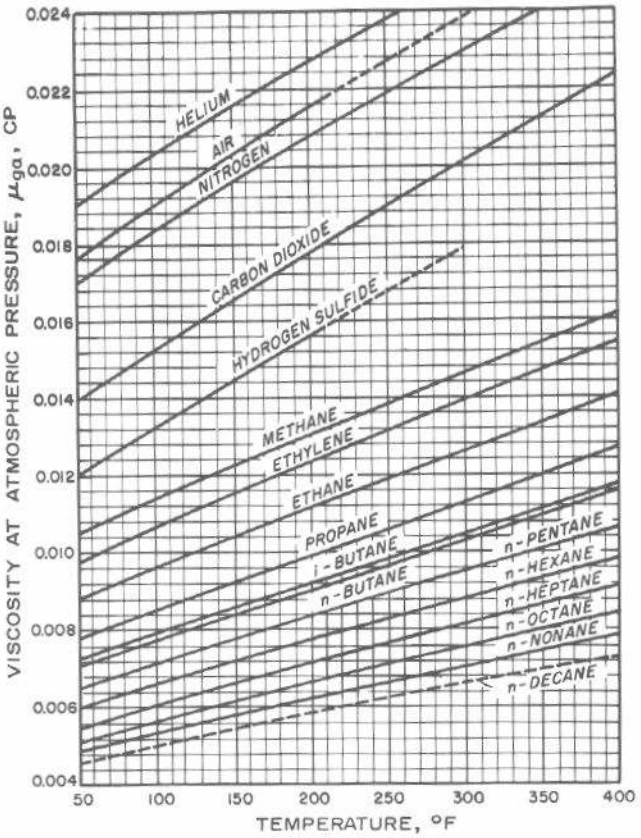

Fig. D.28 Viscosity of pure hydrocarbon gases at 1 atm. After Carr, Kobayashi, and Burrows.[15]

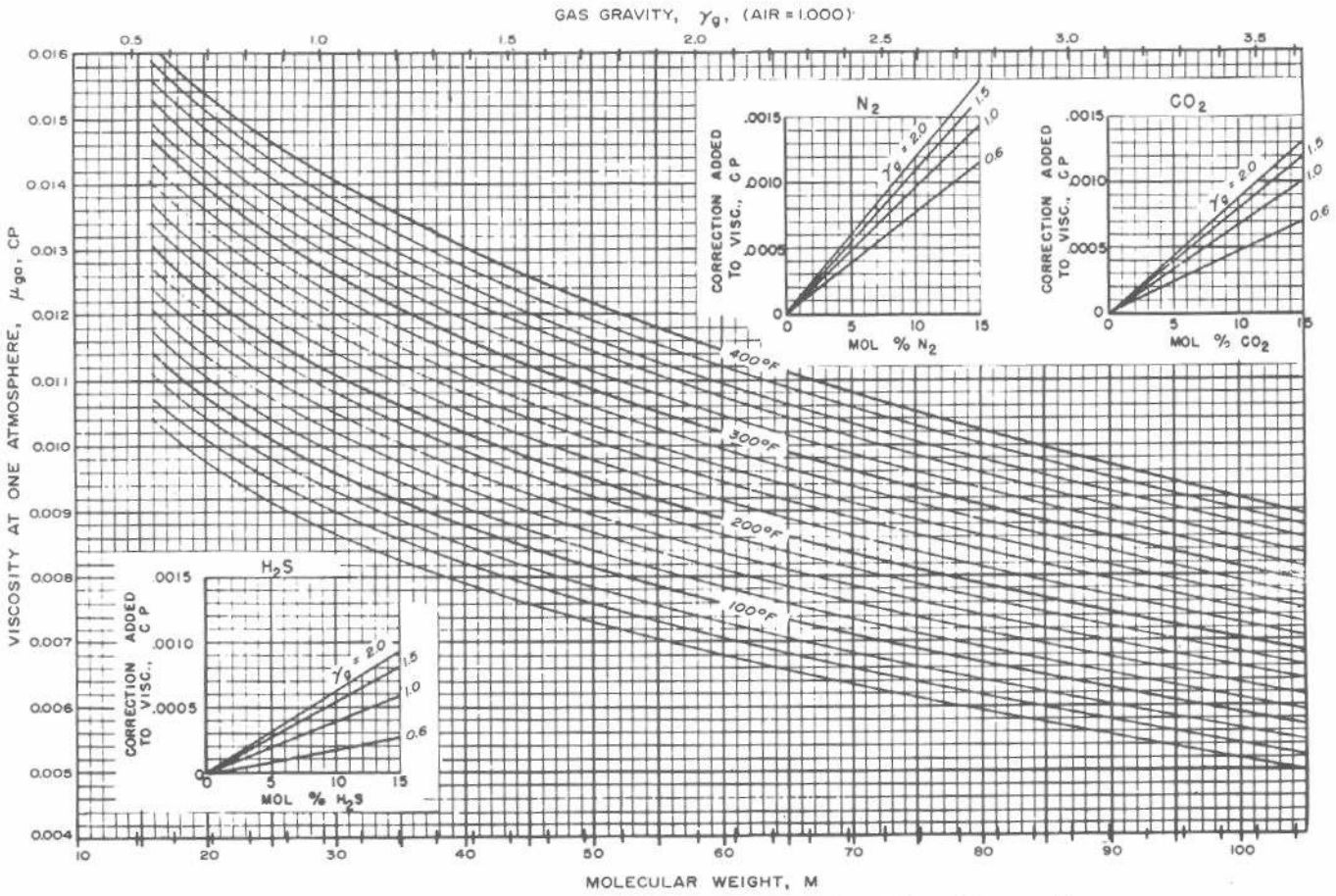

Fig. D.29 Viscosity of natural gases at 1 atm. After Carr, Kobayashi, and Burrows.[15]

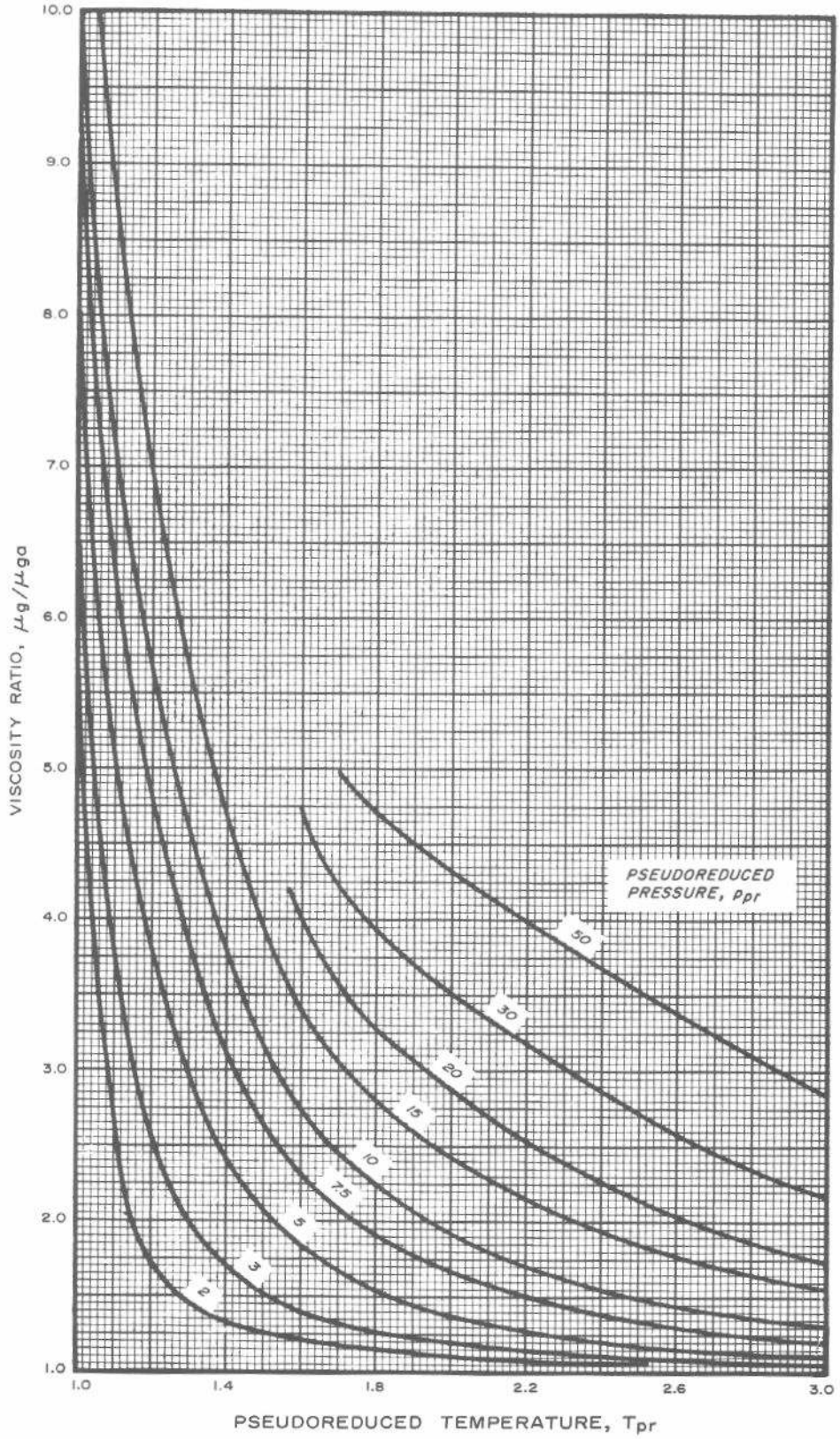

Fig. D.30 Effect of temperature and pressure on gas viscosity; μ_{ga} is estimated from Eq. D.17 or Fig. D.29. After Carr, Kobayashi, and Burrows.[15]

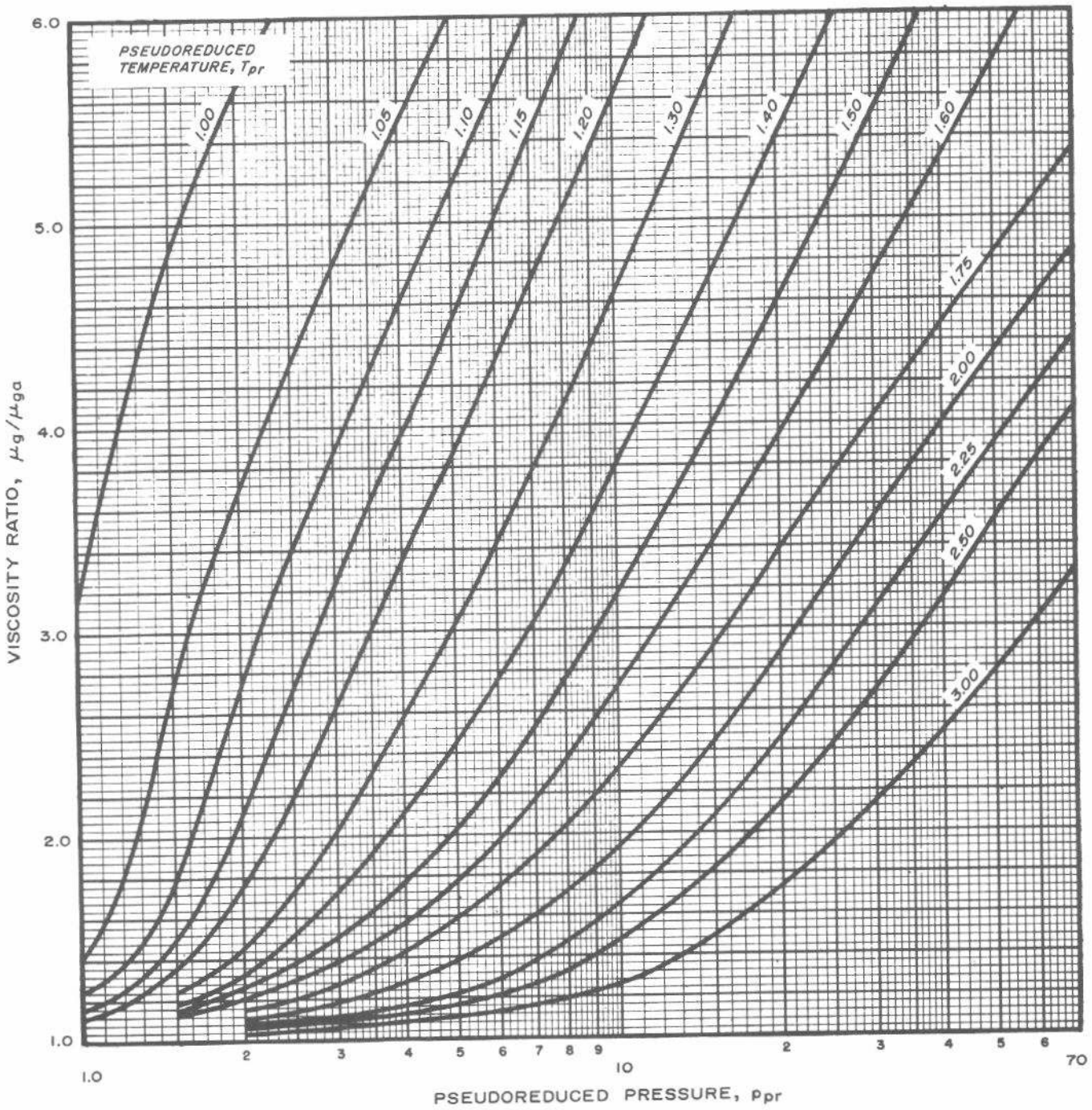

Fig. D.31 Effect of pressure and temperature on gas viscosity; μ_{ga} is estimated from Eq. D.17 or Fig. D.29. After Carr, Kobayashi, and Burrows.[15]

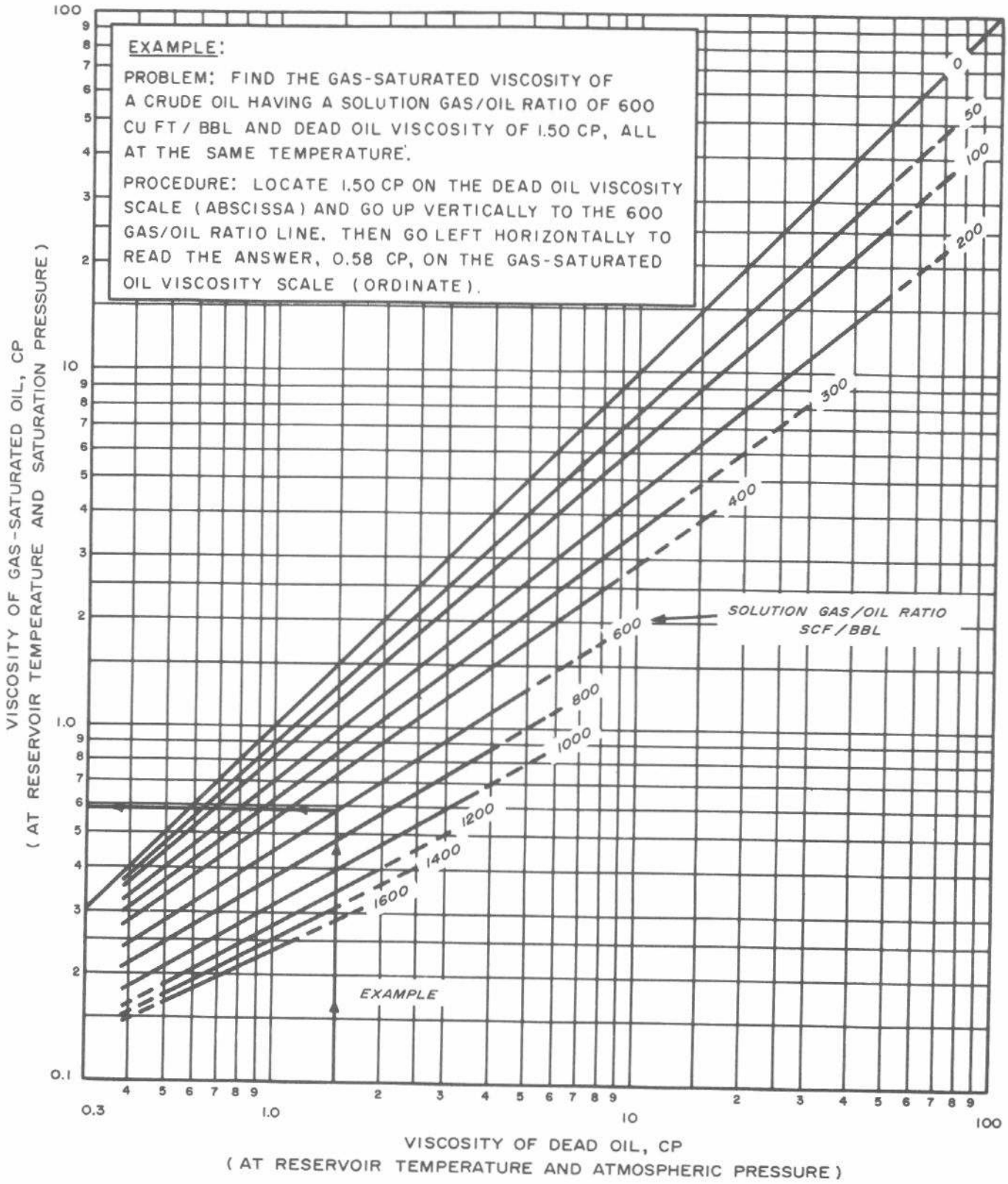

Fig. D.32 Viscosity of gas-saturated crude oil at reservoir temperature and pressure. Dead oil viscosity from laboratory data, or from Fig. D.33. After Chew and Connally.[16]

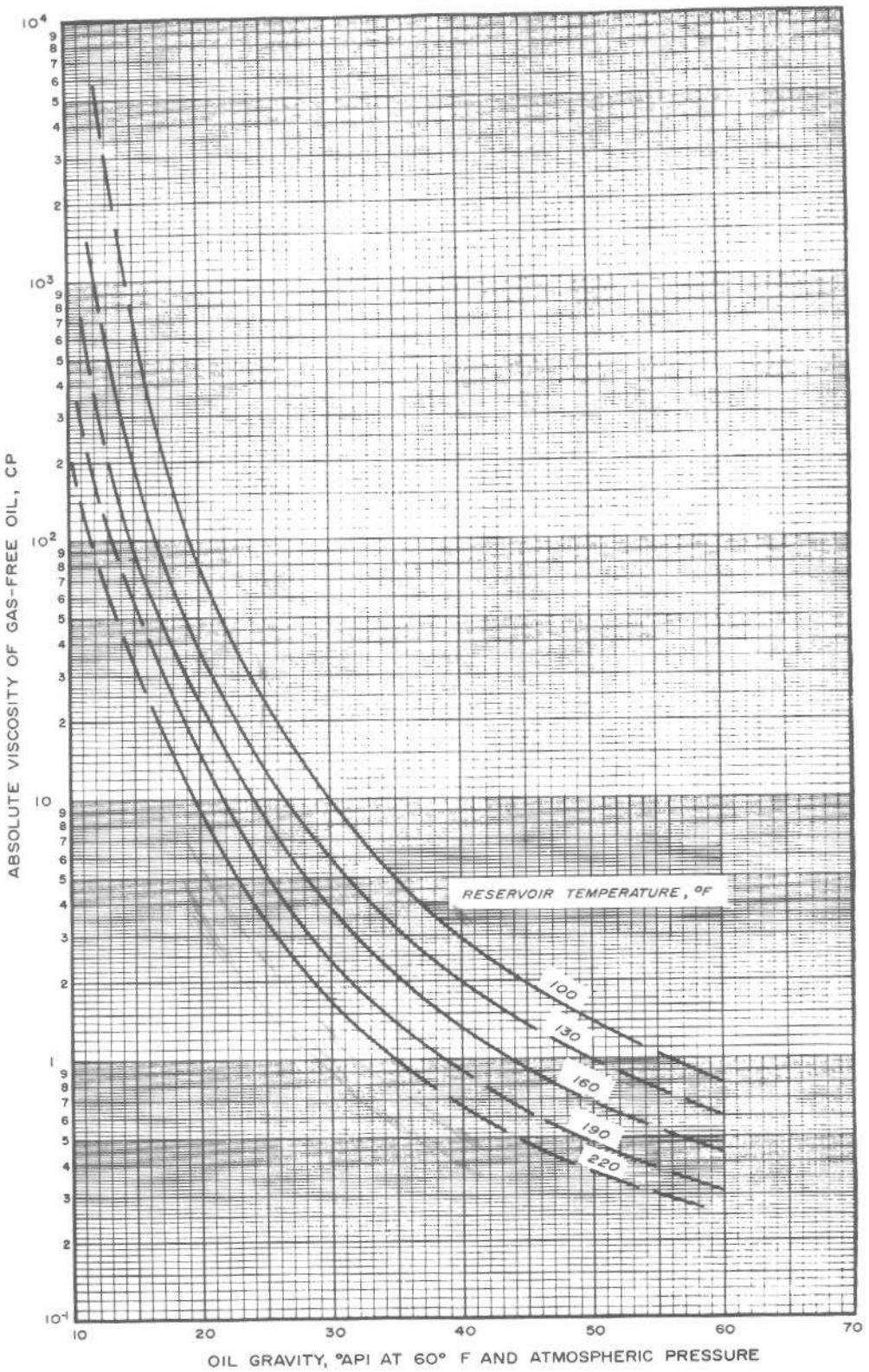

Fig. D.33 Dead oil viscosity at reservoir temperature and atmospheric pressure. After Beal.[17]

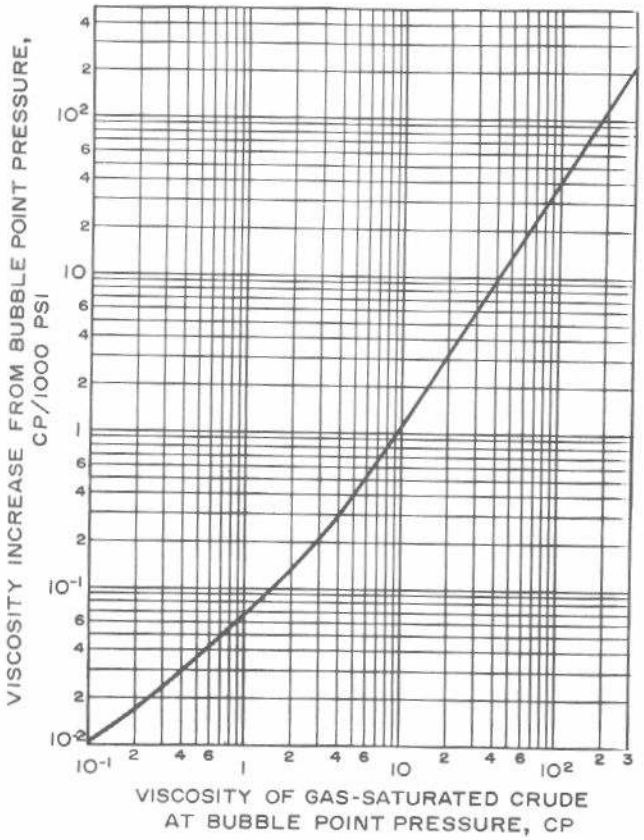

Fig. D.34 Rate of increase of oil viscosity above bubble-point pressure. After Beal.[17]

To estimate oil viscosity above the bubble-point pressure, use Fig. D.34. The figure shows the increase in viscosity above the bubble-point viscosity per 1,000 psi. It is based on a small amount of data, and so should be used only as a rough guide.

D.9 Water Viscosity

Fig. D.35 provides a means for estimating water viscosity as a function of salinity and temperature; a pressure correction is included. There are no provisions in Fig. D.35 for modifying the viscosity of water as a function of gas saturation. As for oil, it is best to measure water viscosity as a function of pressure at reservoir temperature. The water should have the gas saturation and salinity existing in the reservoir.

References

1. *Engineering Data Book*, 9th ed., Gas Processors Suppliers Assn., Tulsa (1972) Sec. 16.
2. Trube, Albert S.: "Compressibility of Undersaturated Hydrocarbon Reservoir Fluids," *Trans.*, AIME (1957) **210**, 341-344.
3. Brown, George G., Katz, Donald L., Oberfell, George G., and Alden, Richard C.: *Natural Gasoline and the Volatile Hydrocarbons*, Natural Gasoline Assn. of America, Tulsa (1948).
4. "Measuring, Sampling, and Testing Crude Oil," API Standard 2500, American Petroleum Institute. Reproduced in Frick, Thomas C. and Taylor, R. William: *Petroleum Production Handbook*, McGraw-Hill Book Co., Inc., New York (1962) **1**, Chap. 16.
5. Standing, M. B.: *Volumetric and Phase Behavior of Oil Field Hydrocarbon Systems*, Reinhold Publishing Corp., New York (1952).
6. Cronquist, Chapman: "Dimensionless PVT Behavior of Gulf Coast Reservoir Oils," *J. Pet. Tech.* (May 1973) 538-542.
7. Standing, Marshall B. and Katz, Donald L.: "Density of Natural Gases," *Trans.*, AIME (1942) **146**, 140-149.
8. Dodson, C. R. and Standing, M. B.: "Pressure-Volume-Temperature and Solubility Relations for Natural-Gas-Water Mixtures," *Drill. and Prod. Prac.*, API (1944) 173-179.
9. Newman, G. H.: "Pore-Volume Compressibility of Consolidated, Friable, and Unconsolidated Reservoir Rocks Under Hydrostatic Loading," *J. Pet. Tech.* (Feb. 1973) 129-134.
10. Hall, Howard N.: "Compressibility of Reservoir Rocks," *Trans.*, AIME (1953) **198**, 309-311.
11. van der Knaap, W.: "Nonlinear Behavior of Elastic Porous Media," *Trans.*, AIME (1959) **216**, 179-187.
12. Ramey, H. J., Jr.: "Rapid Method of Estimating Reservoir Compressibility," *J. Pet. Tech.* (April 1964) 447-454; *Trans.*, AIME, **231**.
13. Long, Giordano and Chierici, Gianluigi: "Salt Content Changes Compressibility of Reservoir Brines," *Pet. Eng.* (July 1961) B-25 to B-31.
14. Trube, Albert S.: "Compressibility of Natural Gases," *Trans.*, AIME (1957) **210**, 355-357.
15. Carr, Norman L., Kobayashi, Riki, and Burrows, David B.: "Viscosity of Hydrocarbon Gases Under Pressure," *Trans.*, AIME (1954) **201**, 264-272.
16. Chew, Ju-Nam and Connally, Carl A., Jr.: "A Viscosity Correlation for Gas-Saturated Crude Oils," *Trans.*, AIME (1959) **216**, 23-25.
17. Beal, Carlton: "The Viscosity of Air, Water, Natural Gas, Crude Oil and Its Associated Gases at Oil-Field Temperatures and Pressures," *Trans.*, AIME (1946) **165**, 94-115.
18. Matthews, C. S. and Russell, D. G.: *Pressure Buildup and Flow Tests in Wells*, Monograph Series, Society of Petroleum Engineers of AIME, Dallas (1967) **1**, Appendix G.

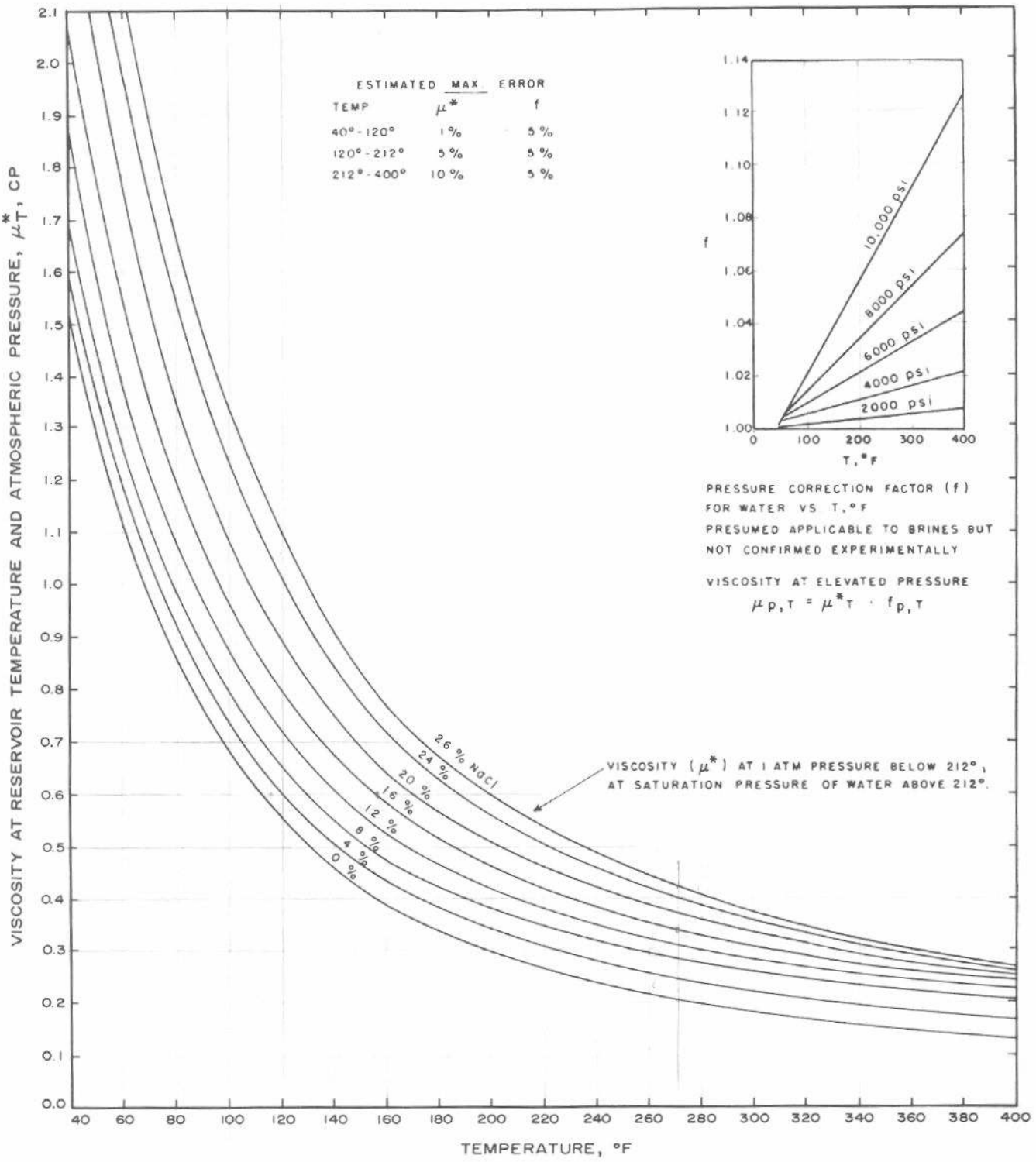

Fig. D.35 Water viscosity at various salinities and temperatures. After Matthews and Russell, data of Chesnut.[18]

Appendix E

Summary of Well Test Analysis Methods

E.1 Introduction

This monograph considers many types of well tests and discusses the influence of many factors on well-test response. Although some analysis techniques are unique, most have similarities. This appendix summarizes the equations and data plots for a variety of single-well-test analysis methods. Although the monograph is consistent in nomenclature and sign convention, and although many of the equations used are the same, there are some slight variations from one test type to another that are most clearly described in the tabular form presented here. This appendix also shows buildup-curve shapes resulting from various influences.

E.2 Pressure-Buildup Curve Shapes

Conceptually, graphs of pressure buildup, drawdown, injectivity, or falloff behavior in individual wells can be divided into three areas: (1) front-end effects (wellbore storage, fractures, damage); (2) the semilog straight line for which most analysis techniques apply; and (3) boundary effects. Those three portions are illustrated for a pressure buildup case in Fig. E.1. Throughout the text, criteria have been given for when each effect can be expected to be significant.

Wellbore storage effects always take priority at early time and can completely obscure early-time formation response. Thus, afterflow can be devastating to test analysis methods that depend heavily on early-time data. Fig. E.1 shows that fracture cases and large-negative-skin cases approach the semilog straight line from above when wellbore storage is small. As also shown in that figure, that behavior can be hidden by large wellbore storage effects, so the buildup curve may have the characteristic shape associated with wellbore storage only, or with a positive skin. There is no guarantee that a fractured-well pressure buildup curve will approach the semilog straight line from above.

Analysis methods that use late-time pressure data can be highly sensitive to variations in boundary conditions. Attempting to find a semilog straight line in late-time data affected by boundary or interference effects from offset wells can give highly misleading results. Generally, it is advisable to make time checks to estimate the end of the semilog straight line. Application of late-time analysis methods, such as the Muskat method, to middle-time data can also give misleading results. In some situations, as when wellbore storage effects are extremely severe or induced fractures are deep ($x_e/x_f < 10$), a classic semilog straight line may never develop, or its slope may be incorrect so that correction factors must be applied to apparent semilog slopes. (Correction factors are given for vertically fractured wells in Section 11.3.) Sometimes type-curve matching techniques may be used for those situations as well as for situations with severe wellbore storage. Curve matching is described in detail in Section 3.3 and is illustrated in other places in the monograph.

E.3 Well-Test Analysis Equations

Table E.1 summarizes analysis equations for unfractured, single-well drawdown, buildup, injectivity, and falloff tests. The equation numbers given in that table refer to the equations listed below. Also shown are the sections containing thorough discussions of the tests, cautions, and alternate analysis techniques. Table E.1 is presented to provide a quick reference and summary only, and should not be used as a replacement for material presented elsewhere in the monograph. To do so blindly will lead to incorrect analysis results.

Time Axis

$$\sum_{j=1}^{N} \frac{(q_j - q_{j-1})}{q_N} \log(t - t_{j-1}). \quad \ldots\ldots\ldots\ldots \text{(E.1)}$$

$$\sum_{j=1}^{N} \frac{q_j}{q_N} \log\left(\frac{t_N - t_{j-1} + \Delta t}{t_N - t_j + \Delta t}\right). \quad \ldots\ldots\ldots\ldots \text{(E.2)}$$

Permeability

$$k = \frac{-162.6\, qB\mu}{mh}. \quad \ldots\ldots\ldots\ldots\ldots\ldots \text{(E.3)}$$

$$k = \frac{162.6\, B\mu}{m'h}. \quad \ldots\ldots\ldots\ldots\ldots\ldots \text{(E.4)}$$

$$k = \frac{162.6\,B\mu}{m_q\,(p_i - p_{wf})\,h} \quad \text{(E.5)}$$

$$k = \frac{162.6\,qB\mu}{mh} \quad \text{(E.6)}$$

$$k = \frac{141.2\,qB\mu}{h\,(\bar{p} - p_{ws})_{\text{int}}}\, p_{D\text{Mint}}(t_{pDA}). \quad \text{Use Fig. 5.10.} \quad \text{(E.7)}$$

Skin Factor

$$s = 1.1513\left[\frac{p_{1\text{hr}} - p_i}{m} - \log\left(\frac{k}{\phi\mu c_t r_w{}^2}\right) + 3.2275\right]. \quad \text{(E.8)}$$

$$s = 1.1513\left[\frac{\Delta p_{1\text{hr}} - p_{ws}(\Delta t{=}0)}{m} - \log\left(\frac{k}{\phi\mu c_t r_w{}^2}\right) + 3.2275\right]. \quad \text{(E.9)}$$

$$s = 1.1513\left[\frac{b'}{m'} - \log\left(\frac{k}{\phi\mu c_t r_w{}^2}\right) + 3.2275\right]. \quad \text{(E.10)}$$

$$s = 1.1513\left[\frac{(1/q)_{1\text{hr}}}{m_q} - \log\left(\frac{k}{\phi\mu c_t r_w{}^2}\right) + 3.2275\right]. \quad \text{(E.11)}$$

$$s = 1.1513\left[\frac{p_{1\text{hr}} - p_{wf}(\Delta t{=}0)}{m} - \log\left(\frac{k}{\phi\mu c_t r_w{}^2}\right) + 3.2275\right]. \quad \text{(E.12)}$$

$$s = 1.1513\left[\frac{\Delta p_{1\text{hr}}}{m} - \log\left(\frac{k}{\phi\mu c_t r_w{}^2}\right) + 3.2275\right]. \quad \text{(E.13)}$$

Connected Pore Volume

$$\phi hA = -\frac{0.23395\,qB}{c_t m^*}. \quad \text{(E.14)}$$

$$\phi hA = -\frac{0.00471\,kh}{\mu c_t m_M} \quad \text{Closed square.} \quad \text{(E.15a)}$$

$$\phi hA = -\frac{0.00233\,kh}{\mu c_t m_M} \quad \text{Square with constant-pressure boundaries.} \quad \text{(E.15b)}$$

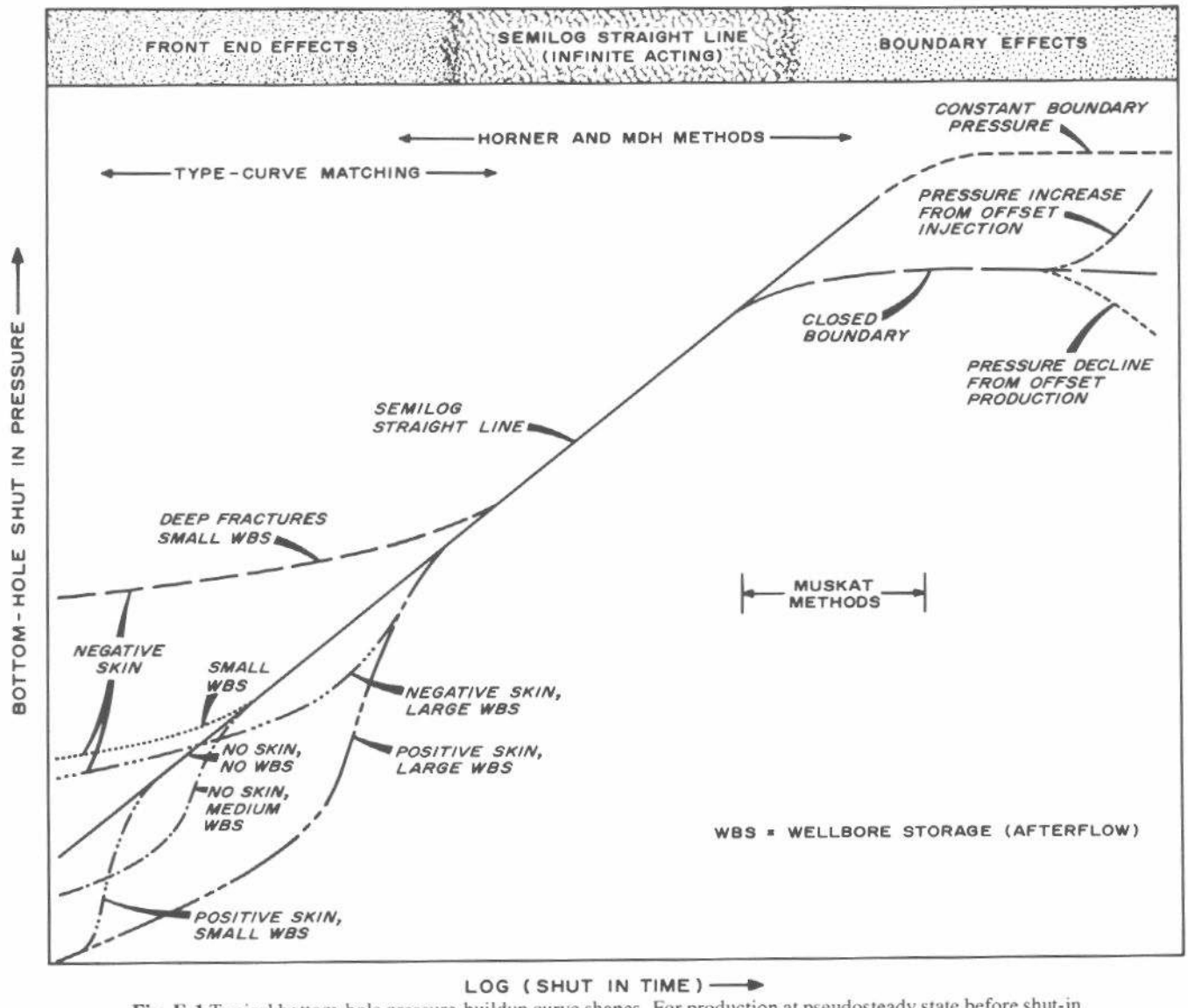

Fig. E.1 Typical bottom-hole pressure-buildup curve shapes. For production at pseudosteady state before shut-in.

TABLE E.1—SUMMARY OF COMMON WELL-TEST ANALYSIS EQUATIONS. EQUATIONS ARE IN SECTION E.3 OR REFERENCED CHAPTER.

Test Type	Analysis Method	Analysis Graph Axes: Pressure	Analysis Graph Axes: Time	Slope Data: Sign of Slope	Slope Data: Relation to m[9]	Permeability Equation	Skin-Factor Equation	Connected Pore-Volume Equation	Limits of Straight-Line Equation: Beginning	Limits of Straight-Line Equation: End	Section Number in Text	Comments
Drawdown	MDH	p_{wf}	$\log t$	−	$+m$	E.3	E.8	N/A	E.16	E.21	3.2	
	Developed system	[1]$p_{wf}-m^*\Delta t$	$\log \Delta t$	−	$+m$	E.3	E.9	N/A	E.16	E.21	3.4	
	Reservoir limit	p_{wf}	t	−	$+m^*$	N/A	N/A	E.14	E.17	—	3.5	
	Variable rate	$(p_i-p_{wf})/q_N$	Eq. E.1	+	$+m'$	E.4	E.10	N/A	E.16	E.21	4.2	Many specialized forms. Line limits approximate.
	Constant pressure	$1/q$	$\log t$	+	$+m_q$	E.5	E.11	N/A	E.18	—	4.6	Also curve matching with Fig. 4.12.
Buildup	Horner	p_{ws}	[2]$\log[(t_p+\Delta t)/\Delta t]$	−	$-m$	E.6	E.12	N/A	E.19	[3]E.22	5.2, 5.3	
	MDH	p_{ws}	$\log \Delta t$	+	$+m$	E.6	E.12	N/A	E.19	[4]E.22	5.3	
	Muskat	$\log(\bar{p}-p_{ws})$	Δt	−	$+m_M$	[5]E.7	N/A	E.15	[6]E.20	[6]E.20	5.3	Square system only.
	Developed system	[7]$\Delta p_{\Delta t}$	$\log \Delta t$	+	$+m$	E.6	E.13	N/A	E.19	[4]E.22	5.3	Line limits approximate.
	Developed system	[1]$p_{ws}-m^*\Delta t$	$\log \Delta t$	+	$+m$	E.6	E.9	N/A	E.19	[4]E.22	5.3	Line limits approximate.
	Variable production rate	p_{ws}	Eq. E.2	−	$-m$	E.6	E.12	N/A	—	—	5.4	Short production time only; see Section 5.4.
Injectivity	MDH	p_{wf}	$\log t$	+	$+m$	E.3	E.8	N/A	E.16	E.21	7.2	[8]See footnotes.
	Developed system	[1]$p_{wf}-m^*\Delta t$	$\log \Delta t$	+	$+m$	E.3	E.9	N/A	E.16	E.21	3.4	[8]See footnotes.
	Reservoir limit	p_{wf}	t	+	$+m^*$	N/A	N/A	E.14	E.17	—	3.5	[8]See footnotes.
	Variable rate	$(p_i-p_{wf})/q_N$	Eq. E.1	+	$+m'$	E.4	E.10	N/A	E.16	E.21	4.2	[8]Many specialized forms.
	Constant pressure	$1/q$	$\log t$	−	$+m_q$	E.5	E.11	N/A	E.18	—	4.6	[8]Also curve matching with Fig. 4.12.
Falloff	Horner	p_{ws}	[2]$\log[(t_p+\Delta t)/\Delta t]$	+	$-m$	E.6	E.12	N/A	E.19	[3]E.22	7.3	[8]See footnotes.
	MDH	p_{ws}	$\log \Delta t$	−	$+m$	E.6	E.12	N/A	E.19	[4]E.22	5.3	[8]See footnotes.
	Muskat	$\log(\bar{p}-p_{ws})$	Δt	+	$+m_M$	[5]E.7	N/A	E.15	[6]E.20	[6]E.20	5.3	[8]Square system only.
	Developed system	[7]$\Delta p_{\Delta t}$	$\log \Delta t$	−	$+m$	E.6	E.13	N/A	E.19	[4]E.22	5.3	[8]Line limits approximate.
	Developed system	[1]$p_{ws}-m^*\Delta t$	$\log \Delta t$	−	$+m$	E.6	E.9	N/A	E.19	[4]E.22	5.3	[8]Line limits approximate.
	Variable injection rate	p_{ws}	Eq. E.2	+	$-m$	E.6	E.12	N/A	—	—	5.4	[8]Short injection time only; see Section 5.4.

1. Requires linear pressure change before testing.
2. t_p from Eq. 5.9
3. Use Fig. 5.6
4. Use Fig. 5.7.
5. Use Fig. 5.10.
6. Use Fig. 5.11.
7. Extrapolate prior pressure trend to get $\Delta p_{\Delta t}$.
8. Liquid filled, unit mobility ratio assumed.
9. Use as an equation, (slope value) = $\pm m$.

Beginning Time for Analyzed Straight Line

$$t \simeq \frac{(200{,}000 + 12{,}000\,s)\,C}{(kh/\mu)} \quad \text{(E.16)}$$

$$t \simeq \frac{\phi\mu c_t A}{0.0002637\,k}\,(t_{DA})_{pss} \quad \text{(E.17)}$$

$$t \simeq \frac{19 \times 10^6\,\phi\mu c_t r_w{}^2}{k} \quad \text{(E.18)}$$

$$\Delta t \simeq \frac{170{,}000\,C e^{0.14s}}{(kh/\mu)} \quad \text{(E.19)}$$

$$\Delta t = \frac{\phi\mu c_t A}{0.0002637\,k}\,(\Delta t_{DA})_{sl}. \quad \text{Use with Fig. 5.11.} \quad \text{(E.20)}$$

End Time for Semilog Straight Line

$$t \simeq \frac{\phi\mu c_t A}{0.0002637\,k}\,(t_{DA})_{eia} \quad \text{(E.21)}$$

$$\Delta t \simeq \frac{\phi\mu c_t A}{0.0002637\,k}\,(\Delta t_{DA})_{esl}. \quad \text{Use with Figs. 5.6 and 5.7.} \quad \text{(E.22)}$$

Nomenclature

a = distance to an image well, Appendix B, ft
a_D = dimensionless distance to an image well, Appendix B
A = area, sq ft
b = intercept on Cartesian plot of transient-test pressure data, psi
b' = intercept on semilog plot of transient-test pressure data normalized by rate, psi/(STB/D)
B = formation volume factor, RB/STB
B_g = gas formation volume factor, RB/scf
B_o = oil formation volume factor, RB/STB
B_w = water formation volume factor, RB/STB
c = compressibility, psi^{-1}
c_f = formation (rock, pore volume) compressibility, psi^{-1}
c_g = gas compressibility, psi^{-1}
c_o = oil compressibility, psi^{-1}
c_{oa} = apparent oil-phase compressibility, including effects of dissolved gas, psi^{-1}
c_t = system total compressibility, psi^{-1}, Eq. 2.38
c_w = water compressibility, psi^{-1}
c_{wa} = apparent water-phase compressibility, including effects of dissolved gas, psi^{-1}
C = wellbore storage constant (coefficent, factor) RB/psi
C_A = shape constant or factor
C_D = dimensionless wellbore storage constant (coefficient, factor)
D = non-Darcy flow coefficient, D/Mcf
E_k = error in permeability estimated by simplified two-rate test analysis, fraction
E_s = error in skin factor estimated by simplified two-rate test analysis, dimensionless skin units
Ei = exponential integral, Eq. 2.7
e = 2.7182 . . .
erf = error function
exp = e
F_{cor} = correction factor when calculating permeability for a vertically fractured well, Section 11.3
F_{fl} = ratio of porosity-compressibility product of fracture to total porosity-compressibility product of reservoir rock
F_{HL} = Higgins-Leighton shape factor
F' = ratio of pulse length to total cycle length, Eq. 9.13
g = acceleration of gravity, ft/sec^2
g_c = units conversion factor, 32.17 lb_m ft/(lb_f sec^2)
G_P = primal geometric fraction for vertical pulse testing
G_R = reciprocal geometric fraction for vertical pulse testing
G^* = geometric fraction for vertical interference testing
h = formation thickness, ft
h_D = dimensionless thickness for horizontal fracture cases, Appendix C and Section 11.3
J = productivity index, (STB/D)/psi
J' = modified productivity index for a deliverability test
J^* = productivity index for a deliverability test
k = permeability, md
k_f = fracture permeability, md
k_{ma} = matrix permeability, md
k_{max} = maximum directional permeability, md
k_{min} = minimum directional permeability, md
k_o = permeability to oil, md
k_r = permeability in the radial (horizontal) direction, md
k_{rg} = relative permeability to gas, fraction
k_{ro} = relative permeability to oil, fraction
k_{rw} = relative permeability to water, fraction
k_s = permeability in the skin zone
k_z = permeability in the vertical direction, md
$\bar{k}$ = average permeability for anisotropic system, md
K = Secenov's coefficient, litre/gram-equivalent
log = logarithm, base 10
ln = logarithm, base e
L = length or distance, ft
m = ± slope of linear portion of semilog plot of pressure transient data, psi/cycle
$m(p)$ = real gas "potential" or pseudo pressure, Eq. 2.32, psi^2/cp
m_H = slope of a Hall plot, psi/(STB/D)
m_M = slope of the straight-line portion of a Muskat plot of pressure buildup data, cycle/hour
m_q = slope of the $1/q$ vs $\log t$ plot for a constant-pressure test, (D/STB)/cycle
m_{Hf} = slope of p_{ws} vs $\sqrt{t}$ plot for horizontal-fracture well test data, psi/$\sqrt{\text{hours}}$
m_{Vf} = slope of p_{ws} vs $\sqrt{t}$ plot for vertical-fracture well test data, psi/$\sqrt{\text{hours}}$
m' = slope of the data plot for a multiple-rate test, psi/(cycle STB/D)
m'_1 = slope (based on q_1) of the data plot for a two-rate test, psi/cycle
m'_3 = slope (based on q_3) of the data plot for a drawdown after a shut-in period, psi/cycle
m'' = slope of simplified or special data plot for a multiple-rate test, psi/cycle
m^* = slope of the straight line on a linear plot of p_w vs t, psi/hour
M = mobility ratio
M = molecular weight, lb_m/mole
n = concentration of dissolved solids, gram-equivalents/litre, Appendix D

n = power in productivity-index formula
p = pressure, psi
p_c = critical pressure, psia
p_D = dimensionless pressure
$(p_D)_M$ = dimensionless pressure at the match point for type-curve analysis
p_{DMBH} = Matthews-Brons-Hazebroek-type dimensionless pressure
$\bar{p}_{DMBH}$ = Matthews-Brons-Hazebroek dimensionless pressure for a square, water-drive system based on average pressure
p_{DMBHe} = Matthews-Brons-Hazebroek dimensionless pressure for a square, water-drive system based on boundary pressure
p_{DMDH} = Miller-Dyes-Hutchinson-type dimensionless pressure
p_{DMint} = dimensionless pressure of extrapolated straight line at intercept of a Muskat plot
p_{DR} = dimensionless pressure ratio used in type-curve matching DST flow-period data
$\bar{p}_D$ = dimensionless average reservoir pressure for water-drive reservoir
p_e = external pressure, psi
p_{ext} = pressure correctly extrapolated from past behavior, psi
p_{ff} = final flowing pressure in a DST (subscript 1 or 2 indicates flow period), psi
p_{fhm} = final hydrostatic mud pressure in a DST, psi
p_{fsi} = final shut-in pressure in a DST, psi
p_i = initial pressure, psi
p_{if} = initial flowing pressure in a DST (subscript 1 or 2 indicates flow period), psi
p_{ihm} = initial hydrostatic mud pressure in a DST, psi
p_{int} = pressure at intercept (abscissa value = 0) of various kinds of $f(p_w)$ vs $f(t)$ plots, psi
p_{isi} = initial shut-in pressure in a DST, psi
p_o = pressure in drillstring just before a flow period of a DST, psi
p_{pc} = pseudocritical pressure, psia
p_{pr} = pseudoreduced pressure
p_{sc} = pressure at standard conditions, psi
p_{tf} = tubing or wellhead flowing pressure, psi
p_{ts} = tubing or wellhead shut-in pressure, psi
p_w = bottom-hole pressure, psi
$p_w(\Delta t = 0)$ = bottom-hole pressure just before starting a transient well test, psi
p_{wext} = bottom-hole pressure correctly extrapolated from past behavior, psi
p_{wf} = flowing bottom-hole pressure, psi
p_{ws} = shut-in bottom-hole pressure, psi
p_{1hr} = pressure on straight-line portion of semilog plot 1 hour after beginning a transient test; usually a special kind of p_{int}, psi
$\bar{p}$ = average reservoir pressure, psi
p^* = false pressure, pressure obtained when linear portion of the plot of p_{ws} vs $\log\left[(t_p + \Delta t)/\Delta t\right]$ is extrapolated to $(t_p + \Delta t)/\Delta t = 1$, psi
δp = pressure offset between two semilog straight lines in transient-test data plot for a naturally fractured system, psi
Δp = pressure change (or pulse response amplitude in pulse testing), psi
Δp_{bsl} = Δp at beginning of semilog straight line, psi
Δp_{DV} = dimensionless response amplitude for vertical pulse testing
$(\Delta p_{DV})_\infty$ = dimensionless response amplitude for vertical pulse testing in an infinite-acting system
Δp_{el} = Δp at end of linear flow period (half-slope log-log line, or $\sqrt{t}$ straight line) for a vertical fracture, psi
Δp_M = pressure change from transient test data at the match point for type-curve analysis, psi
Δp_{our} = pressure drop at a well owing to operation of other wells in the reservoir, psi
Δp_s = pressure drop across skin, psi
Δp_{tw} = pressure difference between wellhead and bottom hole, psi
Δp_{1hr} = pressure difference on straight-line portion of semilog plot 1 hour after beginning a transient test; used in any kind of Δp vs log Δt plot, psi
$\Delta p_{\Delta t}$ = difference between observed and extrapolated pressure at time Δt, Eq. 5.22, psi
q = flow rate, > 0 for production, < 0 for injection, STB/D for liquid, Mscf/D for gas
q_D = dimensionless flow rate
$(q_D)_M$ = dimensionless flow rate at match point for type-curve matching
q_g = gas flow rate, Mcf/D
q_o = oil flow rate, STB/D
q_M = flow rate at match point for type-curve matching, STB/D
q_N = flow rate during Nth rate period in a variable-rate test, STB/D or Mcf/D
q_{sf} = sand-face flow rate expressed at standard conditions, STB/D
q_w = water flow rate, STB/D
$\bar{q}$ = average flow rate, STB/D
q^* = modified flow rate for pressure buildup analysis with variable rate before shut-in, STB/D
$(1/q)_{1hr}$ = ordinate value at 1 hour on straight-line plot of $(1/q)$ vs log t, D/STB
r = radius, ft
r_d = radius of drainage as defined in Section 2.12, ft
r_D = dimensionless radial distance
r_e = external radius, ft
r_f = horizontal fracture radius, ft
r_{ff} = radial distance to fluid front number 1, ft
r_{inf} = influence radius for interference testing, ft
r_s = radius of skin zone, ft
r_w = wellbore radius, ft
r_{wa} = apparent or effective wellbore radius (includes effects of wellbore damage or improvement), ft
r_{wb} = radius to a water bank, ft
R_s = solution gas-oil ratio, scf/STB
R_{sw} = solution gas-water ratio, scf/STB
s = van Everdingen-Hurst skin factor
s_{cp} = pseudo skin factor resulting from sand consolidation
s_p = pseudo skin factor resulting from partial completion or restricted flow entry
s_{wcp} = pseudo skin factor resulting from slanted well
s'' = additional skin factor resulting from anisotropic effects
S_g = gas saturation, fraction
S_o = oil saturation, fraction
S_w = water saturation, fraction
t = time, hours
t_{bsl} = time to beginning of the semilog straight line, hours
t_D = dimensionless time
$(t_D/r_D^2)_M$ = dimensionless time parameter from type curve at the match point for type-curve analysis
t_{DA} = dimensionless time based on drainage area
t_{De} = dimensionless time based on external radius, r_e
$(t_{DA})_{pss}$ = dimensionless time at the beginning of pseudosteady-state flow
t_{Drf} = dimensionless time based on horizontal fracture radius
t_{Dxf} = dimensionless time based on half-fracture length of a vertical fracture

t_{eia} = time at the end of the infinite-acting period, hours
t_{esl} = time to end of the semilog straight line, hours
t_L = time lag used in pulse testing, hours
$(t_L)_D$ = dimensionless time lag used in pulse testing
$(t_L)_\infty$ = time lag in vertical pulse testing for an infinite-acting system, hours
t_M = time value from transient-test data at the match point for type-curve analysis, hours
t_p = equivalent time well was on production or injection before shut-in, hours
$t_p{}^*$ = modified production time for pressure buildup analysis with variable rate before shut-in, hours
t_{pDA} = dimensionless production time based on drainage area
t_{pss} = time at the beginning of pseudosteady-state flow, hours
t_R = readjustment time, hours
t_s = stabilization time, hours
t_x = intersection time of two semilog straight-line segments on transient-test data plot, hours
t_1 = any time in a transient test, hours
t_2 = any time in a transient test, hours
t^* = time that transient-test data start deviating from semilog straight line, hours
Δt = running testing time, hours
Δt_C = total cycle length in pulse testing, hours
$(\Delta t_{DA})_{esl}$ = dimensionless time at end of Horner or Miller-Dyes-Hutchinson straight line for pressure buildup test analysis
$(\Delta t_{DA})_{sl}$ = dimensionless time at beginning or end of Muskat straight line for pressure buildup analysis
Δt_{Dfx} = dimensionless intersection time of two semilog straight lines for falloff test in a composite system
$\Delta t_{Df1}{}^*$ = dimensionless time for deviation of data from first semilog straight line for falloff test in a composite system
Δt_{dyn} = time for reading dynamic pressure (used in reservoir simulation) from straight line of a buildup plot, hours
Δt_{fx} = time of intersection of two semilog straight lines for falloff test in a composite system, hours
$\Delta t_{f1}{}^*$ = time of deviation of data from first semilog straight line for falloff test in a composite system, hours
$(\Delta t)_M$ = time at match point for type-curve matching, hours
$\Delta t_{\bar{p}}$ = shut-in time corresponding to Dietz's average reservoir pressure, hours
Δt_P = pulse length used in pulse testing, hours
Δt_{PDV} = dimensionless pulse length used in vertical pulse testing
Δt_{si} = shut-in time before drawdown test, hours
T = temperature, °R
T_c = critical temperature, °R
T_{pc} = pseudocritical temperature, °R
T_{pr} = pseudoreduced temperature
T_{sc} = temperature at standard conditions, °R
V = volume, bbl
V_p = pore volume, bbl
V_{pi} = drainage pore volume of Well i, bbl
V_{pt} = total system pore volume, bbl
V_P = volume produced, bbl
V_u = wellbore volume per unit length, bbl/ft
V_w = wellbore volume, bbl
ΔV = change in volume, bbl
W_i = cumulative water injection, bbl
x = x coordinate, ft
x_D = dimensionless x coordinate, Fig. 2.15 and Appendix B
x_e = x distance from a centered well to the edge of its square drainage region (half-length of the side of a square), ft
x_f = x distance from a well in the center of a square drainage region to the end of a vertical fracture that is parallel to the x axis (half-length of a vertical fracture), ft
x' = transformed x coordinate for an anisotropic system, ft
Δx = x length of a grid in a reservoir simulator, ft
y = y coordinate, ft
y_D = dimensionless y coordinate, Fig. 2.15 and Appendix B
y_i = mole fraction of Component i in the gas phase
y' = transformed y coordinate in an anisotropic system, ft
Δy = y length of a grid in a reservoir simulator, ft
z = real gas deviation factor
z_i = real gas deviation factor at initial conditions
ΔZ_P = vertical distance from upper formation boundary to center of upper perforations; for vertical well testing; Fig. 10.25; ft
ΔZ_R = vertical (response) distance between upper and lower perforations; for vertical pulse testing; Fig. 10.25; ft
ΔZ_{uf} = vertical distance from lower formation boundary to flow perforations; for vertical well testing; Fig. 10.25; ft
ΔZ_{us} = vertical distance from lower formation boundary to observation (static) perforations; for vertical well testing; Fig. 10.25; ft
Δ = difference
γ = specific gravity; referenced to water for liquids, to air for gases
ϵ = interporosity flow parameter
θ = angle between positive x axis and direction of k_{max} in an anisotropic reservoir, degrees
λ = mobility, md/cp
λ_g = mobility of gas phase, md/cp
λ_o = mobility of oil phase, md/cp
λ_t = total flowing mobility, md/cp
λ_w = mobility of water phase, md/cp
μ = viscosity, cp
μ_g = gas viscosity, cp
$\mu_{g@}$ = gas viscosity at atmospheric pressure and reservoir temperature, cp
μ_{gi} = gas viscosity at initial conditions, cp
μ_o = oil viscosity, cp
μ_w = water viscosity, cp
ρ = density, lb_m/cu ft
ρ_w = water density, lb_m/cu ft
ϕ = porosity, fraction

Subscripts

a = apparent
b = base
bsl = beginning of semilog straight line
C = calculated
dyn = dynamic pressure value for use in reservoir simulation
D = dimensionless
e = external
eia = end of infinite-acting period
el = end of linear flow period
esl = end of straight-line portion
ext = on extrapolated pressure trend
E = estimated
f = flowing
f = in fracture

F = future
g = gas
i = initial, index, component number
int = intercept value, value of ordinate at zero abscissa value
j = index
ma = in formation matrix
M = match point in type-curve matching
n = total in summation
N = last rate interval in a multiple-rate flow test
N = total in summation
N = number of components in a mixture
o = oil
OB = observed value
s or si = shut-in or static
s = skin zone
sl = beginning or end of straight-line portion
t = total
tr = true
w = water
w = well
wb = wellbore
x = intersection point of two semilog straight-line segments on transient-test data plot
1hr = data from straight-line portion of semilog plot at 1 hour of test time, extrapolated if necessary
1, 2 = layer, zone numbers, or time numbers
∞ = infinite-acting system

Bibliography

A

Abramowitz, Milton and Stegun, Irene A. (ed.): *Handbook of Mathematical Functions With Formulas, Graphs and Mathematical Tables*, National Bureau of Standards Applied Mathematics Series-55 (June 1964) 227-253.

Adams, A. R., Ramey, H. J., Jr., and Burgess, R. J.: "Gas Well Testing in a Fractured Carbonate Reservoir," *J. Pet. Tech.* (Oct. 1968) 1187-1194; *Trans.*, AIME, **243.**

Agarwal, Ram G., Al-Hussainy, Rafi, and Ramey, H. J., Jr.: "An Investigation of Wellbore Storage and Skin Effect in Unsteady Liquid Flow: I. Analytical Treatment," *Soc. Pet. Eng. J.* (Sept. 1970) 279-290; *Trans.*, AIME, **249.**

Agostini, M. D.: "Wireline Formation-Tester Performance on the North West Shelf," *Australian Pet. Expl. Assn. J.* (1975) **15,** Part 1, 127-132.

Al-Hussainy, R. and Ramey, H. J., Jr.: "Application of Real Gas Flow Theory to Well Testing and Deliverability Forecasting," *J. Pet. Tech.* (May 1966) 637-642; *Trans.*, AIME, **237.**

Al-Hussainy, R., Ramey, H. J., Jr., and Crawford, P. B.: "The Flow of Real Gases Through Porous Media," *J. Pet. Tech.* (May 1966) 624-636; *Trans.*, AIME, **237.**

Ammann, Charles B.: "Case Histories of Analyses of Characteristics of Reservoir Rock From Drill-Stem Tests," *J. Pet. Tech.* (May 1960) 27-36.

Amyx, James W., Bass, Daniel M., Jr., and Whiting, Robert L.: *Petroleum Reservoir Engineering: Physical Properties*, McGraw-Hill Book Co., Inc., New York (1960).

Aronofsky, J. A. and Jenkins, R.: "A Simplified Analysis of Unsteady Radial Gas Flow," *Trans.*, AIME (1954) **201,** 149-154.

Arps, J. J. and Smith, A. E.: "Practical Use of Bottom-Hole Pressure Buildup Curves," *Drill. and Prod. Prac.*, API (1949) 155-165.

B

Baldwin, David E., Jr.: "A Monte Carlo Model for Pressure Transient Analysis," paper SPE 2568 presented at the SPE-AIME 44th Annual Fall Meeting, Denver, Sept. 28-Oct. 1, 1969.

Banks, K. M.: "Recent Achievements With the Formation Tester in Canada," *J. Cdn. Pet. Tech.* (July-Sept. 1963) 84-94.

Barbe, J. A. and Boyd, B. L.: "Short-Term Buildup Testing," *J. Pet. Tech.* (July 1971) 800-804.

Beal, Carlton: "The Viscosity of Air, Water, Natural Gas, Crude Oil and Its Associated Gases at Oil-Field Temperatures and Pressures," *Trans.*, AIME (1946) **165,** 94-115.

Bixel, H. C., Larkin, B. K., and van Poollen, H. K.: "Effect of Linear Discontinuities on Pressure Build-Up and Drawdown Behavior," *J. Pet. Tech.* (Aug. 1963) 885-895; *Trans.*, AIME, **228.**

Bixel, H. C. and van Poollen, H. K.: "Pressure Drawdown and Buildup in the Presence of Radial Discontinuities," *Soc. Pet. Eng. J.* (Sept. 1967) 301-309; *Trans.*, AIME, **240.**

Breitenbach, E. A., Thurnau, D. H., and van Poollen, H. K.: "Solution of the Immiscible Fluid Flow Simulation Equations," *Soc. Pet. Eng. J.* (June 1969) 155-169.

Brigham, W. E.: "Planning and Analysis of Pulse-Tests," *J. Pet. Tech.* (May 1970) 618-624; *Trans.*, AIME, **249.**

Brill, J. P., Bourgoyne, A. T., and Dixon, T. N.: "Numerical Simulation of Drillstem Tests as an Interpretation Technique," *J. Pet. Tech.* (Nov. 1969) 1413-1420.

Brons, F. and Marting, V. E.: "The Effect of Restricted Fluid Entry on Well Productivity," *J. Pet. Tech.* (Feb. 1961) 172-174; *Trans.*, AIME, **222.**

Brons, F. and Miller, W. C.: "A Simple Method for Correcting Spot Pressure Readings," *J. Pet. Tech.* (Aug. 1961) 803-805; *Trans.*, AIME, **222.**

Brown, George G., Katz, Donald L., Oberfell, George G., and Alden, Richard C.: *Natural Gasoline and the Volatile Hydrocarbons*, Natural Gasoline Assn. of America, Tulsa (1948).

Brownscombe, E. R.: "A Field Calibration Technique for Bottom-Hole Pressure Measurement," *Pet. Eng.* (Aug. 1947) 84-88.

Brownscombe, E. R. and Conlon, D. R.: "Precision in Bottom-Hole Pressure Measurements," *Trans.*, AIME (1946) **165,** 159-174.

Bruce, G. H., Peaceman, D. W., Rachford, H. H., Jr., and Rice, J. D.: "Calculations of Unsteady-State Gas Flow Through Porous Media," *Trans.*, AIME (1953) **198,** 79-92.

Burnett, O. W. and Mixa, E.: "Application of the Formation Interval Tester in the Rocky Mountain Area," *Drill. and Prod. Prac.*, API (1964) 131-140.

Burns, William A., Jr.: "New Single-Well Test for Determining Vertical Permeability," *J. Pet. Tech.* (June 1969) 743-752; *Trans.*, AIME, **246.**

C

Cannon, John R. and Dogru, Ali H.: "Estimation of Permeability and Porosity From Well Test Data," paper SPE 5345 presented at the SPE-AIME 45th Annual California Regional Meeting, Ventura, April 2-4, 1975.

Carr, Norman L., Kobayashi, Riki, and Burrows, David B.: "Viscosity of Hydrocarbon Gases Under Pressure," *Trans.*, AIME (1954) **201,** 264-272.

Carter, R. D.: "Pressure Behavior of a Limited Circular Composite Reservoir," *Soc. Pet. Eng. J.* (Dec. 1966) 328-334; *Trans.*, AIME, **237.**

Chatas, Angelos T.: "A Practical Treatment of Non-Steady State Flow Problems in Reservoir Systems," *Pet. Eng.*, Part 1 (May 1953) B-42 through B-50; Part 2 (June 1953) B-38 through B-50; Part 3 (Aug. 1953) B-44 through B-56.

Chen, Hsiu-Kuo and Brigham, W. E.: "Pressure Buildup for a Well With Storage and Skin in a Closed Square," paper SPE 4890 presented at the SPE-AIME 44th Annual California Regional Meeting, San Francisco, April 4-5, 1974.

Chew, Ju-Nam and Connally, Carl A., Jr.: "A Viscosity Correlation for Gas-Saturated Crude Oils," *Trans.*, AIME (1959) **216,** 23-25.

Cinco, H., Miller, F. G., and Ramey, H. J., Jr.: "Unsteady-State Pressure Distribution Created by a Directionally Drilled Well," *J. Pet. Tech.* (Nov. 1975) 1392-1400; *Trans.*, AIME, **259.**

Cinco-Ley, Heber, Ramey, H. J., Jr., and Miller, Frank G.: "Pseudo-Skin Factors for Partially Penetrating Directionally Drilled Wells," paper SPE 5589 presented at the SPE-AIME 50th Annual Fall Technical Conference and Exhibition, Dallas, Sept. 28-Oct. 1, 1975.

Cinco-Ley, Heber, Ramey, Henry J., Jr., and Miller, Frank G.: "Unsteady-State Pressure Distribution Created by a Well With an Inclined Fracture," paper SPE 5591 presented at the SPE-AIME 50th Annual Fall Technical Conference and Exhibition, Dallas, Sept. 28-Oct. 1, 1975.

Cinco-L., Heber, Samaniego-V., F., and Dominguez-A., N.: "Transient Pressure Behavior for a Well With a Finite Conductivity Vertical Fracture," paper SPE 6014 presented at the SPE-AIME 51st Annual Fall Technical Conference and Exhibition, New Orleans, Oct. 3-6, 1976.

Cinco-L., Heber, Samaniego-V., F., and Dominguez-A., N.: "Unsteady-State Flow Behavior for a Well Near a Natural Fracture," paper SPE 6019 presented at the SPE-AIME 51st Annual Fall Technical Conference and Exhibition, New Orleans, Oct. 3-6, 1976.

Clark, K. K.: "Transient Pressure Testing of Fractured Water Injection Wells," *J. Pet. Tech.* (June 1968) 639-643; *Trans.*, AIME, **243.**

Coats, K. H., Dempsey, J. R., and Henderson, J. H.: "A New Technique for Determining Reservoir Description From Field Performance Data," *Soc. Pet. Eng. J.* (March 1970) 66-74; *Trans.*, AIME, **249.**

Cobb, William M. and Dowdle, Walter L.: "A Simple Method for Determining Well Pressure in Closed Rectangular Reservoirs," *J. Pet. Tech.* (Nov. 1973) 1305-1306.

Cobb, William M., Ramey, H. J., Jr., and Miller, Frank G.: "Well-Test Analysis for Wells Producing Commingled Zones," *J. Pet. Tech.* (Jan. 1972) 27-37; *Trans.*, AIME, **253.**

Cobb, William M. and Smith, James T.: "An Investigation of Pressure Buildup Tests in Bounded Reservoirs," paper SPE 5133 presented at the SPE-AIME 49th Annual Fall Meeting, Houston, Oct. 6-9, 1974. An abridged version appears in *J. Pet. Tech.* (Aug. 1975) 991-996; *Trans.*, AIME, **259.**

Collins, Royal Eugene: *Flow of Fluids Through Porous Materials,* Reinhold Publishing Corp., New York (1961) 108-123.

"Conversion of Operational and Process Measurement Units to the Metric (SI) System," *Manual of Petroleum Measurement Standards,* Pub. API 2564, API (March 1974) Chap. 15, Sec. 2.

Cooper, Hilton, H., Jr., Bredehoeft, John D., and Papadopulos, Istavros S.: "Response of a Finite-Diameter Well to an Instantaneous Charge of Water," *Water Resources Res.* (1967) **3,** No. 1, 263-269.

Crawford, G. E., Hagedorn, A. R., and Pierce, A. E.: "Analysis of Pressure Buildup Tests in a Naturally Fractured Reservoir," *J. Pet. Tech.* (Nov. 1976) 1295-1300.

Cronquist, Chapman: "Dimensionless PVT Behavior of Gulf Coast Reservoir Oils," *J. Pet. Tech.* (May 1973) 538-542.

Culham, W. E.: "Amplification of Pulse-Testing Theory," *J. Pet. Tech.* (Oct. 1969) 1245-1247.

Culham, W. E.: "Pressure Buildup Equations for Spherical Flow Regime Problems," *Soc. Pet. Eng. J.* (Dec. 1974) 545-555.

Cullender, M. H.: "The Isochronal Performance Method of Determining the Flow Characteristics of Gas Wells," *Trans.*, AIME (1955) **204,** 137-142.

D

Denson, A. H., Smith, J. T., and Cobb, W. M.: "Determining Well Drainage Pore Volume and Porosity From Pressure Buildup Tests," *Soc. Pet. Eng. J.* (Aug. 1976) 209-216; *Trans.*, AIME, **261.**

de Swaan O., A.: "Analytic Solutions for Determining Naturally Fractured Reservoir Parameters by Well Testing," *Soc. Pet. Eng. J.* (June 1976) 117-122; *Trans.*, AIME, **261.**

Dietz, D. N.: "Determination of Average Reservoir Pressure From Build-Up Surveys," *J. Pet. Tech.* (Aug. 1965) 955-959; *Trans.*, AIME, **234.**

Dixon, Thomas N., Seinfeld, John H., Startzman, Richard A., and Chen, W. H.: "Reliability of Reservoir Parameters From History Matched Drill Stem Tests," paper SPE 4282 presented at the SPE-AIME Third Symposium on Numerical Simulation of Reservoir Performance, Houston, Jan. 10-12, 1973.

Dodson, C. R. and Standing, M. B.: "Pressure-Volume-Temperature and Solubility Relations for Natural-Gas-Water Mixtures," *Drill. and Prod. Prac.*, API (1944) 173-179.

Dolan, John P., Einarsen, Charles A., and Hill, Gilman A.: "Special Application of Drill-Stem Test Pressure Data," *Trans.*, AIME (1957) **210,** 318-324.

Dowdle, Walter L.: "Discussion of Pressure Falloff Analysis in Reservoirs With Fluid Banks," *J. Pet. Tech.* (July 1974) 818; *Trans.*, AIME, **257.**

Doyle, R. E. and Sayegh, E. F.: "Real Gas Transient Analysis of Three-Rate Flow Tests," *J. Pet. Tech.* (Nov. 1970) 1347-1356.

Driscoll, Vance J.: "Use of Well Interference and Build-Up Data for Early Quantitative Determination of Reserves, Permeability and Water Influx," *J. Pet. Tech.* (Oct. 1963) 1127-1136; *Trans.*, AIME, **228.**

Duvaut, G.: "Drainage des Systèmes Hétérogènes," *Revue IFP* (Oct. 1961) 1164-1181.

E

Earlougher, Robert C., Jr.: "Comparing Single-Point Pressure Buildup Data With Reservoir Simulator Results," *J. Pet. Tech.* (June 1972) 711-712.

Earlougher, Robert C., Jr.: "Discussion of Interference Analysis for Anisotropic Formations — A Case History," *J. Pet. Tech.* (Dec. 1975) 1525; *Trans.*, AIME, **259.**

Earlougher, R. C., Jr.: "Estimating Drainage Shapes From Reservoir Limit Tests," *J. Pet. Tech.* (Oct. 1971) 1266-1268; *Trans.*, AIME, **251.**

Earlougher, R. C., Jr.: "Estimating Errors When Analyzing Two-Rate Flow Tests," *J. Pet. Tech.* (May 1973) 545-547.

Earlougher, Robert C., Jr.: "Variable Flow Rate Reservoir Limit Testing," *J. Pet. Tech.* (Dec. 1972) 1423-1429.

Earlougher, Robert C., Jr., and Kersch, Keith M.: "Analysis of Short-Time Transient Test Data by Type-Curve Matching," *J. Pet. Tech.* (July 1974) 793-800; *Trans.*, AIME, **257.**

Earlougher, Robert C., Jr., and Kersch, Keith M.: "Field Examples of Automatic Transient Test Analysis," *J. Pet. Tech.* (Oct. 1972) 1271-1277.

Earlougher, Robert C., Jr., Kersch, K. M., and Kunzman, W. J.: "Some Characteristics of Pressure Buildup Behavior in Bounded Multiple-Layer Reservoirs Without Crossflow," *J. Pet. Tech.* (Oct. 1974) 1178-1186; *Trans.*, AIME, **257.**

Earlougher, Robert C., Jr., Kersch, K. M., and Ramey, H. J., Jr.: "Wellbore Effects in Injection Well Testing," *J. Pet. Tech.* (Nov. 1973) 1244-1250.

Earlougher, R. C., Jr., Miller, F. G., and Mueller, T. D.: "Pressure Buildup Behavior in a Two-Well Gas-Oil System," *Soc. Pet. Eng. J.* (June 1967) 195-204; *Trans.*, AIME, **240.**

Earlougher, R. C., Jr., and Ramey, H. J., Jr.: "Interference Analysis in Bounded Systems," *J. Cdn. Pet. Tech.* (Oct.-Dec. 1973) 33-45.

Earlougher, Robert C., Jr., and Ramey, H. J., Jr.: "The Use of Interpolation to Obtain Shape Factors for Pressure Buildup Calculations," *J. Pet. Tech.* (May 1968) 449-450.

Earlougher, Robert C., Jr., Ramey, H. J., Jr., Miller, F. G., and Mueller, T. D.: "Pressure Distributions in Rectangular Reservoirs," *J. Pet. Tech.* (Feb. 1968) 199-208; *Trans.*, AIME, **243.**

Edwards, A. G. and Shryock, S. H.: "New Generation Drill Stem Testing Tools/Technology," *Pet. Eng.* (July 1974) 46, 51, 56, 58, 61.

Edwards, A. G. and Winn, R. H.: "A Summary of Modern Tools and Techniques Used in Drill Stem Testing," Pub. T-4069, Halliburton Co., Duncan, Okla. (Sept. 1973).

Eilerts, C. Kenneth: "Methods for Estimating Deliverability After Massive Fracture Completions in Tight Formations," paper SPE 5112 presented at the SPE-AIME Deep Drilling and Production Symposium, Amarillo, Tex., Sept. 8-10, 1974.

El-Hadidi, Samir M. and Ritter, A. W.: "Interpretation of Bottom-Hole Pressure Build-Up Tests on Fractured Oil Reservoirs," paper SPE 6020 presented at the SPE-AIME 51st Annual Fall Technical Conference and Exhibition, New Orleans, Oct. 3-6, 1976.

Elkins, Lincoln F. and Skov, Arlie M.: "Determination of Fracture Orientation From Pressure Interference," *Trans.*, AIME (1960) **219,** 301-304.

Engineering Data Book, 9th ed., Gas Processors Suppliers Assn., Tulsa (1972) Sec. 1.

Ershaghi, Iraj, Rhee, Shie-Woo, and Yang, Hsun-Tiao: "Analysis of Pressure Transient Data in Naturally Fractured Reservoirs With Spherical Flow," paper SPE 6018 presented at the SPE-AIME 51st Annual Fall Technical Conference and Exhibition, New Orleans, Oct. 3-6, 1976.

Evans, John G.: "The Use of Pressure Buildup Information to Analyze Non-Respondent Vertically Fractured Oil Wells," paper SPE 3345 presented at the SPE-AIME Rocky Mountain Regional Meeting, Billings, Mont., June 2-4, 1971.

Evers, John F. and Soeiinah, Edy: "Transient Tests and Long-Range Performance Predictions in Stress-Sensitive Reservoirs," paper SPE 5423 presented at the SPE-AIME Northern Plains Section Regional Meeting, Omaha, May 15-16, 1975.

F

Falade, Gabriel K. and Brigham, William E.: "The Analysis of Single-Well Pulse Tests in a Finite-Acting Slab Reservoir," paper SPE 5055B presented at the SPE-AIME 49th Annual Fall Meeting, Houston, Oct. 6-9, 1974.

Falade, Gabriel K. and Brigham, William E.: "The Dynamics of Vertical Pulse Testing in a Slab Reservoir," paper SPE 5055A presented at the SPE-AIME 49th Annual Fall Meeting, Houston, Oct. 6-9, 1974.

Felsenthal, Martin: "Step-Rate Tests Determine Safe Injection Pressures in Floods," *Oil and Gas J.* (Oct. 28, 1974) 49-54.

Fetkovich, M. J.: "The Isochronal Testing of Oil Wells," paper SPE 4529 presented at the SPE-AIME 48th Annual Fall Meeting, Las Vegas, Sept. 30-Oct. 3, 1973.

G

Gibson, J. A. and Campbell, A. T., Jr.: "Calculating the Distance to a Discontinuity From D.S.T. Data," paper SPE 3016 presented at the SPE-AIME 45th Annual Fall Meeting, Houston, Oct. 4-7, 1970.

Gladfelter, R. E., Tracy, G. W., and Wilsey, L. E.: "Selecting Wells Which Will Respond to Production-Stimulation Treatment," *Drill. and Prod. Prac.*, API (1955) 117-129.

Gogarty, W. B., Kinney, W. L., and Kirk, W. B.: "Injection Well Stimulation With Micellar Solutions," *J. Pet. Tech.* (Dec. 1970) 1577-1584.

Gray, K. E.: "Approximating Well-to-Fault Distance From Pressure Buildup Tests," *J. Pet. Tech.* (July 1965) 761-767.

Greenkorn, R. A. and Johnson, C. R.: "Method for Defining Reservoir Heterogeneities," U.S. Patent No. 3,285,064 (Nov. 15, 1966).

Griffith, H. D. and Collins, T.: "Determining Average Reservoir Properties From Gathering-Line Transient Analysis for a Multiwell Reservoir," *J. Pet. Tech.* (July 1975) 835-842.

Gringarten, Alain C.: "Unsteady-State Pressure Distributions Created by a Well With a Single Horizontal Fracture, Partial Penetration, or Restricted Flow Entry," PhD dissertation, Stanford U. (1971) 106. (Order No. 71-23,512 University Microfilms, P. O. Box 1764, Ann Arbor, Mich. 48106.)

Gringarten, Alain C. and Ramey, Henry J., Jr.: "An Approximate Infinite Conductivity Solution for a Partially Penetrating Line-Source Well," *Soc. Pet. Eng. J.* (April 1975) 140-148; *Trans.*, AIME, **259.**

Gringarten, Alain C. and Ramey, Henry J., Jr.: "Unsteady-State Pressure Distributions Created by a Well With a Single Horizontal Fracture, Partial Penetration, or Restricted Entry," *Soc. Pet. Eng. J.* (Aug. 1974) 413-426; *Trans.*, AIME, **257.**

Gringarten, A. C., Ramey, H. J., Jr., and Raghavan, R.: "Applied Pressure Analysis for Fractured Wells," *J. Pet. Tech.* (July 1975) 887-892; *Trans.*, AIME, **259.**

Gringarten, Alain C., Ramey, Henry J., Jr., and Raghavan, R.: "Pressure Analysis for Fractured Wells," paper SPE 4051 presented at the SPE-AIME 47th Annual Fall Meeting, San Antonio, Tex., Oct. 8-11, 1972.

Gringarten, Alain C., Ramey, Henry J., Jr., and Raghavan, R.: "Unsteady-State Pressure Distributions Created by a Well With a Single Infinite-Conductivity Vertical Fracture," *Soc. Pet. Eng. J.* (Aug. 1974) 347-360.

Gringarten, A. C. and Witherspoon, P. A.: "A Method of Analyzing Pump Test Data From Fractured Aquifers," *Proc.*, Symposium on Percolation Through Fissured Rock, International Society for Rock Mechanics, Stuttgart (Sept. 18-19, 1972).

"Guide for Calculating Static Bottom-Hole Pressures Using Fluid-Level Recording Devices," ERCB Report 74-S, Energy Resources Conservation Board, Calgary, Alta., Canada (Nov. 1974).

"Guide for the Planning, Conducting, and Reporting of Subsurface Pressure Tests," ERCB Report 74-T, Energy Resources Conservation Board, Calgary, Alta., Canada (Nov. 1974).

Gutek, A. M. H. and Clark, K. K.: "Vertical Permeability Measurements, Swan Hills Reef Complex," paper SPE 4122 presented at the SPE-AIME 47th Annual Fall Meeting, San Antonio, Tex., Oct. 8-11, 1972.

H

Hall, H. N.: "How to Analyze Waterflood Injection Well Performance," *World Oil* (Oct. 1963) 128-130.

Hall, Howard N.: "Compressibility of Reservoir Rocks," *Trans.*, AIME (1953) **198,** 309-311.

Harrill, J. R.: "Determining Transmissivity From Water-Level Recovery of a Step-Drawdown Test," Prof. Paper 700-C, USGS (1970) C212 through C213.

Hartsock, J. H. and Warren, J. E.: "The Effect of Horizontal Hydraulic Fracturing on Well Performance," *J. Pet. Tech.* (Oct. 1961) 1050-1056; *Trans.*, AIME, **222.**

Hawkins, Murray F., Jr.: "A Note on the Skin Effect," *Trans.*, AIME (1956) **207,** 356-357.

Hazebrock, P., Rainbow, H., and Matthews, C. S.: "Pressure Fall-Off in Water Injection Wells," *Trans.*, AIME (1958) **213,** 250-260.

Hernandez, Victor M. and Swift, George W.: "A Method for Determining Reservoir Parameters From Early Drawdown Data," paper SPE 3982 presented at the SPE-AIME 47th Annual Fall Meeting, San Antonio, Oct. 8-11, 1972.

Higgins, R. V., Boley, D. W., and Leighton, A. J.: "Aids to Forecasting the Performance of Waterfloods," *J. Pet. Tech.* (Sept. 1964) 1076-1082; *Trans.*, AIME, **231.**

Higgins, R. V. and Leighton, A. J.: "A Method of Predicting Performance of Five-Spot Waterfloods in Stratified Reservoirs Using Streamlines," *Report of Investigations 5921,* USBM (1962).

Higgins, R. V. and Leighton, A. J.: "Quick Way to Find Reservoir Pressure Distribution," *Oil and Gas J.* (Jan. 6, 1969) 67-70.

Hirasaki, George J.: "Pulse Tests and Other Early Transient Pressure Analyses for In-Situ Estimation of Vertical Permeability," *Soc. Pet. Eng. J.* (Feb. 1974) 75-90; *Trans.*, AIME, **257.**

Hopkins, Robert A.: *The International (SI) Metric System and How It Works,* Polymetric Services, Inc., Tarzana, Calif. (1974).

Horner, D. R.: "Pressure Build-Up in Wells," *Proc.*, Third World Pet. Cong., The Hague (1951) Sec. II, 503-523.

Howard, G. C. and Fast, C. R.: *Hydraulic Fracturing,* Monograph Series, Society of Petroleum Engineers of AIME, Dallas (1970) **2.**

Hubbert, M. King: "The Theory of Ground-Water Motion," *J. of Geol.* (Nov.-Dec. 1940) **XLVIII,** 785-944.

Hurst, William: "Establishment of the Skin Effect and Its Impediment to Fluid Flow Into a Well Bore," *Pet. Eng.* (Oct. 1953) B-6 through B-16.

Hurst, William: "Interference Between Oil Fields," *Trans.*, AIME (1960) **219,** 175-192.

Hurst, William, Clark, J. Donald, and Brauer, E. Bernard: "The Skin Effect in Producing Wells," *J. Pet. Tech.* (Nov. 1969) 1483-1489; *Trans.*, AIME, **246.**

Huskey, William L. and Crawford, Paul B.: "Performance of Petroleum Reservoirs Containing Vertical Fractures in the Matrix," *Soc. Pet. Eng. J.* (June 1967) 221-228; *Trans.*, AIME, **240.**

J

Jacob, C. E. and Lohman, S. W.: "Nonsteady Flow to a Well of Constant Drawdown in an Extensive Aquifer," *Trans.*, AGU (Aug. 1952) 559-569.

Jahns, Hans O.: "A Rapid Method for Obtaining a Two-Dimensional Reservoir Description From Well Pressure Response Data," *Soc. Pet. Eng. J.* (Dec. 1966) 315-327; *Trans.*, AIME, **237.**

Jargon, J. R.: "Effect of Wellbore Storage and Wellbore Damage at the Active Well on Interference Test Analysis," *J. Pet. Tech.* (Aug. 1976) 851-858.

Jargon, J. R. and van Poollen, H. K.: "Unit Response Function From Varying-Rate Data," *J. Pet. Tech.* (Aug. 1965) 965-969; *Trans.*, AIME, **234.**

Johnson, C. R.: "Portable 'Radar' for Testing Reservoirs Developed by Esso Production Research," *Oil and Gas J.* (Nov. 20, 1967) 162-164.

Johnson, C. R., Greenkorn, R. A., and Woods, E. G.: "Pulse-Testing: A New Method for Describing Reservoir Flow Properties Between Wells," *J. Pet. Tech.* (Dec. 1966) 1599-1604; *Trans.*, AIME, **237.**

Johnson, C. R. and Raynor, R.: "System for Measuring Low Level Pressure Differential," U.S. Patent No. 3,247,712 (April 26, 1966).

Jones, L. G.: "Reservoir Reserve Tests," *J. Pet. Tech.* (March 1963) 333-337; *Trans.*, AIME, **228.**

Jones, L. G. and Watts, J. W.: "Estimating Skin Effect in a Partially Completed Damaged Well," *J. Pet. Tech.* (Feb. 1971) 249-252; *Trans.*, AIME, **251.**

Jones, Park: "Drawdown Exploration Reservoir Limit, Well and Formation Evaluation," paper 824-G presented at the SPE-AIME Permian Basin Oil Recovery Conference, Midland, April 18-19, 1957.

Jones, Park: "Reservoir Limit Test," *Oil and Gas J.* (June 18, 1956) 184-196.

K

Kamal, M. and Brigham, W. E.: "Design and Analysis of Pulse Tests With Unequal Pulse and Shut-In Periods," *J. Pet. Tech.* (Feb. 1976) 205-212; *Trans.*, AIME, **261.**

Kamal, M. and Brigham, W. E.: "The Effect of Linear Pressure Trends on Interference Tests," *J. Pet. Tech.* (Nov. 1975) 1383-1384.

Kamal, Medhat and Brigham, William E.: "Pulse-Testing Response for Unequal Pulse and Shut-In Periods," *Soc. Pet. Eng. J.* (Oct. 1975) 399-410; *Trans.*, AIME, **259.**

Kaplan, Wilfred: *Advanced Calculus,* Addison Wesley Publishing Co., Inc., Reading, Mass. (1952) 220.

Katz, Donald L., Cornell, David, Kobayashi, Riki L., Poettmann, Fred H., Vary, John A., Elenbaas, John R., and Weinaug, Charles F.: *Handbook of Natural Gas Engineering,* McGraw-Hill Book Co., Inc., New York (1959) Chap. 11.

Kazemi, H.: "A Reservoir Simulator for Studying Productivity Variation and Transient Behavior of a Well in a Reservoir Undergoing Gas Evolution," *J. Pet. Tech.* (Nov. 1975) 1401-1412; *Trans.*, AIME, **259.**

Kazemi, Hossein: "Damage Ratio From Drill-Stem Tests With Variable Back Pressure," paper SPE 1458 presented at the SPE-AIME 36th Annual California Regional Meeting, Santa Barbara, Nov. 17-18, 1966.

Kazemi, Hossein: "Determining Average Reservoir Pressure From Pressure Buildup Tests," *Soc. Pet. Eng. J.* (Feb. 1974) 55-62; *Trans.*, AIME, **257.**

Kazemi, Hossein: "Discussion of Variable Flow Rate Reservoir Limit Testing," *J. Pet. Tech.* (Dec. 1972) 1429-1430.

Kazemi, Hossein: "Locating a Burning Front by Pressure Transient Measurements," *J. Pet. Tech.* (Feb. 1966) 227-232; *Trans.*, AIME, **237.**

Kazemi, Hossein: "Pressure Buildup in Reservoir Limit Testing of Stratified Systems," *J. Pet. Tech.* (April 1970) 503-511; *Trans.*, AIME, **249.**

Kazemi, H.: "Pressure Transient Analysis of Naturally Fractured Reservoirs With Uniform Fracture Distribution," *Soc. Pet. Eng. J.* (Dec. 1969) 451-462; *Trans.*, AIME, **246.**

Kazemi, Hossein, Merrill, L. S., and Jargon, J. R.: "Problems in Interpretation of Pressure Fall-Off Tests in Reservoirs With and Without Fluid Banks," *J. Pet. Tech.* (Sept. 1972) 1147-1156.

Kazemi, Hossein and Seth, Mohan S.: "Effect of Anisotropy and Stratification on Pressure Transient Analysis of Wells With Restricted Flow Entry," *J. Pet. Tech.* (May 1969) 639-647; *Trans.*, AIME, **246.**

Kazemi, H., Seth, M. S., and Thomas, G. W. "The Interpretation of Interference Tests in Naturally Fractured Reservoirs With Uniform Fracture Distribution," *Soc. Pet. Eng. J.* (Dec. 1969) 463-472; *Trans.*, AIME, **246.**

Khurana, A. K.: "Influence of Tidal Phenomena on Interpretation of Pressure Build-Up and Pulse Tests," *Australian Pet. Expl. Assn. J.* (1976) **16,** Part 1, 99-105.

Knutson, G. C.: "A Computer-Oriented Method of Pressure Build-Up Analysis," *J. Cdn. Pet. Tech.* (July-Sept. 1967) 111-114.

Kohlhaas, Charles A.: "A Method for Analyzing Pressures Measured During Drillstem-Test Flow Periods," *J. Pet. Tech.* (Oct. 1972) 1278-1282; *Trans.*, AIME, **253.**

Kohlhaas, C. A. and Miller, F. G.: "Rock-Compaction and Pressure-Transient Analysis With Pressure-Dependent Rock Properties," paper SPE 2563 presented at the SPE-AIME 44th Annual Fall Meeting, Denver, Sept. 28-Oct. 1, 1969.

Kolb, R. H.: "Two Bottom-Hole Pressure Instruments Providing Automatic Surface Recording," *Trans.*, AIME (1960) **219,** 346-349.

Kumar, Anil and Ramey, Henry J., Jr.: "Well-Test Analysis for a Well in a Constant-Pressure Square," paper SPE 4054 presented at the SPE-AIME 47th Annual Fall Meeting, San Antonio, Tex., Oct. 8-11, 1972. An abridged version appears in *Soc. Pet. Eng. J.* (April 1974) 107-116.

L

Laird, A. and Birks, J.: "Performance and Accuracy of Amerada Bottom-Hole Pressure Recorder With Special Reference to Use in Drill Stem Formation Tests and Repeatability of Reservoir Pressures Obtained Therein," *J. Inst. Pet.* (1951) **37,** 678-695.

Langston, E. P.: "Field Application of Pressure Buildup Tests, Jay-Little Escambia Creek Fields," paper SPE 6199 presented at the SPE-AIME 51st Annual Fall Technical Conference and Exhibition, New Orleans, Oct. 3-6, 1976.

Larkin, Bert K.: "Solutions to the Diffusion Equation for a Region Bounded by a Circular Discontinuity," *Soc. Pet. Eng. J.* (June 1963) 113-115; *Trans.*, AIME, **228.**

Lee, W. J., Jr.: "Analysis of Hydraulically Fractured Wells With Pressure Buildup Tests," paper SPE 1820 presented at the SPE-AIME 42nd Annual Fall Meeting, Houston, Oct. 1-4, 1967.

Lee, W. John: "Wellbore Storage: How It Affects Pressure Buildup and Pressure Drawdown Tests," paper presented at the SPWLA 12th Annual Logging Symposium, Dallas, May 2-5, 1971.

Lee, W. John, Harrell, Robert R., and McCain, William D., Jr.: "Evaluation of a Gas Well Testing Method," paper SPE 3872 presented at the SPE-AIME Northern Plains Section Regional Meeting, Omaha, May 18-19, 1972.

Lefkovits, H. C., Hazebroek, P., Allen, E. E., and Matthews, C. S.: "A Study of the Behavior of Bounded Reservoirs Composed of Stratified Layers," *Soc. Pet. Eng. J.* (March 1961) 43-58; *Trans.*, AIME, **222.**

Lescarboura, Jaime A.: "New Downhole Shut-in Tool Boosts BHP Test Accuracy," *World Oil* (Nov. 1974) 71-73.

"Letter Symbols for Petroleum Reservoir Engineering, Natural Gas Engineering, and Well Logging Quantities," Society of Petroleum Engineers of AIME, Dallas (1965); *Trans.*, AIME (1965) **234,** 1463-1496.

Levorsen, A. I.: *Geology of Petroleum,* 2nd ed., W. H. Freedman and Co., San Francisco (1967) 125.

Locke, C. D. and Sawyer, W. K.: "Constant Pressure Injection Test in a Fractured Reservoir — History Match Using Numerical Simulation and Type-Curve Analysis," paper SPE 5594 presented at the SPE-AIME 50th Annual Fall Technical Conference and Exhibition, Dallas, Sept. 28-Oct. 1, 1975.

Long, Giordano and Chierici, Gianluigi: "Salt Content Changes Compressibility of Reservoir Brines," *Pet. Eng.* (July, 1961) B-25 through B-31.

Loucks, T. L. and Guerrero, E. T.: "Pressure Drop in a Composite Reservoir," *Soc. Pet. Eng. J.* (Sept. 1961) 170-176; *Trans.*, AIME, **222.**

M

Maer, N. K., Jr.: "Type Curves for Analysis of Afterflow-Dominated Gas Well Buildup Data," *J. Pet. Tech.* (Aug. 1976) 915-924.

Martin, John C.: "Simplified Equations of Flow in Gas Drive Reservoirs and the Theoretical Foundation of Multiphase Pressure Buildup Analyses," *Trans.*, AIME (1959) **216,** 309-311.

Mathur, Shri B.: "Determination of Gas Well Stabilization Factors in the Hugoton Field," *J. Pet. Tech.* (Sept. 1969) 1101-1106.

Matthews, C. S.: "Analysis of Pressure Build-Up and Flow Test Data," *J. Pet. Tech.* (Sept. 1961) 862-870.

Matthews, C. S., Brons, F., and Hazebroek, P.: "A Method for Determination of Average Pressure in a Bounded Reservoir," *Trans.*, AIME (1954) **201,** 182-191.

Matthews, C. S. and Lefkovits, H. C.: "Studies on Pressure Distribution in Bounded Reservoirs at Steady State," *Trans.*, AIME (1955) **204,** 182-189.

Matthews, C. S. and Russell, D. G.: *Pressure Buildup and Flow Tests in Wells,* Monograph Series, Society of Petroleum Engineers of AIME, Dallas (1967) **1.**

Matthies, E. Peter: "Practical Application of Interference Tests," *J. Pet. Tech.* (March 1964) 249-252.

McAlister, J. A., Nutter, B. P., and Lebourg, M.: "A New System of Tools for Better Control and Interpretation of Drill-Stem Tests," *J. Pet. Tech.* (Feb. 1965) 207-214; *Trans.*, AIME, **234.**

McKinley, R. M.: "Estimating Flow Efficiency From Afterflow-Distorted Pressure Buildup Data," *J. Pet. Tech.* (June 1974) 696-697.

McKinley, R. M.: "Wellbore Transmissibility From Afterflow-Dominated Pressure Buildup Data," *J. Pet. Tech.* (July 1971) 863-872; *Trans.*, AIME, **251.**

McKinley, R. M., Vela, Saul, and Carlton, L. A.: "A Field Application of Pulse-Testing for Detailed Reservoir Description," *J. Pet. Tech.* (March 1968) 313-321; *Trans.*, AIME, **243.**

McLeod, H. O., Jr., and Coulter, A. W., Jr.: "The Stimulation Treatment Pressure Record — An Overlooked Formation Evaluation Tool," *J. Pet. Tech.* (Aug. 1969) 951-960.

"Measuring, Sampling, and Testing Crude Oil," API Standard 2500, American Petroleum Institute. Reproduced in Frick, Thomas C. and Taylor, R. William: *Petroleum Production Handbook,* McGraw-Hill Book Co., Inc., New York (1962) **1,** Chap. 16.

Merrill, L. S., Jr., Kazemi, Hossein, and Gogarty, W. Barney: "Pressure Falloff Analysis in Reservoirs With Fluid Banks," *J. Pet. Tech.* (July 1974) 809-818; *Trans.*, AIME, **257.**

Miller, C. C., Dyes, A. B., and Hutchinson, C. A., Jr.: "The Estimation of Permeability and Reservoir Pressure From Bottom Hole Pressure Build-Up Characteristics," *Trans.*, AIME (1950) **189,** 91-104.

Miller, G. B., Seeds, R. W. S., and Shira, H. W.: "A New, Surface-Recording, Down-Hole Pressure Gauge," paper SPE 4125 presented at the SPE-AIME 47th Annual Fall Meeting, San Antonio, Tex., Oct. 8-11, 1972.

Moran, J. H. and Finklea, E. E.: "Theoretical Analysis of Pressure Phenomena Associated With the Wireline Formation Tester," *J. Pet. Tech.* (Aug. 1962) 899-908; *Trans.*, AIME, **225.**

Morris, Earl E. and Tracy, G. W.: "Determination of Pore Volume in a Naturally Fractured Reservoir," paper SPE 1185 presented at the SPE-AIME 40th Annual Fall Meeting, Denver, Oct. 3-6, 1965.

Morse, J. V. and Ott, Frank III: "Field Application of Unsteady-State Pressure Analysis in Reservoir Diagnosis," *J. Pet. Tech.* (July 1967) 869-876.

Mueller, Thomas D. and Witherspoon, Paul A.: "Pressure Interference Effects Within Reservoirs and Aquifers," *J. Pet. Tech.* (April 1965) 471-474; *Trans.*, AIME, **234.**

Murphy, W. C.: "The Interpretation and Calculation of Formation Characteristics From Formation Test Data," Pamphlet T-101, Halliburton Co., Duncan, Okla. (1970).

Muskat, Morris: *Physical Principles of Oil Production*, McGraw-Hill Book Co., Inc., New York (1949) Chap. 12.

Muskat, Morris: "Use of Data on the Build-Up of Bottom-Hole Pressures," *Trans.*, AIME (1937) **123,** 44-48.

N

Najurieta, Humberto L.: "A Theory for the Pressure Transient Analysis in Naturally Fractured Reservoirs," paper SPE 6017 presented at the SPE-AIME 51st Annual Fall Technical Conference and Exhibition, New Orleans, Oct. 3-6, 1976.

Nestlerode, W. A.: "Permanently Installed Bottom-Hole Pressure Gauge," paper 875-16-L presented at the API Div. of Production Meeting, Denver, April 11-13, 1962.

Newman, G. H.: "Pore-Volume Compressibility of Consolidated, Friable, and Unconsolidated Reservoir Rocks Under Hydrostatic Loading," *J. Pet. Tech.* (Feb. 1973) 129-134.

Nowak, T. J. and Lester, G. W.: "Analysis of Pressure Fall-Off Curves Obtained in Water Injection Wells to Determine Injective Capacity and Formation Damage," *Trans.*, AIME (1955) **204,** 96-102.

O

Odeh, A. S.: "Flow Test Analysis for a Well With Radial Discontinuity," *J. Pet. Tech.* (Feb. 1969) 207-210; *Trans.*, AIME, **246.**

Odeh, A. S.: "Pseudo Steady-State Flow Capacity of Oil Wells With Limited Entry, and With an Altered Zone Around the Wellbore," paper SPE 6132 presented at the SPE-AIME 51st Annual Fall Technical Conference and Exhibition, New Orleans, Oct. 3-6, 1976.

Odeh, A. S.: "Steady-State Flow Capacity of Wells With Limited Entry to Flow," *Soc. Pet. Eng. J.* (March 1968) 43-51; *Trans.*, AIME, **243.**

Odeh, A. S.: "Unsteady-State Behavior of Naturally Fractured Reservoirs," *Soc. Pet. Eng. J.* (March 1965) 60-64; *Trans.*, AIME, **234.**

Odeh, A. S. and Al-Hussainy, R.: "A Method for Determining the Static Pressure of a Well From Buildup Data," *J. Pet. Tech.* (May 1971) 621-624; *Trans.*, AIME, **251.**

Odeh, A. S. and Jones, L. G.: "Pressure Drawdown Analysis, Variable-Rate Case," *J. Pet. Tech.* (Aug. 1965) 960-964; *Trans.*, AIME, **234.**

Odeh, A. S. and Jones, L. G.: "Two-Rate Flow Test, Variable-Rate Case — Application to Gas-Lift and Pumping Wells," *J. Pet. Tech.* (Jan. 1974) 93-99; *Trans.*, AIME, **257.**

Odeh, A. S., Moreland, E. E., and Schueler, S.: "Characterization of a Gas Well From One Flow-Test Sequence," *J. Pet. Tech.* (Dec. 1975) 1500-1504; *Trans.*, AIME, **259.**

Odeh, A. S. and Selig, F.: "Pressure Build-Up Analysis, Variable-Rate Case," *J. Pet. Tech.* (July 1963) 790-794; *Trans.*, AIME, **228.**

Otoumagie, Robert and Menzie, D. E.: "Analysis of Pressure Buildup in an Infinite Two-Layered Oil Reservoir Without Crossflow," paper SPE 6130 presented at the SPE-AIME 51st Annual Fall Technical Conference and Exhibition, New Orleans, Oct. 3-6, 1976.

P

Papadopulos, Istavros S.: "Nonsteady Flow to a Well in an Infinite Anisotropic Aquifer," *Proc.*, 1965 Dubrovnik Symposium on Hydrology of Fractured Rocks, Inter. Assoc. of Sci. Hydrology (1965) **I,** 21-31.

Papadopulos, Istavros S., Bredehoeft, John D., and Cooper, Hilton H., Jr.: "On the Analysis of 'Slug Test' Data," *Water Resources Res.* (Aug. 1973) **9,** No. 4, 1087-1089.

Papadopulos, Istavros S. and Cooper, Hilton H., Jr.: "Drawdown in a Well of Large Diameter," *Water Resources Res.* (1967) **3,** No. 1, 241-244.

Perrine, R. L.: "Analysis of Pressure Buildup Curves," *Drill. and Prod. Prac.*, API (1956) 482-509.

Pierce, Aaron E.: "Case History: Waterflood Performance Predicted by Pulse Testing," paper SPE 6196 presented at the SPE-AIME 51st Annual Fall Technical Conference and Exhibition, New Orleans, Oct. 3-6, 1976.

Pierce, A. E., Vela, Saul, and Koonce, K. T.: "Determination of the Compass Orientation and Length of Hydraulic Fractures by Pulse Testing," *J. Pet. Tech.* (Dec. 1975) 1433-1438.

Pinson, A. E., Jr.: "Concerning the Value of Producing Time Used in Average Pressure Determinations From Pressure Buildup Analysis," *J. Pet. Tech.* (Nov. 1972) 1369-1370.

Pinson, A. E., Jr.: "Conveniences in Analyzing Two-Rate Flow Tests," *J. Pet. Tech.* (Sept. 1972) 1139-1141.

Pirson, Richard S. and Pirson, Sylvain J.: "An Extension of the Pollard Analysis Method of Well Pressure Build-Up and Drawdown Tests," paper SPE 101 presented at the SPE-AIME 36th Annual Fall Meeting, Dallas, Oct. 8-11, 1961.

Pitzer, Sidney C., Rice, John D., and Thomas, Clifford E.: "A Comparison of Theoretical Pressure Build-Up Curves With Field Curves Obtained From Bottom-Hole Shut-In Tests," *Trans.*, AIME (1959) **216,** 416-419.

Pollard, P.: "Evaluation of Acid Treatments From Pressure Build-Up Analysis," *Trans.*, AIME (1959) **216,** 38-43.

Polubarinova-Kochina, P. Ya.: *Theory of Ground Water Movement*, Princeton U. Press, Princeton, N.J. (1962) 343-369.

Prasad, Raj K.: "A Practical Way to Find Minimum Drainage Area for a Well," *Oil and Gas J.* (July 30, 1973) 118-120.

Prasad, Raj K.: "Pressure Transient Analysis in the Presence of Two Intersecting Boundaries," *J. Pet. Tech.* (Jan. 1975) 89-96; *Trans.*, AIME, **259.**

Prats, Michael: "A Method for Determining the Net Vertical Permeability Near a Well From In-Situ Measurements," *J. Pet. Tech.* (May 1970) 637-643; *Trans.*, AIME, **249.**

Prats, M. and Scott, J. B.: "Effect of Wellbore Storage on Pulse-Test Pressure Response," *J. Pet. Tech.* (June 1975) 707-709.

R

Raghavan, R.: "Well Test Analysis: Wells Producing by Solution Gas Drive," *Soc. Pet. Eng. J.* (Aug. 1976) 196-208; *Trans.*, AIME, **261.**

Raghavan, R., Cady, Gilbert V., and Ramey, Henry J., Jr.: "Well-Test Analysis for Vertically Fractured Wells," *J. Pet. Tech.* (Aug. 1972) 1014-1020; *Trans.*, AIME, **253.**

Raghavan, R. and Clark, K. K.: "Vertical Permeability From Limited Entry Flow Tests in Thick Formations," *Soc. Pet. Eng. J.* (Feb. 1975) 65-73; *Trans.*, AIME, **259.**

Raghavan, R. and Hadinoto, Nico: "Analysis of Pressure Data for Fractured Wells: The Constant Pressure Outer Boundary," paper SPE 6015 presented at the SPE-AIME 51st Annual Fall Technical Conference and Exhibition, New Orleans, Oct. 3-6, 1976.

Raghavan, R., Scorer, J. D. T., and Miller, F. G.: "An Investigation by Numerical Methods of the Effect of Pressure-Dependent Rock and Fluid Properties on Well Flow Tests," *Soc. Pet. Eng. J.* (June 1972) 267-275; *Trans.*, AIME, **253.**

Raghavan, R., Topaloglu, H. N., Cobb, W. M., and Ramey, H. J., Jr.: "Well-Test Analysis for Wells Producing From Two Commingled Zones of Unequal Thickness," *J. Pet. Tech.* (Sept. 1974) 1035-1043; *Trans.*, AIME, **257.**

Raghavan, R., Uraiet, A., and Thomas, G. W.: "Vertical Fracture Weight: Effect on Transient Flow Behavior," paper SPE 6016 presented at the SPE-AIME 51st Annual Fall Technical Conference and Exhibition, New Orleans, Oct. 3-6, 1976.

Ramey, H. J., Jr.: "Application of the Line Source Solution to Flow in Porous Media — A Review," *Prod. Monthly* (May 1967) 4-7, 25-27.

Ramey, Henry J., Jr.: "Interference Analysis for Anisotropic Formations — A Case History," *J. Pet. Tech.* (Oct. 1975) 1290-1298; *Trans.*, AIME, **259.**

Ramey, H. J., Jr.: "Non-Darcy Flow and Wellbore Storage Effects in Pressure Build-Up and Drawdown of Gas Wells," *J. Pet. Tech.* (Feb. 1965) 223-233; *Trans.*, AIME, **234.**

Ramey, H. J., Jr.: "Rapid Method of Estimating Reservoir Compressibility," *J. Pet. Tech.* (April 1964) 447-454; *Trans.*, AIME, **231.**

Ramey, H. J., Jr.: "Short-Time Well Test Data Interpretation in the Presence of Skin Effect and Wellbore Storage," *J. Pet. Tech.* (Jan. 1970) 97-104; *Trans.*, AIME, **249.**

Ramey, H. J., Jr.: "Verification of the Gladfelter-Tracy-Wilsey Concept for Wellbore Storage Dominated Transient Pressures During Production," *J. Cdn. Pet. Tech.*, (April-June 1976) 84-85.

Ramey, Henry J., Jr., and Agarwal, Ram G.: "Annulus Unloading Rates as Influenced by Wellbore Storage and Skin Effect," *Soc. Pet. Eng. J.* (Oct. 1972) 453-462; *Trans.*, AIME, **253.**

Ramey, Henry J., Jr., Agarwal, Ram G., and Martin, Ian: "Analysis of 'Slug Test' or DST Flow Period Data," *J. Cdn. Pet. Tech.* (July-Sept. 1975) 37-47.

Ramey, H. J., Jr., and Cobb, William M.: "A General Buildup Theory for a Well in a Closed Drainage Area," *J. Pet. Tech.* (Dec. 1971) 1493-1505.

Ramey, H. J., Jr., and Earlougher, R. C., Jr.: "A Note on Pressure Buildup Curves," *J. Pet. Tech.* (Feb. 1968) 119-120.

Ramey, Henry J., Jr., Kumar, Anil, and Gulati, Mohinder S.: *Gas Well Test Analysis Under Water-Drive Conditions*, AGA, Arlington, Va. (1973).

Rawlins, E. L. and Schellhardt, M. A.: *Back-Pressure Data on Natural-Gas Wells and Their Application to Production Practices*, Monograph 7, USBM (1936).

Reprint Series No. 9 — Pressure Analysis Methods, Society of Petroleum Engineers of AIME, Dallas (1967).

Reprint Series No. 11 — Numerical Simulation, Society of Petroleum Engineers of AIME, Dallas (1973).

"Review of Basic Formation Evaluation," Form J-328, Johnston, Houston (1974).

Ridley, Trevor P.: "The Unified Analysis of Well Tests," paper SPE 5587 presented at the SPE-AIME 50th Annual Fall Technical Conference and Exhibition, Dallas, Sept. 28-Oct. 1, 1975.

Robertson, D. C. and Kelm, C. H.: "Injection-Well Testing To Optimize Waterflood Performance," *J. Pet. Tech.* (Nov. 1975) 1337-1342.

Russell, D. G.: "Determination of Formation Characteristics From Two-Rate Flow Tests," *J. Pet. Tech.* (Dec. 1963) 1347-1355; *Trans.*, AIME, **228.**

Russell, D. G.: "Extensions of Pressure Build-Up Analysis Methods," *J. Pet. Tech.* (Dec. 1966) 1624-1636; *Trans.*, AIME, **237.**

Russell, D. G., Goodrich, J. H., Perry, G. E., and Bruskotter, J. F.: "Methods for Predicting Gas Well Performance," *J. Pet. Tech.* (Jan. 1966) 99-108; *Trans.*, AIME, **237.**

Russell, D. G. and Prats, M.: "The Practical Aspects of Interlayer Crossflow," *J. Pet. Tech.* (June 1962) 589-594.

Russell, D. G. and Truitt, N. E.: "Transient Pressure Behavior in Vertically Fractured Reservoirs," *J. Pet. Tech.* (Oct. 1964) 1159-1170; *Trans.*, AIME, **231.**

S

Samaniego-V., F., Brigham, W. E., and Miller, F. G.: "A Performance Prediction Procedure for Transient Flow of Fluids Through Pressure Sensitive Formations," paper SPE 6051 presented at the SPE-AIME 51st Annual Fall Technical Conference and Exhibition, New Orleans, Oct. 3-6, 1976.

Samaniego-V., F., Brigham, W. E., and Miller, F. G.: "An Investigation of Transient Flow of Reservoir Fluids Considering Pressure-Dependent Rock and Fluid Properties," paper SPE 5593 presented at the SPE-AIME 50th Annual Fall Technical Conference and Exhibition, Dallas, Sept. 28-Oct. 1, 1975.

Schultz, A. L., Bell, W. T., and Urbanosky, H. J.: "Advances in Uncased-Hole, Wireline Formation-Tester Techniques," *J. Pet. Tech.* (Nov. 1975) 1331-1336.

Sinha, B. K., Sigmon, J. E., and Montgomery, J. M.: "Comprehensive Analysis of Drillstem Test Data With the Aid of Type Curves," paper SPE 6054 presented at the SPE-AIME 51st Annual Fall Technical Conference and Exhibition, New Orleans, Oct. 3-6, 1976.

Slater, G. E. and Hegeman, P. S. "Visual Studies of Well Interference," *J. Pet. Tech.* (Feb. 1976) 119-122.

Slider, H. C.: "A Simplified Method of Pressure Buildup Analysis for a Stabilized Well," *J. Pet. Tech.* (Sept. 1971) 1155-1160; *Trans.*, AIME, **251.**

Slider, H. C.: "Application of Pseudo-Steady-State Flow to Pressure-Buildup Analysis," paper SPE 1403 presented at the SPE-AIME Regional Symposium, Amarillo, Tex., Oct. 27-28, 1966.

Smith, R. V. and Dewees, E. J.: "Sources of Error in Subsurface-Pressure-Gage Calibration and Usage," *Oil and Gas J.* (Dec. 9, 1948) 85-98.

Standing, M. B.: "Concerning the Calculation of Inflow Performance of Wells Producing Solution Gas Drive Reservoirs," *J. Pet. Tech.* (Sept. 1971) 1141-1142.

Standing, M. B.: *Volumetric and Phase Behavior of Oil Field Hydrocarbon Systems*, Reinhold Publishing Corp., New York (1952).

Standing, Marshall B. and Katz, Donald L.: "Density of Natural Gases," *Trans.*, AIME (1942) **146,** 140-149.

Startzman, R. A.: "A Further Note on Pulse-Test Interpretation," *J. Pet. Tech.* (Sept. 1971) 1143-1144.

Stegemeier, G. L. and Matthews, C. S.: "A Study of Anomalous Pressure Build-Up Behavior," *Trans.*, AIME (1958) **213,** 44-50.

Strobel, C. J., Gulati, M. S., and Ramey, H. J., Jr.: "Reservoir Limit Tests in a Naturally Fractured Reservoir — A Field Case Study Using Type Curves," *J. Pet. Tech.* (Sept. 1976) 1097-1106; *Trans.*, AIME, **261.**

"Supplements to Letter Symbols and Computer Symbols for Petroleum Reservoir Engineering, Natural Gas Engineering, and Well Logging Quantities," Society of Petroleum Engineers of AIME, Dallas (1972); *Trans.*, AIME (1972) **253,** 556-574.

"Supplements to Letter Symbols and Computer Symbols for Petroleum Reservoir Engineering, Natural Gas Engineering, and Well Logging Quantities," Society of Petroleum Engineers of AIME, Dallas (1975); *Trans.*, AIME (1975) **259,** 517-537.

Swift, S. C. and Brown, L. P.: "Interference Testing for Reservoir Definition — The State of the Art," paper SPE 5809 presented at the SPE-AIME Fourth Symposium on Improved Oil Recovery, Tulsa, March 22-24, 1976.

T

Taylor, George S. and Luthin, James N.: "Computer Methods for Transient Analysis of Water-Table Aquifers," *Water Resources Res.* (Feb. 1969) **5,** No. 1, 144-152.

Theis, Charles V.: "The Relation Between the Lowering of the Piezometric Surface and the Rate and Duration of Discharge of a Well Using Ground-Water Storage," *Trans.*, AGU (1935) 519-524.

Theory and Practice of the Testing of Gas Wells, 3rd ed., Pub. ECRB-75-34, Energy Resources and Conservation Board, Calgary, Alta., Canada (1975).

Thomas, M. D. and Gupta, M. C.: "Can Your DST Results Be Improved?" *Oilweek* (Sept. 21, 1970) 35, 38, 42-44.

Thomas, Rex D. and Ward, Don C.: "Effect of Overburden Pressure and Water Saturation on the Gas Permeability of Tight Sandstone Cores," *J. Pet. Tech.* (Feb. 1972) 120-124.

Tiab, Djebbar and Kumar, Anil: "Application of p_D' Function to Interference Analysis," paper SPE 6053 presented at the SPE-AIME 51st Annual Fall Technical Conference and Exhibition, New Orleans, Oct. 3-6, 1976.

Timmerman, E. H. and van Poollen, H. K.: "Practical Use of Drill-Stem Tests," *J. Cdn. Pet. Tech.* (April-June 1972) 31-41.

Trube, Albert S.: "Compressibility of Natural Gases," *Trans.*, AIME (1957) **210,** 355-357.

Trube, Albert S.: "Compressibility of Undersaturated Hydrocarbon Reservoir Fluids," *Trans.*, AIME (1957) **210,** 341-344.

V

Vairogs, Juris, Hearn, C. L., Dareing, Donald W., and Rhoades, V. W.: "Effect of Rock Stress on Gas Production From Low-Permeability Reservoirs," *J. Pet. Tech.* (Sept. 1971) 1161-1167; *Trans.*, AIME, **251.**

Vairogs, Juris and Rhoades, Vaughan W.: "Pressure Transient Tests in Formations Having Stress-Sensitive Permeability," *J. Pet. Tech.* (Aug. 1973) 965-970; *Trans.*, AIME, **255.**

van der Knaap, W.: "Nonlinear Behavior of Elastic Porous Media," *Trans.*, AIME (1959) **216,** 179-187.

van Everdingen, A. F.: "The Skin Effect and Its Influence on the Productive Capacity of a Well," *Trans.*, AIME (1953) **198,** 171-176.

van Everdingen, A. F. and Hurst, W.: "The Application of the Laplace Transformation to Flow Problems in Reservoirs," *Trans.*, AIME (1949) **186,** 305-324.

van Everdingen, A. F. and Meyer, L. Joffre: "Analysis of Buildup Curves Obtained After Well Treatment," *J. Pet. Tech.* (April 1971) 513-524; *Trans.*, AIME, **251.**

van Poollen, H. K.: "Radius-of-Drainage and Stabilization-Time Equations," *Oil and Gas J.* (Sept. 14, 1964) 138-146.

van Poollen, H. K.: "Status of Drill-Stem Testing Techniques and Analysis," *J. Pet. Tech.* (April 1961) 333-339.

van Poollen, H. K.: "Transient Tests Find Fire Front in an In-Situ Combustion Project," *Oil and Gas J.* (Feb. 1, 1965) 78-80.

van Poollen, H. K., Bixel, H. C., and Jargon, J. R.: "Reservoir Modeling — 1: What It Is, What It Does," *Oil and Gas J.* (July 28, 1969) 158-160.

van Poollen, H. K., Bixel, H. C., and Jargon, J. R.: "Reservoir Modeling — 2: Single-Phase Fluid-Flow Equations," *Oil and Gas J.* (Aug. 18, 1969) 94-96.

van Poollen, H. K., Bixel, H. C., and Jargon, J. R.: "Reservoir Modeling — 3: Finite Differences," *Oil and Gas J.* (Sept. 15, 1969) 120-121.

van Poollen, H. K., Bixel, H. C., and Jargon, J. R.: "Reservoir Modeling — 4: Explicit Finite-Difference Technique," *Oil and Gas J.* (Nov. 3, 1969) 81-87.

van Poollen, H. K., Bixel, H. C., and Jargon, J. R.: "Reservoir Modeling — 5: Implicit Finite-Difference Approximation," *Oil and Gas J.* (Jan. 5, 1970) 88-92.

van Poollen, H. K., Bixel, H. C., and Jargon, J. R.: "Reservoir Modeling — 6: General Form of Finite-Difference Approximations," *Oil and Gas J.* (Jan. 19, 1970) 84-86.

van Poollen, H. K., Bixel, H. C., and Jargon, J. R.: "Reservoir Modeling — 7: Single-Phase Reservoir Models," *Oil and Gas J.* (March 2, 1970) 77-80.

van Poollen, H. K., Bixel, H. C., and Jargon, J. R.: "Reservoir Modeling — 8: Single-Phase Gas Flow," *Oil and Gas J.* (March 30, 1970) 106-107.

van Poollen, H. K., Bixel, H. C., and Jargon, J. R.: "Reservoir Modeling — 9: Here Are Fundamental Equations for Multiphase Fluid Flow," *Oil and Gas J.* (May 11, 1970) 72-78.

van Poollen, H. K., Bixel, H. C., and Jargon, J. R.: "Reservoir Modeling — 10: Applications of Multiphase Immiscible Fluid-Flow Simulator," *Oil and Gas J.* (June 29, 1970) 58-63.

van Poollen, H. K., Bixel, H. C., and Jargon, J. R.: "Reservoir Modeling — 11: Comparison of Multiphase Models," *Oil and Gas J.* (July 27, 1970) 124-130.

van Poollen, H. K., Bixel, H. C., and Jargon, J. R.: "Reservoir Modeling — 12: Individual Wells Pressures in Reservoir Modeling," *Oil and Gas J.* (Oct. 26, 1970) 78-80.

van Poollen, H. K., Bixel, H. C., and Jargon, J. R.: "Reservoir Modeling — 13: (Conclusion) A Review — and A Look Ahead," *Oil and Gas J.* (March 1, 1971) 78-79.

van Poollen, H. K., Breitenbach, E. A., and Thurnau, D. H.: "Treatment of Individual Wells and Grids in Reservoir Modeling," *Soc. Pet. Eng. J.* (Dec. 1968) 341-346.

van Poollen, H. K. and Jargon, J. R.: "Steady-State and Unsteady-State Flow of Non-Newtonian Fluids Through Porous Media," *Soc. Pet. Eng. J.* (March 1969) 80-88; *Trans.*, AIME, **246.**

Vela, Saul and McKinley, R. M.: "How Areal Heterogeneities Affect Pulse-Test Results," *Soc. Pet. Eng. J.* (June 1970) 181-191; *Trans.*, AIME, **249.**

Vogel, J. V.: "Inflow Performance Relationships for Solution-Gas Drive Wells," *J. Pet. Tech.* (Jan. 1968) 83-92; *Trans.*, AIME, **243.**

W

Warren, J. E. and Hartsock, J. H.: "Well Interference," *Trans.*, AIME (1960) **219,** 89-91.

Warren, J. E. and Root, P. J.: "Discussion of Unsteady-State Behavior of Naturally Fractured Reservoirs," *Soc. Pet. Eng. J.* (March 1965) 64-65; *Trans.*, AIME, **234.**

Warren, J. E. and Root, P. J.: "The Behavior of Naturally Fractured Reservoirs," *Soc. Pet. Eng. J.* (Sept. 1963) 245-255; *Trans.*, AIME, **228.**

Wattenbarger, Robert A. and Ramey, H. J., Jr.: "An Investigation of Wellbore Storage and Skin Effect in Unsteady Liquid Flow: II. Finite Difference Treatment," *Soc. Pet. Eng. J.* (Sept. 1970) 291-297; *Trans.*, AIME, **249.**

Wattenbarger, Robert A. and Ramey, H. J., Jr.: "Gas Well Testing With Turbulence, Damage and Wellbore Storage," *J. Pet. Tech.* (Aug. 1968) 877-887; *Trans.*, AIME, **243.**

Wattenbarger, Robert A. and Ramey, Henry J., Jr.: "Well Test Interpretation of Vertically Fractured Gas Wells," *J. Pet. Tech.* (May 1969) 625-632.

Weeks, Edwin P.: "Determining the Ratio of Horizontal to Vertical Permeability by Aquifer-Test Analysis," *Water Resources Res.* (Feb. 1969) **5,** No. 1, 196-214.

Weeks, Steve G. and Farris, Gerald F.: "Permagauge — A Permanent Surface-Recording Downhole Pressure Monitor — Through a Tube," paper SPE 5607 presented at the SPE-AIME 50th Annual Fall Technical Conference and Exhibition, Dallas, Sept. 28-Oct. 1, 1975.

West, W. J., Garvin, W. W., and Sheldon, J. W.: "Solution of the Equations of Unsteady-State Two-Phase Flow in Oil Reservoirs," *Trans.*, AIME (1954) **201,** 217-229.

Winestock, A. G. and Colpitts, G. P.: "Advances in Estimating Gas Well Deliverability," *J. Cdn. Pet. Tech.* (July-Sept. 1965) 111-119.

Witherspoon, Paul A., Narasimhan, T. N., and McEdwards, D. G.: "Results of Interference Tests From Two Geothermal Reservoirs," paper SPE 6052 presented at the SPE-AIME 51st Annual Fall Technical Conference and Exhibition, New Orleans, Oct. 3-6, 1976.

Woods, E. G.: "Pulse-Test Response of a Two-Zone Reservoir," *Soc. Pet. Eng. J.* (Sept. 1970) 245-256; *Trans.*, AIME, **249.**

Z

Zana, E. T. and Thomas, G. W.: "Some Effects of Contaminents on Real Gas Flow," *J. Pet. Tech.* (Sept. 1970) 1157-1168; *Trans.*, AIME, **249.**

Author Index

(List of authors and organizations referred to in the Monograph text, references, and the bibliography.)

Subject Index